5-2015

Investigating the Effects of Particulate Hexavalent Chromium on the Centriole Linkers

Julieta Martino

INVESTIGATING THE EFFECTS OF PARTICULATE HEXAVALENT CHROMIUM ON THE CENTRIOLE LINKERS

By

Julieta Martino

B.S. Universidad Nacional de Córdoba, 2005

A DISSERTATION

Submitted in Partial Fulfillment of the

Requirements for the Degree of

Doctor of Philosophy

(in Biochemistry and Molecular Biology)

The Graduate School

The University of Maine

May 2015

Advisory Committee:

John Pierce Wise, Sr., Professor of Toxicology and Molecular Epidemiology, Department of Applied Medical Sciences, University of Southern Maine, Advisor

Greg Mayer, Assistant Professor of Molecular Toxicology, Department of Environmental Toxicology, Texas Tech University

Stephen C. Pelsue, Associate Professor of Immunology & Molecular Biology, Department of Applied Medical Sciences, University of Southern Maine

W. Douglas Thompson, Professor of Epidemiology, Department of Applied Medical Sciences, University of Southern Maine

Hong Xie, Assistant Research Professor of Toxicology, Department of Applied Medical Sciences, University of Southern Maine

DISSERTATION ACCEPTANCE STATEMENT

On behalf of the Graduate Committee for Julieta Martino, I affirm that this manuscript is the final accepted dissertation. Signatures of all committee members are on file with the Graduate School at the University of Maine, 5755 Stodder Hall, Orono, ME.

John P. Wise, Sr., Professor of Toxicology and Molecular Epidemiology — Date 4/10/15

LIBRARY RIGHTS STATEMENT

In presenting this dissertation in partial fulfillment of the requirements for an advanced degree at The University of Maine, I agree that the Library shall make it freely available for inspection. I further agree that permission for "fair use" copying of this dissertation for scholarly purposes may be granted by the Librarian. It is understood that any copying or publication of this dissertation for financial gain shall not be allowed without my written permission.

Signature: Julieta Martinez

Date: 4/17/2015

INVESTIGATING THE EFFECTS OF PARTICULATE HEXAVALENT CHROMIUM ON THE CENTRIOLE LINKERS

By Julieta Martino

Dissertation Advisor: Dr. John Pierce Wise, Sr.

An Abstract of the Dissertation Presented
in Partial Fulfillment of the Requirements for the
Degree of Doctor of Philosophy
(in Biochemistry and Molecular Biology)
May 2015

Particulate hexavalent chromium (Cr(VI)) compounds are human lung carcinogens. However, their carcinogenicity is poorly understood. The best model for Cr(VI)-induced carcinogenesis involves the acquisition of structural and numerical chromosome instability (CIN). Many mechanisms contribute to CIN. Among these, centrosomes play a pivotal role because they dictate proper segregation of chromosomes during cell division. Cr(VI) causes centrosome amplification, a phenotype where cells have extra centrosomes and hence can undergo unequal distribution of chromosomes resulting in CIN. How Cr(VI) induces these abnormalities is unknown. Moreover, whether Cr(VI)-induced centrosome amplification is a permanent phenotypic change is also unknown. This work investigates the permanence of the centrosome amplification phenotype and explores centrosome defects that can lead to centrosome amplification.

We analyzed centrosome numbers in clonal cell lines developed from repeated exposures to Cr(VI). We found that these cells lines develop a permanent centrosome amplification phenotype after one, two or three exposure to Cr(VI). Moreover, permanent

centrosome amplification correlates with the acquisition of permanent changes in chromosome numbers and hence, numerical CIN.

In addition, we investigated centriole disengagement which is the licensing step of centrosome duplication. We found that chronic exposure to particulate Cr(VI) induces premature centriole disengagement in interphase. Consistent with this, we observed a decrease in securin and increase in active separase and Plk1, which regulate the disruption of the S-M protein linker that holds centrioles together.

Chronic exposure to Cr(VI) also caused premature centrosome separation in interphase, suggesting that Cr(VI) has the potential to affect the other centrosome protein linker (i.e. G1-G2 tether) which holds duplicated centrosomes together. Cr(VI) also decreases protein levels and localization of Nek2 and Eg5, proteins involved in centrosome separation.

Overall, the data indicate that Cr(VI) targets many aspects of centrosome biology. We propose that disruption of the G1-G2 tether leads to premature disruption of the S-M linker causing centriole disengagement and triggering centrosome duplication. This causes centrosome amplification, which leads to numerical CIN and ultimately, neoplastic transformation and cancer.

DEDICATION

This dissertation is dedicated to my family in Argentina: mami, papi, Santi and my grandmas Pocha and Berta, for their enormous and unconditional support, encouragement and love throughout my life. Even though we have been apart for many years, I have always felt you were by my side no matter what. You have laughed, cheered, cried and celebrated with me all these years and I am deeply grateful for our small but tight and loving family. This work is the fruit of all of our efforts.

A special dedication is to my dad Roberto, whose passion for geology, research and science and thirst for knowledge have been extremely influential in my decision to become a biologist. As a child I walked in his lab amidst microscopes, books and minerals, and always looked forward to seeing the rocks, plants and insects he would bring from his trips. He has instilled in me a deep appreciation, curiosity and respect for nature and science and I am extremely thankful for such a gift.

I would also like to dedicate this work to the whales, whose majestic nature inspired me to pursue biology as a career and who continue to fuel my passion and commitment to understanding the causes of disease in humans and wildlife.

ACKNOWLEDGEMENTS

First of all I would like to thank Dr. Wise, my mentor, for allowing me to be part of his lab, for his guidance, support, encouragement and for believing I could grow as a student and finish my PhD. I have learned a tremendous amount under his mentorship and I am very grateful for all the scientific and life wisdom he has shared with me. He also provided me with numerous research, travel and mentoring opportunities which allowed me to grow beyond what a PhD dissertation normally offers. I also thank him for always opening his house for pumpkin carvings, thanksgiving dinners and Christmas parties, and for fostering a great work environment which always felt like a big, fun family.

I would also like to thank my Doctoral Dissertation Committee: Dr. Greg Mayer, Dr. Stephen Pelsue, Dr. Doug Thompson, and Dr. Hong Xie for sharing their knowledge and expertise, and for their guidance and support during all these years. I also thank Drs. Amie Holmes, Scott Kraus, and Vince Markowski who served in my Dissertation Committee in the initial stages of my doctoral work. I am very thankful to my Committee for all the insightful questions, technical advice and moral support, which have greatly enhanced my growth as a student as well as the work of this dissertation.

Special thanks to the Applied Medical Sciences faculty at USM. Dr. Ah-Kau Ng, Dr. Stephen Pelsue and Dr. Monroe Duboise allowed me to use equipment from their laboratories and provided suggestions for experimental troubleshooting. Dr. Doug Thompson provided help and suggestions for statistical analyses.

I am extremely grateful for all of my colleagues at the Wise Laboratory of Environmental and Genetic Toxicology. Numerous high school students and teachers, undergraduates, graduate students, staff and faculty have provided me with a fun, kind and supportive work environment. Special thanks to Dr. Sandra Wise and Dr. Hong Xie

for their continuous guidance and help in all aspects of my graduate experience. Chris Gianios, for his tremendous dedication to the lab computers and software and for always making sure that our data was backed up. I would also like to thank David Kirstein, Jill Sinagra and Shouping Huang, for their hard work as administrative assistants and for taking care of the administrative duties that make our work possible. Thanks to Dr. John Lechner for his support, and for his difficult questions and constructive criticism. Thanks to Therry The, our technician, for his willingness to help with anything and for always having food to cheer me up. Thanks to our previous technician Dr. Britton Goodale who always answered my questions on cell culture and lab duties during my first year at the lab. Thanks to Dr. Nancy Gordon for sharing a cup of tea with me once a week, and answering my chemistry questions. I have had the pleasure to mentor high school and undergraduate students and I thank all of them for their time and help with my experiments: Alex, Kiersten, Ryan, Rachael, Greg, Amanda, Madison and Ania. I have also had the pleasure to work with many outstanding undergraduate students: James, Johnny, Cathy, Matt, Rob, Ryan, Greer, Jenny and Nicole; and Master's students: Fariba, Priya, Joe, Sean, Melissa, Leah, Erin and Jason; all of them were always willing to help and also offered support and encouragement. Special thanks to James for giving me numerous rides, for always asking how I was doing, and for many fun conversations. Thanks to our visiting scientists for sharing their expertise, cultural background and for many talks on the complexities of moving to a foreign land: Dr. Tolga Cavas, Dr. Lina Yang and Drs. Zulal and Vedat Zekeroglu.

My fellow PhD students were one of the most valuable resources while in graduate school: Tania, Qin Qin, Jamie, Sandy, Laura, Amie, Seungbum, Jen, Dan, Naun, Kellie, Cyndi, Carolyne, Kelsey and Rachel. Thanks for your support, for your help with experiments and lab duties, for your suggestions, for the many chats about data

and life, and for always being there for me. The long days in the lab would have not been possible if it weren't for your presence.

I have received tremendous administrative support from both the University of Maine and the University of Southern Maine. Particularly, I would like to thank the staff at the Office of International Programs at the University of Maine for their help with immigration and Fulbright Fellowship paperwork. The staff at the Office of Graduate Studies at the University of Southern Maine and the University of Maine Graduate School helped me with class registration, graduate assistantships, health insurance and graduate school and thesis/graduation paperwork. Thanks to Sharon Watterson and Ann Johnson, administrative specialists at the Applied Medical Sciences Department for their help with program paperwork.

Special thanks to Dr. Charles Moody and Dr. Julie Gosse at the Department of Molecular and Biomedical Sciences at the University of Maine for being a liaison for the Cooperative PhD program in Biochemistry and Molecular Biology between the University of Southern Maine and the University of Maine Orono.

Many thanks to the staff at the Sullivan Recreation and Fitness Complex at the University of Southern Maine for providing students with a friendly atmosphere in which to exercise, and for offering many great classes and programs. Special thanks to Niffy, my trainer, and Jeanette, my yoga instructor, for their teachings and support. I would have not made it sane without my weekly workouts with you ladies!

Thanks to the staff from University Health and Counseling Services at the University of Southern Maine for their kindness and friendliness, and especially to my counselor Dr. Janis Mallon, for listening to me and providing insightful guidance during difficult times.

Thanks to the Fulbright Commission in Argentina and the Institute of International Education for their help with applications to graduate programs in the USA, for

negotiating tuition waivers and for their help with the Delta Kappa Gamma World Fellowship application.

Special thanks to my Maine friends Tania, Pam, Mal, Betsy, Holly, Nadia, John, Robert, Braulio, Tatiana, Suly, Seungbum and Qin, for being part of all the experiences I had while living in Maine. I feel blessed to have had you in all the trips, fairs, concerts, beach days, snow days, dinners…and lobster bakes! Your tremendous love, encouragement and support have been crucial in allowing me to make it through graduate school and living abroad. My friend Nadia opened her house to me during tough financial times. I am deeply thankful for her generosity, for cooking delicious healthy meals while I was writing and for her love.

My friends in Argentina were always present despite the great distance between us: Lau, Mai, Male, Chil, Cari, Maris, Iva, Anis, Romis, Luichi, Chucky and Noe. Thanks for over two decades of friendship!

Thanks to the members of Instituto de Conservación de Ballenas: Mariano, Rox, Diego, Luciano, Cari, Vicky and José, for connecting me to Dr. Wise and supporting my decision to move to Maine to pursue my PhD. Thanks for your support, encouragement and guidance these years and for letting me reach the whales through your wonderful work. Special thanks to Mariano for sharing his insight and experience.

A special thanks to Aaron for his love, company, support and encouragement, for his advice and insight, our many conversations about science and lab work, and for inspiring me to aim higher.

And finally, my deepest gratitude goes to my family in Córdoba, my parents, brother, grandmas, aunts, uncle, cousins and sister-in-law for their love and support in all aspects of my life and throughout these years. I could have not done anything in my life without it.

This dissertation would have not been possible without the funding support from many sources. I received travel awards from the Society of Marine Mammalogy, the Society of Environmental Toxicology and Chemistry, the Society of Toxicology and the Maine Engagement and Innovation Fund, which allowed me to attend meetings to present my work. An International Fulbright Fellowship from the U.S. Department of State, a Delta Kappa Gamma World Fellowship and the Maine Engagement and Innovation Fund provided stipend, tuition and health insurance funding.

This work was supported by the National Institutes of Environmental and Health Sciences grant number ES016893[1] (J.P.W.) and the Maine Center for Toxicology and Environmental Health at the University of Southern Maine.

[1]The content is solely the responsibility of the authors and does not necessarily represent the official views of the National Institutes of Environmental and Health Sciences or the National Institutes of Health.

TABLE OF CONTENTS

LIST OF TABLES

LIST OF FIGURES

LIST OF ABBREVIATIONS

8-OHdG	8-hidroxydeoxyguanosine
APC/C	Anaphase promoting complex/cyclosome
CA	Centrosome amplification
CD	Centriole disengagement
CIN	Chromosome instability
CS	Centrosome separation
Cr	Chromium
Cr(0)	Elemental chromium
Cr(III)	Trivalent chromium
Cr(VI)	Hexavalent chromium
DSBs	Double strand breaks
EPA	Environmental Protection Agency
EGF	Epithelial growth factor
HR	Homologous recombination
M	Mitosis
MIN	Microsatellite instability
MMR	Mismatch repair
Mst2	Mammalian sterile 20-like kinase
MTOC	Microtubule-organizing center
Nek2	NIMA-related kinase 2
NER	Nucleotide excision repair
NSCLC	Non-small cell lung cancer
p-Eg5	Phosphorylated Eg5
PCM	Pericentriolar material

Plk1	Polo-like kinase 1
p-Plk1	Phosphorylated Plk1
PP1	Protein phosphatase 1
ROS	Reactive oxygen species
Sgo	Shugoshin
SPB	Surfactant protein B

CHAPTER 1

INTRODUCTION

1.1. Overview

Hexavalent chromium (Cr(VI) is a metal widely used in the chemical, refractory and metal industries. It is also a well-established human lung carcinogen. Cr(VI)-induced tumors are caused by Cr(VI) particles that are deposited in bronchial bifurcations. These particles dissolve over time and as they do, the chromate anions enter the surrounding cells. Once inside cells, Cr(VI) is reduced and in the process potent genotoxic metabolites are formed. DNA damage is a key aspect of Cr(VI) carcinogenicity. Cr(VI) tumors are characterized by chromosome instability, a phenotype that results in the development of complex karyotypes with abnormal number of chromosomes as well as structural damage to chromosomes. Chromosome instability is a major driving force of Cr(VI) carcinogenicity.

Proper chromosome segregation is key to maintaining normal number and structurally intact chromosomes. Centrosomes are organelles responsible for forming the mitotic spindle that segregates chromosomes during cell division. Many solid tumors, including lung tumors, have extra number of centrosomes that contribute to the acquisition of a chromosome instability phenotype. Centrosome numbers are tightly regulated by the centrosome cycle. However chemicals can negatively impact the centrosome cycle and cause centrosome abnormalities. Metals, including Cr(VI), cause centrosome amplification in human cells, although the underlying mechanisms are currently unknown. Here we present an overview of Cr(VI) uses, exposure and carcinogenicity. We also describe centrosomes and their role in carcinogenesis, as well as the current state of knowledge on metal-induced centrosome abnormalities.

1.2. Chromium

Chromium (Cr) is a naturally occurring metal. It has multiple valence states (-2 to +6) but the most stable are the elemental [Cr(0)], trivalent [Cr(III)] and hexavalent [Cr(VI)]. Even though all of these forms are present in nature, Cr(III) is the most stable and predominant one, mostly found in the mineral chromite [$(Fe, Mg)O(Cr, Al, Fe)_2O_4$]. About 95% of the chromite ores are located in southern South Africa, Zimbabwe and Kazakhstan (USGS, 2012). Cr(VI) in natural form is present in various minerals but in small amounts, and hence, these minerals are not extracted for commercial purposes. The majority of Cr(VI) in the environment is man-made and derives from the production and use of Cr(VI) compounds. Cr(VI) is made by milling and mixing chromite with soda ash and heating the mixture to oxidize Cr(III) to a soluble form of Cr(VI), which is then leached out of the mixture (OSHA, 2006).

Cr is lustrous, hard, and brittle, has a high melting point and is very resistant to corrosion. Cr compounds are also brightly colored in different shades of violets, greens, yellows, oranges and reds. Because these are highly desirable properties in industry, Cr is extracted from the mineral chromite to be used in metal, chemical and refractory industries. Cr has been widely used in industry for over 100 years and for many applications is considered an irreplaceable metal. One of its main uses is production of alloys where Cr serves as an anticorrosive and strengthening agent. The main Cr-containing alloy produced is stainless steel. The bright colored Cr salts are used as pigments in textile dyes, paints, glass, inks and plastics. Other applications that use Cr compounds are leather tanning, chrome plating, wood preservatives, and refractory bricks and linings for industrial furnaces.

Some studies have proposed that Cr(III) is an essential nutrient for glucose metabolism (Schwarz, 1959). However, until this date no disease or negative health effects have been associated with Cr(III) deficiency (Stearns, 2000). The European

Union has recently declared that there is no evidence of beneficial effects associated with Cr intake in healthy subjects and considers that the setting of an adequate intake for Cr is not appropriate (European Food Safety Authority, 2014). Cr(III) could potentially have a therapeutic role in patients with diabetes, but this also remains controversial (Vincent, 2014). Regarding negative health outcomes, Cr(III) is considered relatively non-toxic at the doses normally encountered. Cr(VI), on the other hand, is a very toxic metal and well established human lung carcinogen (IARC, 1990). The first report of a suspected Cr(VI)-induced tumor was in 1890, an adenocarcinoma in the turbinate body of a chrome worker (Newman, 1890). Since then, cell culture, animal and epidemiological studies from workers have provided indisputable evidence for the carcinogenicity of Cr(VI).

1.3. Cr(VI) Exposure

Cr(VI) is naturally found in soil, air and water, and derives from continental dust due to weathering and volcanic emissions. However, most of the Cr(VI) found in the environment has an anthropogenic origin (ATSDR, 2012). Anthropogenic sources include stationary points such as metal, textile and cement industries, and leather tanneries. Burning of fossil fuels and waste, and degradation of Cr-containing products also release Cr(VI). According to the Toxics Release Inventory (ATSDR, 2012), in 2009 about 36 million lbs of Cr compounds were released into U.S. waters, soils and air. Thus, it is no surprise that Cr is one of the primary pollutants present in 1,127 of the 1,699 sites listed on the Environmental Protection Agency (EPA) National Priorities List (ATSDR, 2012). Because of its widespread use and presence, exposure to Cr(VI) can occur through inhalation, ingestion and dermal contact. Of these, inhalation is the main exposure route.

Cr is naturally present in meats, fish, vegetables and fruits, as well as grains and cereals. Cr content in foods is highly variable but it is estimated that mean daily intakes (i.e.: 60 ug) are within the limits established by the World Health Organization (ATSDR, 2012). Cr(VI) is also present in drinking water. The EPA has an enforceable drinking standard of 0.1 mg/L for total Cr. However, a 2010 report by the Environmental Working Group (EWG, 2010) on high Cr(VI) levels in drinking water re-opened the debate on the potential health effects from oral exposure. It is estimated that most ingested Cr(VI) is efficiently reduced to non-toxic Cr(III) by gastric acids (De Flora et al., 1997). Cr(III) is not readily absorbed by cells, making overall Cr(VI) absorption through the gastrointestinal tract less than 10% of the ingested dose (ATSDR, 2012). Further reduction in the blood and liver limits the amount of Cr(VI) available for uptake by cells (De Flora et al., 1997). Due to reduction to Cr(III), Cr(VI) in water has been deemed as safe. However, the National Toxicology Program (NTP) showed an increase in neoplasms in the oral cavity in rats and small intestine in mice exposed chronically to Cr(VI) in drinking water (NTP, 2008). The data on human populations is still inconclusive. The EPA is currently re-evaluating its standard under the light of the newer studies.

Dermal exposure to Cr(VI) is possible through direct contact of the skin with Cr(VI) compounds in industrial settings, Cr(VI)-containing consumer products, as well as contaminated soils. Skin contact causes irritations and ulcerations. Eczema and dermatitis are common allergic responses in sensitized individuals. Some compounds with caustic properties may also induce enough damage to the skin to facilitate entry of Cr(VI) to the bloodstream and cause systemic toxicity (ATSDR, 2012).

Cr(VI) is also present in Co-Cr-Mo alloys used in prosthetics for joint replacements. Metal ions and particles released from these replacements are another potential source of exposure (Jantzen et al., 2013). Although multiple exposure

scenarios are possible, the greatest risk in both the general public and workers is through inhalation.

1.3.1. Cr(VI) in the Air

Even though natural sources contribute to atmospheric Cr, about 60-70% of atmospheric emissions are from anthropogenic sources. Main sources include combustion of fossil fuels, metal industries, cement plants and incineration of waste. Johnson et al. (2006) have estimated that worldwide anthropogenic emissions range between 58 and 112 Gg Cr/yr. It is estimated that a third of the 2,700-2,900 tons of Cr released into the atmosphere each year in the U.S. is in the hexavalent form (ATSDR, 2012). Cr in the air is mostly in particulate form (Kimbrough et al., 1999). The mass mean aerodynamic diameter for particles emitted by different industries is <10um (Kimbrough et al., 1999). It is estimated that particles in this size range can remain airborne for up to 10 days and be subject to long range transport (Kimbrough et al., 1999). More importantly, these particles can reach the tracheobronchiolar and alveolar regions of the lung. Average concentrations from 2,100 monitoring stations in urban, suburban, and rural areas ranged from 0.005 to 0.525 ug/m^3 (EPA 1984, 1990).

1.3.2. Inhalation Exposure in the General Public

The general public is at risk of Cr(VI) inhalation exposure, especially in suburban and urban areas nearby Cr industries. Home exposures from household dusts are likely in areas near industrial facilities and waste sites. In 1992-1993, the average Cr concentration in household dusts from Jersey City, NJ, was 376 ug/g (Freeman et al., 2000). Jersey City harbors several waste sites from chromate industries and Cr-contaminated slag has been extensively used as a landfill in this area. In contrast, average Cr concentration in household dusts after remediation was 73 ug/g (Freeman et al., 2000), suggesting that initial high indoor Cr levels were due to higher Cr levels in the outdoor environment. A similar trend was observed in Cr urine concentrations from

residents of this area (Stern et al.,1992; Freeman et al., 1995). Home based exposures can also occur in families of workers through contaminated clothing and shoes (ATSDR, 2012).

Another source of inhaled Cr are cigarettes. Cigarette smoke contains 0.0002-0.5 ug of Cr per cigarette (Smith et al., 1997). Indoor Cr levels in households where smoking occurs can be 10-400 times greater than those found outside (ATSDR, 2012). Moreover, because chronic inhalation of cigarette smoking causes lung cancer, the risk of lung cancer due to Cr(VI) inhalation is expected to be exacerbated in smokers and passive-smokers (Albert, 1991).

1.3.3. Inhalation Exposure in Occupational Settings

The population at greatest risk for Cr(VI) exposure are Cr workers. OSHA estimates that 558,000 workers in ~80 professions are exposed to Cr(VI) through inhalation of dusts, fumes and mists (OSHA, 2006). Exposure concentrations are up to two orders of magnitude higher than the general population (ATSDR, 2012), with the highest exposures occurring in chromate, chrome pigment, ferrochrome and stainless steel production, welding and electroplating.

The permissible exposure level (PEL) established by OSHA is an 8 h time weighted average (TWA) of 5 ug/m^3 (OSHA, 2006). However, Cr(VI) concentrations in ambient air in chromate factories can range from 5-600 ug/m^3 (Stern, 1982). Concentrations have declined significantly since the 1980s due to emission controls (NTP, 2011).

1.4. Cr(VI) Carcinogenicity

In the 1980s, numerous agencies classified Cr(VI) as carcinogenic to humans (NTP, 1980; EPA, 1984; NIOSH, 1988; IARC, 1990). This classification derives from strong evidence in cohorts of workers exposed to Cr(VI). These studies also helped

establish that the main target for Cr(VI) is the respiratory system. Cr(VI) not only causes lung cancer, but also induces nasal ulcerations and perforations as well as asthma (OSHA, 2006). Studies in rats and mice have suggested that the gastrointestinal tract could be a target for Cr(VI) carcinogenicity (NTP, 2008; Stout et al., 2009). Cr(VI) has also been shown to enhance UV-induced skin cancer in mice (Davidson et al., 2004; Uddin et al., 2007). Both the gastrointestinal tract and skin cancer studies are very recent and the effects on humans are inconclusive. In the below characterization of Cr(VI) carcinogenicity we will focus only on the respiratory system.

1.4.1. Evidence for Cr(VI) Carcinogenicity

1.4.1.1. Human Studies

The first systematic study on Cr(VI)-induced lung cancer in the United States was in 1948 (Machle and Gregorious). This study included data from all chromate production plants in the country and showed that 21.8% of all deaths were due to lung cancer, compared to 1.3% in a control population. Since then, multiple studies in chromate workers have provided strong links between Cr(VI) exposure and lung cancer (Hayes et al., 1979; Mancuso, 1997; Gibb et al., 2000; Luippold et al., 2003). Data collected in cohorts of chromate pigment production workers, platers and stainless steel welders also strongly support that Cr(VI) is a lung carcinogen (Sheffet et al., 1982; Langard and Vigander, 1983; Davies, 1984; Hayes et al., 1989; Moulin, 1997; Sorahan and Harrington, 2000).

From these studies, it has been estimated that the latency period for diagnosis is about 15 years (Machle and Gregorious, 1948; Taylor, 1966; Hayes et al., 1979). Moreover, lung cancer occurrence is correlated with exposure time (Braver et al., 1985). These studies also show that the particulate Cr(VI) compounds are more carcinogenic than the soluble ones (Hayes et al., 1979; Alderson et al., 1981). Initially, factories would add lime (calcium carbonate) to the extraction process to maximize the amount of

extracted Cr(VI). This would produce high levels of the insoluble calcium chromate. After the 1950s, factories underwent modernization, installed better hygiene practices and switched to low-lime or no-lime production. This has greatly reduced the risk of lung cancer in these cohorts but not completely eliminated it (Hayes et al., 1979; Alderson et al., 1981; Luippold et al., 2003). In addition, in 2006 OSHA lowered its permissible exposure limit (PEL) from 52 ug/m^3 to 5 ug/m^3. The current cohorts have not been followed long enough but it could be speculated that future epidemiologic studies will show an even further reduction in the incidence of lung cancers among Cr(VI) workers.

1.4.1.2. Animal Studies

Animal models have also been used to test the carcinogenicity of Cr compounds. Several Cr compounds of various solubilities have been administered to mice and rats by inhalation, intrabronchial implantation and intratracheal instillation. These studies also support that Cr(VI), and not Cr(III), is a lung carcinogen (Nettesheim et al., 1971; Levy and Vennit, 1986; Steinhoff et al., 1986; Snyder et al., 1997). They also show particulate forms are more potent carcinogens than the soluble forms (Levy et al., 1986).

1.4.1.3. Cell Culture Studies

Cellular transformation assays, namely loss of contact inhibition and growth in soft agar, have also been used to test Cr(VI) compounds. Both particulate and soluble Cr(VI) compounds are able to induce cellular transformation in various cell lines (Patierno et al., 1988; Elias et al., 1989; Xie et al., 2007; Rodrigues et al., 2009), with the particulate compounds being more potent than soluble ones (Elias et al., 1989). Moreover, Cr(VI)-transformed cells form tumors when injected in mice (Elias et al., 1989; Rodrigues et al., 2009). Studies in cells also show that the dissolution of Cr(VI) particles is necessary for transformation (Elias et al., 1991). DNA repair deficiency may also play a role in Cr(VI)-induced cellular transformation (Xie et al., 2008).

1.4.2. Physico-Chemical Factors Involved in Cr(VI) Carcinogenicity

1.4.2.1. Valence State

The valence state of Cr plays an important role in its carcinogenicity because it determines its uptake by cells. Cr(III) binds strongly to water and molecules that have oxygen, nitrogen or sulfur in their structures (Zhitcovich, 2004), forming bulky molecules that do not readily cross cell membranes. In contrast, Cr(VI) has a tetrahedral structure that resembles that of phosphate and sulfate, and enters cells by facilitated diffusion through generic anion transporters (DeFlora and Wetterhahn, 1989). Once inside the cell, Cr(VI) undergoes reduction to Cr(III), which rapidly accumulates inside of cells because it is not excreted. Reduction of Cr(VI) to Cr(III) also favors more uptake of Cr(VI). Moreover, reduction forms Cr(V), Cr(IV) and reactive oxygen species. Both Cr(III) and reduction intermediates can bind and damage DNA, but it is unknown which of these is the ultimate carcinogenic species.

1.4.2.2. Reduction

Reduction of Cr(VI) to Cr(III) plays a major role in Cr(VI) carcinogenesis. Extracellular reduction leads to a protective effect as Cr(III) does not easily enter cells. In contrast, intracellular reduction forms reactive intermediates that cause DNA damage (Shi et al., 1999). Cr(VI) can be reduced by numerous reductants including ascorbate, glutathione, cysteine, lipoic acid and diol-containing molecules such as NADPH (Shi et al., 1999). Microsomes, mitochondria, cytochrome P-450 and flavoenzymes have also been shown to reduce Cr(VI) in vitro (Shi et al., 1999). Ascorbate has been proposed to be the main reductant in the rat lung (Suzuki and Fukuda, 1990; Standeven and Wetterhahn, 1992). However, these studies were done treating bronchoalveolar lavage fluid or cytosolic fractions from lung tissues, as opposed to treating whole animals. Rats also have significantly higher levels of lung ascorbate than humans (Slade et al., 1985) and can synthesize it while humans cannot. Both of these factors could favor ascorbate

being the primary reductant in rat lung tissue. Moreover, studies in mice suggest NADPH, not ascorbate, is the main reductant in vivo (Liu et al., 1994; 1995; Liu and Dixon, 1996).

1.4.2.3. Solubility

Solubility is another important factor in Cr(VI) carcinogenesis. Multiple epidemiological studies have shown that the particulate forms are more potent carcinogens than the soluble forms (Hayes et al., 1979; Alderson et al., 1981). Moreover, cancer incidence decreased after factories changed to no lime production which significantly reduces the amount of particulate Cr(VI) compounds that are formed during chromite processing (Hayes et al., 1979; Alderson et al., 1981, Luippold et al., 2003). Animal studies also support the carcinogenicity of particulate forms of Cr(VI) (Levy et al., 1986) and cell culture studies show that they cause neoplastic transformation (Elias et al., 1987; Patierno et al., 1988; Xie et al., 2007).

Tumors in chromate workers and animal studies have shown that particulate Cr(VI) impacts lung bifurcation sites where it accumulates (Ishikawa et al., 1994a), adhering to epithelial cells. Particles dissolve slowly over time creating a prolonged exposure in the surrounding tissue. Moreover, cell studies suggest that cells enhance the dissolution of proximate particles, creating high concentrations of chromate anions in the microenvironment between particles and cells (Wise et al., 1994). This prolonged exposure causes DNA damage, aneuploidy and neoplastic transformation (Xie et al., 2005; Holmes et al., 2006a, 2008). In contrast, soluble compounds are rapidly reduced by the epithelial lining fluid and macrophages and cleared from lungs via the mucociliary escalator (De Flora and Wetterhahn, 1989; De Flora et al., 1997).

1.4.3. Cr(VI) Genotoxicity

One very important aspect of Cr(VI) carcinogenicity is its genotoxicity. Cr(VI) itself is not reactive towards DNA. Instead, DNA damage is caused by Cr(V), Cr(IV),

Cr(III), and/or oxygen- and carbon-based radicals formed during Cr(VI) reduction (O'Brien et al., 2003). The spectrum of damage includes base substitutions, oxidized bases, strand breaks, DNA crosslinks, and binary and ternary DNA adducts (DeFlora, 1990; O'Brien et al., 2003). Cr(VI) also induces gross numerical and structural DNA abnormalities such as aneuploidy, sister chromatid exchanges, chromosome aberrations and micronuclei (Holmes et al., 2008). Cr(VI) genotoxicity has mostly been investigated in cell culture models and numerous reviews have summarized this extensive wealth of data (Leonard and Lauwerys, 1980; De Flora et al., 1990; O'Brien et al., 2003; Zhitcovich, 2004; Holmes et al., 2008; Wise et al., 2008; Nickens et al., 2010). These studies highlight the diversity of DNA damage induced by Cr(VI) and the multiple mechanisms underlying it. In contrast, Cr(III) only damages DNA in *in vitro* systems but is not genotoxic in whole cells or animals (De Flora et al., 1990). These data are consistent with the poor uptake of Cr(III).

1.4.3.1. Oxidative DNA Damage

DNA damage by Cr(VI) can be caused indirectly through the formation of oxygen and carbon radicals formed during intracellular reduction of Cr(VI) (Yao et al., 2008). Cr(VI) can generate the carbon-based radical glutathione-derived thiyl radical ($GS^{\bullet}$) which forms by reaction of Cr(VI) with GSH (Shi et al., 1999). Cr(V) and Cr(IV) react with hydrogen peroxide (H_2O_2) and form hydroxyl radicals ($^{\bullet}OH$) via a Fenton-like reaction (Shi et al., 1999). Hydroxyl radicals cause oxidative DNA damage to bases, such as the common ROS biomarker 8-OHdG, and are responsible for formation of abasic sites and single strand breaks after Cr(VI) exposure (Casadevall and Kortenkamp, 1995). However, most of these studies used very high concentrations of Cr(VI) and hence, may not reflect realistic exposure scenarios. As such, the contribution of these lesions to Cr(VI) carcinogenesis is still under debate (O'Brien et al., 2003).

1.4.3.2. DNA Adducts and Crosslinks

The most important lesions caused by Cr(VI) are those where Cr(III) binds directly to DNA. This is possible due to the presence of six coordination sites on Cr(III) that stably bind DNA and other ligands with high affinity (Zhitcovich, 2004). Cr binds DNA specifically on DNA phosphate groups (Zhitcovich et al., 1996). Binding of Cr(III) to DNA forms binary and ternary Cr-DNA adducts and DNA-DNA interstrand crosslinks (Zhitcovich, 2004). In particular, Cr(III)-mediated DNA adducts with cysteine, glutathione and histidine are very abundant and of relevance due to their high mutagenic potential (Voitkun et al., 1998; Zhitcovich et al., 2001; Quievryn et al., 2003). Cr(III) ternary adducts cause base substitutions that target G/C pairs and lead to T/A transversions and A/T transitions (Voitkun et al., 1998, Zhitcovich et al., 2001; Quievryn et al., 2003). The same mutational spectrum is observed in lungs of Big Blue transgenic mice after intratracheal instillation of Cr(VI) (Cheng et al., 1998; 2000). Ternary adducts and interstrand crosslinks can also cause replication arrest due to polymerase stalling at the sites of the lesions (Bridgewater et al., 1994; O'Brien et al, 2001). Cr-DNA ternary adducts are repaired by nucleotide excision repair (NER) (Reynolds et al., 2004; O'Brien et al., 2005). Strikingly, NER deficiency decreases mutagenicity and clastogenicity of Cr(VI) suggesting a role of NER in Cr(VI)-induced DNA damage (Brooks et al., 2008). Other studies have shown NER deficient cells exhibit increased apoptosis and clonogenic lethality after Cr(VI) exposure (Reynolds et al., 2004; O'Brien et al., 2005). Altogether, the data suggest that a proficient NER may enhance DNA damage and survival in Cr(VI)-treated cells.

1.4.3.3. DNA Double Strand Breaks

DNA double strand breaks (DSBs) also form after Cr(VI) exposure (Ha et al., 2004; Xie et al., 2005; Xie et al., 2009) . DSBs caused by Cr(VI) are formed in asynchronous cell populations and abrogated when cells are arrested at G0/G1 phase

indicating that DSBs formation after Cr(VI) exposure is dependent on DNA replication (Ha et al., 2004). Specifically, DSBs form during S and G2 phases likely due to replication arrest or fork collapse when the replication machinery encounters an adduct or single strand break (Ha et al., 2004; Reynolds et al., 2007). Mismatch repair (MMR) has also been implicated in the formation of DSBs after Cr(VI) exposure (Reynolds et al., 2009). Cells deficient in MMR have less Cr(VI)-induced DSBs as measured by γ-H2A.X foci formation (Peterson-Roth et al., 2005). DSBs are normally repaired through homologous recombination (HR) repair which is also involved in the repair of Cr(VI)-induced DSBs (Bryant et al., 2006; Xie et al., 2008). Interestingly, chronic exposure to Cr(VI) in human lung cells inhibits Rad51 foci formation, a key step in HR (Qin et al., 2014). HR deficiency is very detrimental and leads to neoplastic transformation in Cr(VI)-exposed cells (Xie et al., 2007).

1.4.3.4. Structural Chromosome Damage

Failure to repair DNA DSBs can have devastating consequences because unrepaired DSBs give rise to structural chromosome damage (i.e.: clastogenesis) in the form of complex chromosome aberrations. Cr(VI) exposure causes chromosome aberrations after acute and longer exposures in human lung cells (Wise et al., 2002; Holmes et al., 2006a; Wise et al., 2006a; Wise et al., 2010). For particulate Cr(VI) compounds, it has been demonstrated that it is the chromate anion and not the cation or particle that is responsible for the clastogenic effects (Wise et al., 2004a; Xie et al., 2004).

1.4.3.5. In Vivo Genotoxicity

Genotoxicity assays carried out in workers, mainly platers and welders, using peripheral blood lymphocytes demonstrate that *in vivo* Cr(VI) induces micronuclei, strand breaks, sister chromatid exchanges, chromosome aberrations and crosslinks (IARC, 1990; ATSDR, 2012; O'Brien et al., 2003; Proctor et al., 2014). Oxidative DNA damage

is also detected after Cr(VI) exposure in humans and animals. Urinary concentrations of 8-hydroxydeoxyguanosine (8-OHdG), a major product of DNA oxidation, are increased in the urine of Cr(VI) workers and correlate with urinary Cr levels and concentrations of airborne Cr in factories (Kuo et al., 2003). An increase in 8-OHdG has also been observed in lung tissue of rats exposed to Cr(VI) by intratracheal instillation or inhalation (Izotti et al., 1998, Maeng et al., 2003). These studies are in accordance with *in vitro* and cell culture studies and reinforce the potent genotoxicity of Cr(VI).

1.4.4. Characteristics of Cr(VI)-Induced Tumors

The analysis of lung tissues from Cr(VI) workers has also contributed to the understanding of Cr(VI) carcinogenesis. The most common types of Cr(VI)-induced lung cancer are squamous cell carcinoma and small-cell lung carcinoma (Ishikawa et al., 1994b). Cr(VI)-induced tumors have a tendency to originate in the central part of the lung, specifically at bronchial bifurcations. The bifurcation ridges, and in particular the ridge centers, are hot spots of Cr deposits even 15 years after cessation of exposure (Ishikawa et al., 1994a). This supports the idea that Cr(VI) particles persist in the lung and dissolve slowly over time. Cr concentration in the lung ranges from 8-468 ug/g dry tissue, with highest Cr concentrations in the lungs of workers with lung tumors. Moreover, Cr accumulation increases with each generation of tracheobronchial branching and also correlates with the degree of malignancy (Kondo et al., 2003).

Tumors from chromate workers have also been analyzed for expression of key oncogenes and tumor suppressor genes. Cr(VI)-induced tumors from chromate workers have fewer p53 mutations and no ras mutations, when compared to lung tumors from the general population (Kondo et al., 1997; Ewis et al., 2001). These tumors also have reduced expression of p53, $p16^{INK4a}$ and bcl-2 proteins (Katabami et al., 2000). In contrast, cyclin D1, a protein that regulates cell cycle progression during G1 phase, is overexpressed (Katabami et al., 2000). Cr(VI) tumors have also been analyzed for

proteins related to lung function. Specifically, surfactant protein B (SP-B) variants are overrepresented in Cr(VI) tumors (Ewis et al., 2006). SP-B is part of the lung surfactant liquid which coats inhaled particles and aids with mucociliary clearance of the respiratory tract, among other functions (Akella and Desphande, 2013). Interestingly, these variants have been shown to increase susceptibility to squamous cell carcinoma in individuals not exposed to Cr(VI) (Seifart et al., 2002).

Microsatellite instability (MIN) is also a common feature of Cr(VI) tumors (Hirose et al., 2002). Microsatellites are DNA regions characterized by repetitive short nucleotide sequences. MIN refers to variations in the number of repetitive unit sequences in microsatellites caused by defective mismatch repair (MMR) (Loeb, 1994). In a study by Hirose et al. (2002) 92% of Cr(VI) tumors had MIN in one or more markers compared to 50% found in lung tumors not caused by Cr(VI) exposure. MIN also correlated with duration of exposure. Expression of MMR proteins hMLH1 and hMSH2 was also analyzed in the above set of tumors (Takahashi et al., 2005). The repression rate of hMLH1 and hMSH2 in Cr(VI) lung tumors tumors was 56% and 75%, respectively, compared to 20% and 23% in non Cr(VI) lung tumors. Hypermethylation of the hMLH1 promoter region could be partially responsible for the decreased expression in Cr(VI) tumors (Takahashi et al., 2005; Sun et al., 2009).

Cr(VI) has the ability to bind to histones likely through electrostatic interactions (Levina et al., 2006). It can also crosslink the histone deacetylase 1-DNA methyltransferase 1 complex to chromatin, specifically to the CYP1A1 promoter region (Schnekenburger et al., 2007). The above interactions suggest Cr(VI) may be able to induce epigenetic changes. Kondo et al. (2006) have shown that tumors from chromate workers have reduced $p16^{INK4a}$ expression which correlates with hypermethylation of $p16^{INK4a}$ in its promoter region. Hypermethylation of the hMLH1 and APC genes has also been described (Takahashi et al., 2005; Ali et al., 2011). Overall, the studies suggest

Cr(VI) tumors have a higher methylation frequency of tumor suppressor genes than lung tumors not induced by Cr(VI).

1.5. Mechanisms of Cr(VI)-Induced Carcinogenicity

All cancer cells share similar characteristics or “hallmarks” of cancer (Hanahan and Weinberg, 2000). These include the ability to resist cell death, sustain proliferative signaling, evade growth suppressors and immune destruction, reprogram energy metabolism, enable replicative immortality, induce angiogenesis, and activate invasion and metastasis (Hanahan and Weinberg, 2000; 2011). However, cells can acquire these hallmarks by different mechanisms, which can currently be summarized through three carcinogenesis paradigms: multi-stage carcinogenesis, epigenetic modification and genomic instability.

1.5.1. Multi-Stage Carcinogenesis

The multi-stage carcinogenesis paradigm (Vogelstein and Kinzler, 1993) entails that mutations in key proto-oncogenes and tumor suppressor genes lead to tumorigenesis through a step by step process in which each mutation confers the cell a proliferative advantage as well as aid in tumor progression and malignancy. Under this paradigm, a chemical carcinogen would need to cause a significant number of mutations in target genes.

As described before, Cr(VI) causes mutations in cell culture systems. However, mutation studies often use very high cytotoxic doses that do not reflect likely exposure scenarios (Holmes et al., 2008). Moreover, the bulk of the mutagenesis data comes from shuttle vector assays carrying specific Cr-induced lesions. Shuttle vectors are made of DNA that lacks proteins, nucleosomes and overall chromatin structure. As such, the host cell DNA repair machinery might act differently on these lesions than on those formed on

genomic DNA. Given these considerations, it is possible that these studies may overestimate Cr(VI) mutagenesis.

In addition, Cr(VI)-induced tumors do not show frequent mutations in key genes such as ras and p53 (Kondo et al., 1997; Ewis et al., 2001). This is in discordance with the multistage carcinogenesis paradigm. It is also very different than what is commonly observed in other lung tumors where ras is mutated in 20-30% of tumors, while p53 is mutated in 50-90% (Mitsuuchi and Testa, 2002). This striking difference suggests Cr(VI)-induced carcinogenesis does not involve mutagenesis as a central mechanism.

1.5.2. Epigenetics

In the epigenetic paradigm, the driving forces for tumorigenesis are epigenetic changes. Epigenetic changes refer to heritable changes in the genome that do not involve changes in the DNA sequence (Feinberg, 2004). These include cytosine methylation, post-translational modifications on histones and changes in chromatin structure or organization (Feinberg, 2004). The ability of Cr(VI) to induce epigenetic changes has been studied in cell lines as well as tumors.

A set of lung tumors from Japanese chromate workers was analyzed for methylation changes at different genes involved in DNA repair and cell cycle. Overall, these tumors had hypermethylation of $p16^{INK4}$, hMLH1 and APC genes (Kondo et al., 2006; Ali et al., 2011). In the case of $p16^{INK4}$ and hMLH1, hypermethylation correlated with decreased protein expression (Kondo et al., 2006; Ali et al., 2011). Wang et al. (2012) analyzed global methylation in a cohort of chromate workers from China using DNA extracted from blood. They showed global DNA hypomethylation which correlated with the presence of urinary 8-OHdG and DNA strand breaks in peripheral lymphocytes.

Cell culture studies also show evidence of epigenetic changes by Cr(VI). Klein et al. (2002) used a transgenic Chinese hamster cell lung model to analyze methylation status of the transgene *gpt* after Cr(VI) treatment. Cr(VI) caused partial methylation of

the *gpt* reporter and silenced the expression of the *gpt* gene. Mouse Hepa-1 cells were co-exposed to Cr(VI) and benzo[a]pyrene [B(a)P]), a carcinogen that induces gene expression through the aryl hydrocarbon receptor (AhR). Cr(VI) caused crosslinking of histone deacetylase 1-DNA methyltransferase 1 complex to the CYP1A1 promoter, inhibiting histone and acetylation marks usually induced by transactivation of the AhR (Schnekenburger et al., 2007). Cr(VI) also increases global H3K9 di and tri methylation in A549 cells and BEAS-2B cell lines (Sun et al., 2009). Moreover, the methylation patterns are localized to specific regions of the nucleus, with H3K9 dimethylation being mostly peripheral and H3K9 trimethylation localizing to the central region of the nucleus. Increased levels of methyltransferase G9a might be responsible for increased H3K9 dimethlyation seen after Cr(VI) exposure (Sun et al., 2009). In the case of H3K9 dimethylation, methylation was enriched in the promoter region of hMLH1, which correlated with decreased hMLH1 mRNA levels. Similar results have been observed in Cr(VI) tumors (Hirose et al., 2002; Ali et al., 2011).

Overall, the data from these studies show Cr(VI) is able to induce epigenetic changes in cell lines and human subjects. More importantly, epigenetic changes are observed in Cr(VI) tumors. The timing of these changes, either early or late, in the carcinogenesis process is currently unknown. In addition, it is very likely that for these changes to have an effect they would have to be permanent or present for long periods of time. The cell culture studies were mostly done with short time exposures which may not reflect the more realistic, chronic exposure scenarios. Even if changes are permanent, they might not be able to transform cells on their own. Given that Cr(VI) is a potent genotoxicant, epigenetic changes could exacerbate Cr(VI)-induced DNA damage by affecting proteins involved in DNA repair. Together, the currently available epigenetic data cannot explain the carcinogenicity of Cr(VI).

1.5.3. Genomic Instability

The genomic instability paradigm supports that disruption of the processes that maintain the stability of the genome leads to an accelerated rate of genetic changes at a whole genome level (Lengauer et al., 1998). There are two types of genomic instability, microsatellite and chromosomal instability. Microsatellite instability (MIN) is characterized by changes in the lengths of microsatellites, DNA regions with repetitive short nucleotide sequences (Loeb, 1994). Chromosome instability (CIN) involves gain or losses of partial or whole chromosomes (Lengauer et al., 1998).

1.5.3.1. Microsatellite Instability (MIN)

Microsatellites are prone to mutations due to replication errors caused by polymerases at these regions (Karran, 1996). Polymerases can sometimes add the wrong nucleotide or stutter or slip causing insertion or deletion loops. These lesions if left unrepaired result in base substitutions and changes in the length of microsatellites. In normal cells, insertion/deletion loops and base pair mismatches are fixed by mismatch repair (MMR). If MMR is defective, the replication lesions are not fixed and cells acquire MIN (Karran, 1996).

MIN has been described in lung tumors from Cr(VI)-exposed workers (Hirose et al., 2002). MIN of two or more loci was observed in 79% of these tumors, compared to 15% in controls. A higher frequency of MIN was also associated with longer exposure time and repression of the MMR protein hMLH1 (Hirose et al., 2002; Takahashi et al., 2005). Decreased expression of hMLH1 has also been observed in human lung cells after Cr(VI) exposure (Sun et al., 2009). Cell culture studies have also reported that deficient MMR might enhance survival and prevent apoptosis due to decreased DNA double strand break formation (Peterson-Roth et al., 2005; Reynolds et al., 2007). Interestingly, MMR might also be involved in potentiating Cr(VI)-induced DNA double strand breaks through the repair of Cr-DNA adducts (Peterson-Roth et al., 2005;

Reynolds et al., 2007, 2009; Reynolds and Zhitkovich, 2007). These data suggest MMR might play dual roles in Cr(VI) toxicity and together with the tumor data pinpoint MMR and MIN as important mechanisms in Cr(VI) carcinogenesis.

1.5.3.2. Chromosome Instability (CIN)

Exposure to Cr(VI) also causes CIN. CIN refers to an increased rate of gain or losses of partial or whole chromosomes (Lengauer et al., 1998). Numerical CIN specifically refers to gain or losses of whole chromosomes, while structural CIN refers to DNA breaks and translocations, insertions and deletions (Lengauer et al., 1998). CIN is very common in solid tumors, including those of the lung, and accounts for their gross karyotype abnormalities (Testa et al., 1992; Lengauer et al., 1998).

Numerical CIN has not been analyzed in Cr(VI) tumors or investigated using *in vivo* models. However, chromosome losses and gains are common in lung tumors of different etiology (Balsara and Testa, 1992; Testa et al., 1992). Near triploid and tetraploid complements are also frequent (Balsara and Testa, 1992; Testa et al., 1992). Cell culture studies show Cr(VI) is able to induce numerical CIN in human lung cells. A soluble form of Cr(VI), potassium dichromate, was able to induce aneuploidy in the form of hypodiploidy (i.e.: less than 2N) after a 30 h treatment (Güerci et al., 2000; Seoane et al., 2002). Particulate forms of Cr(VI) have also been studied. Both lead and zinc chromate induced aneuploidy, in the forms of hypodiploidy, hyperdiploidy and tetraploidy, after chronic exposure (i.e.: 48-120 h) (Holmes et al., 2006b; Holmes et al., 2010). Lead chromate-induced aneuploid cells were able to survive and form colonies suggesting that the phenotype is persistent (Holmes et al., 2006b). In support of this, human lung epithelial cells transformed by lead chromate also show increased aneuploidy (Xie et al., 2007).

Structural CIN is also very prevalent in lung tumors (Balsara and Testa, 1992; Testa et al., 1992). It is indicated by the presence of chromosomal translocations,

insertions and deletions. No studies have analyzed these events in Cr(VI) tumors or using *in vivo* models. However, chromosomal aberrations that can lead to structural CIN have been studied extensively using the chromosome damage, sister chromatid exchange and micronucleus assays. These studies show that Cr(VI), both soluble and particulate forms, can cause multiple chromosomal aberrations in human lung fibroblasts and epithelial cells (Wise et al., 2002; Wise et al., 2004a; Holmes et al., 2006a; Wise et al., 2006a; Reynolds et al., 2007; Wise et al., 2010). In the case of lead chromate, it was also shown that it is the chromate anion and not the lead cation or internalized particles that cause chromosomal aberrations (Wise et al., 2004a; Xie et al., 2004). Micronuclei and sister chromatid exchanges after Cr(VI) exposure have also been described in non-human cell lines (ATSDR, 2012). Animal studies have mostly analyzed micronuclei formation, and have yielded both positive and negative results (ATSDR, 2012). However, these studies used intraperitoneal or oral exposure of soluble compounds, which are not good models for studying Cr(VI) lung carcinogenesis. Increased frequency of micronuclei, sister chromatid exchanges and chromosomal aberrations have been observed in peripheral blood lymphocytes of Cr(VI) workers (IARC, 1990; ATSDR, 2012). The ultimate DNA lesion leading to structural CIN are DNA double strand breaks (DSBs). Intratracheal instillation of sodium dichromate in the lungs of rats induced DNA fragmentation measured by DNA electrophoresis (Izotti et al., 1998). DNA DSBs, measured by the comet assay and γ.H2AX foci formation, also form in human lung cells after Cr(VI) exposure (Xie et al., 2004; 2009; Ha et al., 2004; Wakeman et al., 2004; Reynolds et al., 2007a, Wise et al., 2010).

In summary, human, animal and cell culture studies show Cr(VI) causes both MIN as well as numerical and structural CIN. Even though, the underlying causes are still unknown, the above studies strongly support that genomic instability is a feasible mechanism for Cr(VI) carcinogenesis.

1.6. Mechanisms Involved in Chromosome Instability

Multiple mechanisms have been implicated in the acquisition of a CIN phenotype. These include chromosome condensation, sister chromatid cohesion, kinetochore structure and function, cell cycle checkpoints, DNA repair, centrosome duplication and microtubule formation and dynamics (Langauer et al., 1998; Negrini et al., 2010). Despite great advances in the understanding of the molecular basis of each of these mechanisms, our current knowledge of how they contribute to genomic instability and tumorigenesis is still very limited.

1.6.1. Possible Mechanisms Underlying Cr(VI)-Induced CIN

Our understanding of how Cr(VI) causes genomic instability is also very limited. However, a few studies have begun to help elucidate the complexity of Cr(VI) carcinogenesis. Human lung cells exposed to lead and zinc chromate show a time-dependent and concentration-dependent increase in centrosome amplification (Holmes et al., 2006b, Holmes et al., 2010). Centrosomes are major contributors to numerical CIN. Cr(VI)-treated cells show evidence of bypass of the spindle checkpoint that controls proper microtubule-kinetochore attachments (Wise et al., 2006b; Holmes et al., 2010). Spindle checkpoint bypass leads to abnormal mitotic phenotypes such as premature anaphase, premature centromere division and centromere spreading, which also cause numerical CIN (Holmes et al., 2010b). Moreover, these phenotypes suggest potential defects in the cohesion of sister chromatids. At the molecular level, Cr(VI) decreases expression of spindle checkpoint proteins Mad2 and Cdc20 (Holmes et al., 2010; Karri et al., 2013). It also decreases Cdc20 localization to kinetochores and the interaction of Cdc20 with Mad2 (Karri et al., 2013). The above studies show that Cr(VI) can alter pathways that control numerical stability of the genome.

Exposure to Cr(VI) also affects DNA repair pathways involved in maintaining structural CIN. Qin et al. (2014) have shown that chronic exposure to Cr(VI) decreases

expression of homologous recombination (HR) repair proteins as well as RAD51 foci formation. Interestingly, this decreased response is followed by overexpression of non-homologous end joining proteins, an alternative DNA DSB repair pathway that is more error-prone than HR (Qin, 2013). Moreover, HR deficient cell lines exposed to Cr(VI) have increased structural CIN and neoplastic transformation (Bryant et al., 2006; Stackpole et al., 2007; Xie et al., 2008). The data from these studies indicate that inhibition of key DNA repair pathways contribute to structural CIN observed after Cr(VI) exposure.

Figure 1.1. shows our proposed model for Cr(VI) carcinogenicity based on our current knowledge of Cr(VI) genotoxicity and its effects on cellular molecular pathways. This project focuses specifically on centrosome amplification and attempts to investigate how Cr(VI) causes this phenotype.

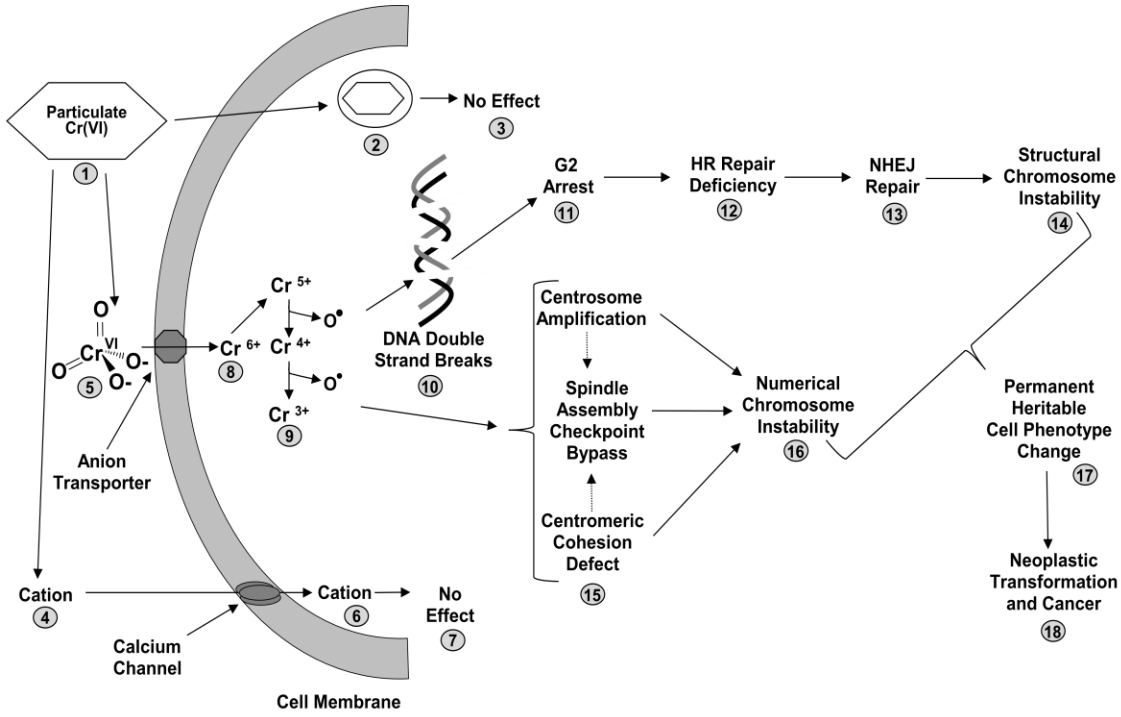

Figure 1.1. Mechanism for Cr(VI) Carcinogenesis. This figure shows a proposed mechanism of how Cr(VI) induces cancer. A cell is exposed to particulate Cr(VI) (1). Particles can be phagocytosed but they have no effect (2,3). Alternatively, the particle dissolves extracellularly into the cation and chromate anion [Cr(VI)] (4,5). The cation enters cells through calcium channels but has no effect (6,7). The chromate anion enters cells by facilitated diffusion using the generic anion transporter (8). Once inside, Cr(VI) is reduced to Cr(V), Cr(IV) and Cr(III) (9). The reduction also generates reactive radicals (9). Both Cr intermediates and reactive radicals damage DNA, ultimately forming DNA DSBs (10). Cells arrest in G2 phase and attempt to repair the damage (11). However, Cr(VI) suppresses HR repair (12) and activates NHEJ repair (13). This switch from an error-free to an error-prone repair pathway leads to structural CIN (14). The reduction intermediates (9) can also cause other types of damage that manifest as centrosome amplification, spindle assembly checkpoint bypass and defects in sister chromatid cohesion (15). These abnormalities contribute to numerical CIN (16). Structural and numerical CIN (14, 16) are permanent and heritable phenotypes (17) and cause neoplastic transformation (18). The growth of neoplastically transformed cells forms a tumor and leads to cancer (18).

1.7. The Centrosome

In 1902 Theodor Boveri, one of the fathers of genetics, postulated that cancer cells arose from chromosomal imbalances due to multipolar spindles (Boveri, 1902; Wunderlich, 2002). This was the first theory on the genetic origin of cancer and still prevails after 100+ years. Boveri also named an organelle that had a central position in the cell as the centrosome and proposed that abnormal duplication of centrosomes lead to the chromosomal imbalances in cancer cells (Wunderlich, 2002). A century later, we now know that centrosome abnormalities are indeed frequent in tumors and contribute to tumorigenesis (D'Assoro et al., 2002; Chan, 2011).

Centrosomes are small organelles, 1-2 um^3 in volume, that nucleate and organize microtubules. Microtubules are one of the building blocks for the cell's cytoskeleton, which regulates cell size, shape, adhesion, polarity, and migration, as well as intracellular transport. Centrosomes also nucleate the microtubules that form the mitotic spindle, and as such, play a major role in proper chromosome segregation and cytokinesis. Centrosomes also serve as signaling centers for control of cell cycle progression (Doxsey, 2001).

Structurally, each centrosome is composed of two centrioles in orthogonal position embedded in a matrix of proteins named the pericentriolar material (PCM) (Figure 1.2). Centrioles resemble open-ended cylinders which are formed by nine triplets of microtubules. The main functions of centrioles are to regulate the duplication of the centrosome and serve as a core for building the PCM (Marshall, 2007). The PCM holds γ-tubulin ring complexes which act as a base template for microtubule nucleation (Moritz et al., 1995). The two centrioles are structurally different and one centriole has appendages on its distal end while the other does not. Accordingly, centrioles are referred to as mother and daughter, respectively.

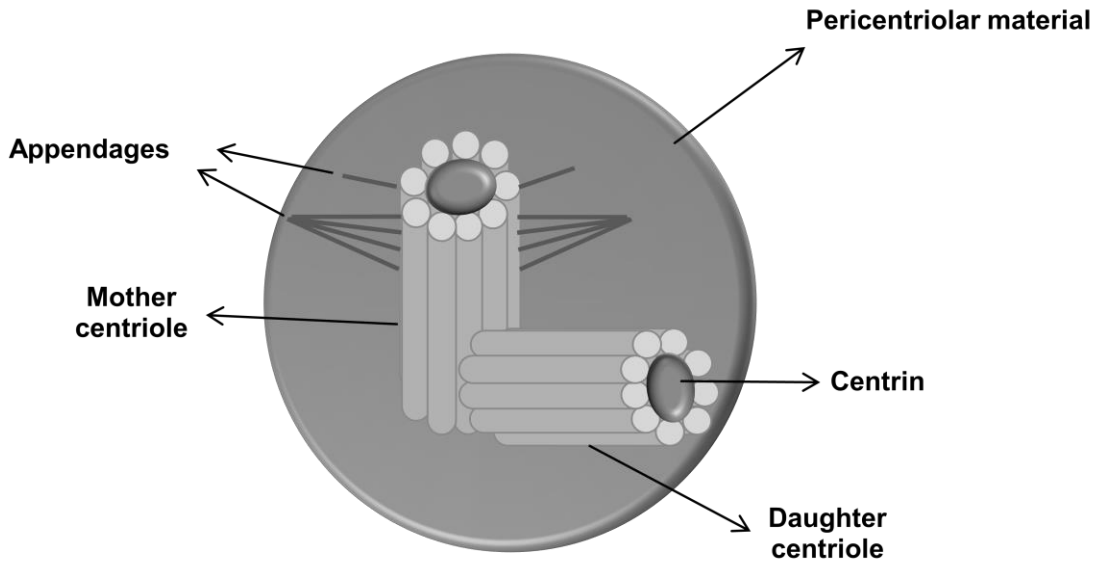

Figure 1.2. The Centrosome. This figure shows the basic composition of a centrosome. At the center, there are two centrioles arranged in an orthogonal position. Each centriole is a cylinder-like structure formed by nine triplets of microtubules. Their distal end contains the protein centrin, commonly used as a centrin marker. The "mother" centriole is distinguished by the presence of distal and sub-distal appendages. Centrioles are embedded in the pericentriolar material (PCM), a highly organized matrix of proteins.

1.7.1. Centrosome Duplication and the Centrosome Cycle

When a cell enters a new cell cycle, in G1 phase, it has one centrosome. However, this centrosome must be duplicated once, and only once, before mitosis. Centrosome duplication ensures a correct number of centrosomes for bipolar orientation of the mitotic spindle and for the future two daughter cells. To guarantee proper centrosome duplication, the centrosome cycle is tightly regulated and coordinated with overall cell cycle progression (Sluder, 2005).

The centrosome cycle (Fig 1.3) begins as cells enter G1 phase. The first step involves the separation of mother and daughter centrioles and is referred to as centriole disengagement (Tsou and Stearns, 2006a). Initially, both centrioles still share the same PCM but as G1 progresses, each centriole acquires its individual PCM. Centriole duplication begins at the G1/S phase transition, as each disengaged centriole begins to

grow a procentriole from the proximal end and in an orthogonal position (Robbins et al., 1968; Kuriyama and Borisy, 1981). Centriole duplication requires activity of Cdk2-Cyclin A/E and Plk4 (Lacey et al., 1999; Matsumoto et al., 1999; Hadenback et al., 2005). Procentrioles elongate during S and G2 phases until they reach full length (i.e.: 0.5 um). During G2, the PCM achieves greater capacity for microtubule nucleation, a process termed centrosome maturation. Up to this phase, both centrosomes remain attached to each other and serve as one microtubule organizing center (MTOC). At the G2/M transition, they are split away from each other through the action of the Nek2 kinase (Fry et al., 1998a; Faragher and Fry, 2003). The motor protein Eg5 separates both centrosomes by pushing them apart (Blangy et al, 1995). Centrosome separation begins during prophase and establishes the bipolarity of the mitotic spindle (Mardin and Schiebel, 2012). At the end of mitosis, cytokinesis yields two daughter cells, with one centrosome each.

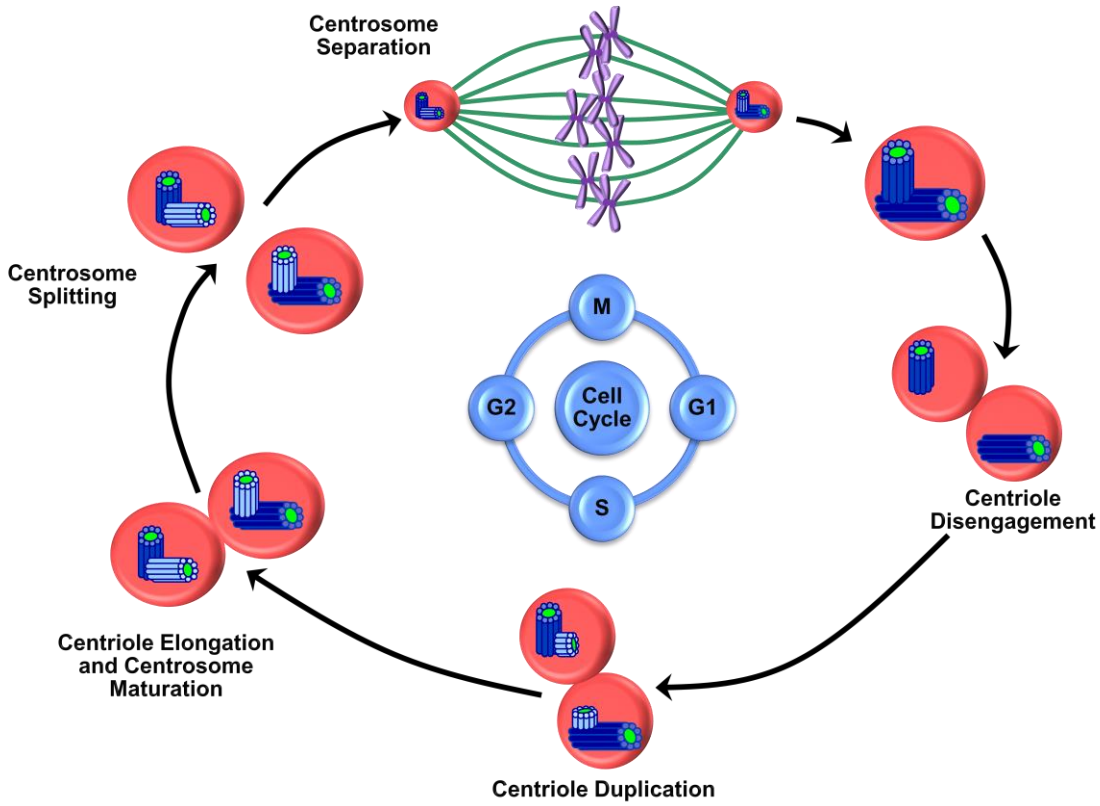

Figure 1.3. The Centrosome Cycle. This figure shows the main steps involved in the centrosome cycle. The cycle begins in G1 phase with the disengagement of mother and daughter centrioles. Each disengaged centriole duplicates a new centriole during S phase. These newly formed centrioles elongate during G2 phase. In G2, centrosomes mature and acquire greater microtubule nucleating capacity. At the G2/M transition, duplicated centrosomes split. During prophase they separate from each other and form the bipolar spindle.

1.7.2. The Centriole Linkers

An important aspect of the centrosome cycle is the formation of protein linkers between the centrioles. These linkers form and split at specific phases of the cell cycle and serve to coordinate centrosome cycle events with events at the cell cycle level. There are two centriole linkers: the S-M linker and the G1-G2 tether (Nigg and Stearns, 2011).

1.7.2.1. The S-M Linker and Regulation of Centriole Disengagement

The S-M linker is formed in S phase and splits as cells exit mitosis (M), hence its name (Nigg and Stearns, 2011). It is formed between a mother centriole and the centriole that grows perpendicular from it during S phase. The purpose of this linker is to keep mother and daughter centrioles engaged throughout the cell cycle. Centriole disengagement is only needed in G1 phase to allow for a new round of duplication.

A small set of proteins have been implicated as being part of the S-M linker (Figure 1.4). Cohesin (Nakamura et al., 2009; Schöckel et al., 2011), the same protein complex that holds sister chromatids together, was shown to localize to centrosomes (Guan et al., 2008; Nakamura et al., 2009). Moreover, depletion of Scc1, a cohesin subunit, causes premature centriole disengagement in mitosis (Nakamura et al., 2009). A small form of Shugoshin (Sgo), sSgo, also localizes to centrosomes and might function in protecting cohesin from premature cleavage (Wang et al., 2008). Cells with silenced Sgo1 show centriole disengagement in mitosis that is rescued by overexpression of sSgo1 (Wang et al., 2008). Kendrin/Pericentrin B, a component of the pericentriolar material, may also provide external support to keep the centrioles engaged (Lee and Rhee, 2012; Matsuo et al., 2012). Centriole disengagement was inhibited in cells with depleted Pericentrin B and rescued with a cleavage-resistant mutant protein. However, cells rescued with wild type protein showed centriole disengagement (Lee and Rhee, 2012).

Upstream of cohesin, sSgo and Pericentrin B, is the protease separase. Separase activity is regulated by the degradation of its inhibitor, securin (Cohen et al., 1996; Ciosk et al., 1998). Securin binding blocks the access to the active site of separase (Waizenegger et al., 2002). Upon securin degradation, separase is free to cleave substrates. Among its substrates, is the cohesin subunit Scc1 (Nakamura et al., 2009; Schöckel et al., 2011). Ectopic activation of separase causes premature centriole

disengagement, which can be prevented by expression of a non-cleavable form of Scc1 (Schöckel et al., 2011). Separase has also been shown to cleave Pericentrin B (Lee and Rhee, 2012; Matsuo et al., 2012).

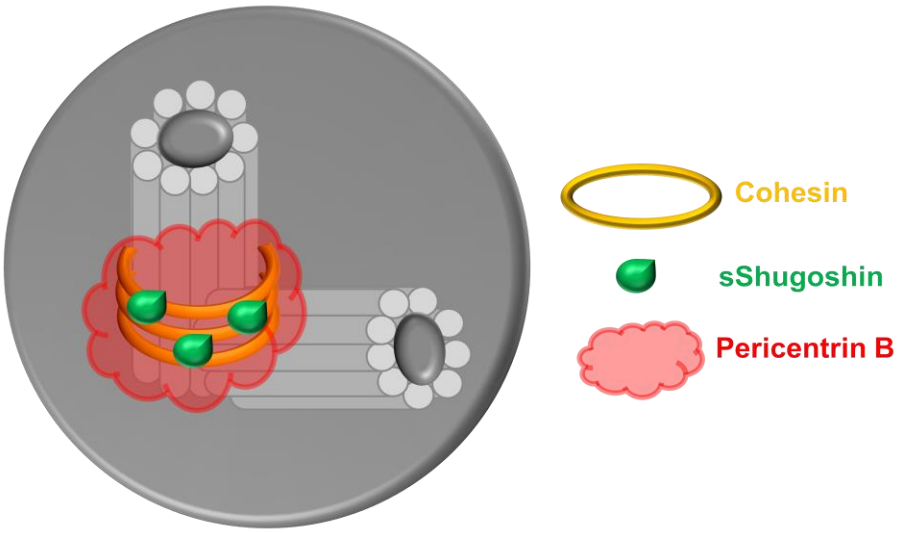

Figure 1.4. The S-M Linker. This figure shows the components of the S-M linker. Mother and daughter centrioles are immersed in the pericentrolar material and engaged to each other through cohesin rings. A small variant of Shugoshin (sSgo) protects cohesin from degradation. Pericentrin B, a PCM protein, wraps around the mother centriole providing further support and engagement.

1.7.2.2. The G1-G2 Tether and Centrosome Separation

As mentioned earlier, at the beginning of G1 phase the S-M linker splits and mother and daughter centrioles disengage. However, they become reconnected through a new linker. This linker is named G1-G2 tether, as it forms in G1 phase and remains present until G2 phase (Nigg and Stearns, 2011). Given that the disengaged mother and daughter centrioles will each form a new centrosome, the G1-G2 tether serves the purpose to keep these two centrosomes together until mitosis. Even though the cell has two centrosomes, because they are connected, they will behave as one microtubule organizing center (Nigg and Stearns, 2011).

The G1-G2 tether is established between the proximal ends of centrioles and it involves the proteins C-Nap1, Rootletin, Cep135, Cep68, LRRC35 and Centlein, (Fry et al., 1998b; Bahe et al., 2005; Graser et al., 2007; Kim et al., 2008; He et al., 2013; Hardy et al., 2014; Fang et al., 2014) (Figure 1.5). C-Nap1 is a coiled-coiled protein that localizes to the free proximal end of centrioles (Fry et al., 1998b). This interaction appears to be mediated through Cep135, which also localizes to the free proximal end of centrioles (Kim et al., 2008; Hardy et al., 2014). C-Nap1 serves as a docking site for Rootletin, LRRC35 and Cep68 which form a fiber-like structure that holds the centrosomes together (Bahe et al., 2005; Graser et al., 2007; He et al., 2013). C-Nap1 interacts directly with Rootletin fibers (Yang et al., 2006). Interaction of C-Nap1 and Cep68 is indirect and mediated through a protein named Centlein (Fang et al., 2014).

The G1-G2 tether is split at the G2/M transition (Fry et al., 1998a; Faragher and Fry 2003). The kinase NIMA-related kinase 2 (Nek2) phosphorylates C-Nap1, Rootletin, LRRC45 proteins causing them to dissociate from centrosomes (Mayor et al., 2002; Bahe et al., 2005; Mardin et al., 2010; He et al., 2013). Nek2 activation is due to autophosphorylation (Fry et al., 1995; Helps et al., 2000) but its ability to remain active depends on multiple proteins. Nek2 is in a complex with protein phosphatase 1 (PP1) and mammalian sterile 20-like kinase (Mst2) (Helps et al., 2000; Mardin et al, 2011). PP1 dephosphorylates Nek2, as well as Nek2 substrates such as C-Nap1 (Helps et al., 2000). However, phosphorylation of Mst2 by Polo like kinase 1 (Plk1) prevents binding of PP1 to the Nek2-Mst2 complex (Mardin et al., 2011). Under this scenario, the complex is released from its inhibitory partner allowing Nek2 to remain active and phosphorylate the linker components. Once the G1-G2 tether is split at the G2/M transition, centrosomes are free to separate in prophase (Mardin et al., 2011). Centrosome separation is an active process and requires the activity of the motor protein Eg5 (Blangy et al., 1995).

Centrosome separation positions centrosomes in opposite poles of the cell and allows for proper bipolar spindle formation (Tanembaum and Medema, 2010).

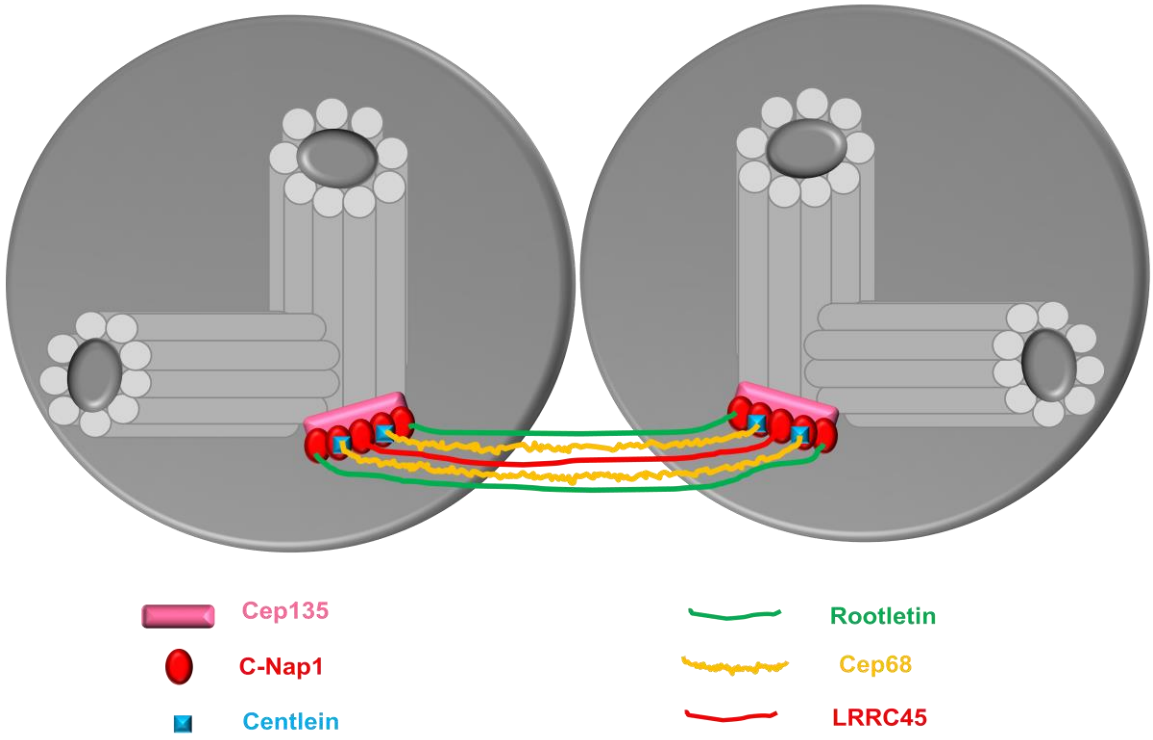

Figure 1.5. The G1-G2 Tether. This figure shows the proteins that form the G1-G2 tether. Cep135 localizes to the proximal end of centrioles C-Nap 1 interacts with Cep135 and serves as a docking site for the formation of fibers made by Rootletin, Cep68 and LRRC45. C-Nap1 interacts directly with Rootletin and possibly LRRC45. However, the interaction with Cep68 is indirect through Centlein.

1.7.2.3. Importance of the Centriole Linkers

The two different linkers formed between centrioles serve to coordinate centrosome cycle events with cell cycle events (Nigg and Stearns, 2011; Mardin and Schiebel, 2012). The S-M linker keeps mother and daughter centrioles together until the next cell cycle when centrioles are required to disengage in order to be duplicated. The G1-G2 tether retains newly duplicated centrosomes close to each other until their separation is needed during prophase. Multiple studies have shown that untimely disruption of the centriole linkers can lead to deleterious phenotypes. Premature

centriole disengagement has been extensively linked to centrosome amplification (Maiato and Logarinho, 2014). Delayed centrosome separation causes an increase in the time spent in mitosis which leads to chromosome segregation errors due to improper attachments between kinetochores and microtubules (Indjeian and Murray, 2007; Kaseda et al, 2012; Mchedlishvilli et al., 2012; Silkworth et al., 2012). In contrast, premature centrosome separation has been shown to enhance proliferation and survival which in a normal cell might not be problematic, but in a genetically unstable cell could contribute to tumor growth (Mardin et al., 2013). These studies shed some light on the potential roles of the centriole linkers as well as emphasize the importance of proper timing of centriole disengagegent and centrosome separation.

1.7.3. Role of Centrosomes in Carcinogenesis

It is very important that cells duplicate their centrosome once and only once during the cell cycle. Proper regulation and timing of the centrosome cycle is key in maintaining a normal number of centrosomes (Doxsey, 2002). Abnormalities in the centrosome cycle can lead to centrosome amplification (CA), a phenotype where cells acquire greater than two centrosomes. Extra centrosomes are a problem because they form multipolar spindles or bipolar spindles with multiple centrosomes at each pole, causing improper attachment of microtubules to the kinetochores and unequal segregation of DNA (Doxsey 2002; Sluder and Nordberg 2004). This can result in chromosome instability, a major driving force for tumorigenesis (D'Assoro et al, 2002; Fukasawa, 2005, Pihan et al, 2003).

Centrosome amplification is commonly found in human tumors and tumor-derived cell lines (Pihan et al., 1998; Chan, 2011). Abnormalities in size, shape and position are also frequent (Pihan et al., 1998; Chan, 2011). Centrosome amplification and other centrosomal defects are also present in pre-invasive carcinomas suggesting that centrosome abnormalities are an early event in tumorigenesis (Pihan et al., 2003).

In addition, centrosome defects are increased in higher degree *in situ* carcinomas suggesting that these defects play a role in the progression of pre-cancerous lesions (Pihan et al., 2001; Pihan et al., 2003).

Lung tumors also exhibit centrosome amplification. Pihan et al. (1998) analyzed a series of malignant tumors from different tissues, including lung. All tumor cells from the lung tumor had centrosome amplification while none was observed in non-tumor cells (Pihan et al., 1998). In non-small cell lung cancers (NSCLC), Jung et al. (2007) also observed abnormalities in number, size and shape of centrosomes in 29% of the tumors analyzed. In addition, 93% of the tumors with centrosome abnormalities were aneuploid, supporting the idea that centrosome defects cause numerical CIN (Jung et al., 2007). Interestingly, cells surrounding the lung tumor also showed early signs of centrosome abnormalities. Koutsami et al. (2006) also analyzed NSCLC tissues. They observed centrosome amplification and structural defects of centrosomes in 53% of the samples. A positive correlation with aneuploidy was also established. Similar to the Jung et al. (2007) study, centrosome amplification and defects were present in adjacent hyperplastic regions as well. These studies suggest that centrosome abnormalities are common and early events in lung carcinogenesis. Their prevalence and early appearance likely contribute to the widespread CIN observed in lung tumors and lung tumor-derived cell lines (Balsara et al., 1992; Haruki et al., 2001, Masuda and Takahashi, 2002).

1.8. Metal-Induced Centrosome Amplification

Centrosome amplification and associated defects, such as spindle polarity, have been studied in different cell lines exposed to inorganic and organic forms of metals. These studies and their main findings are summarized in Table 1.1 and most have also been previously reviewed by Holmes and Wise (2010). The majority of the studies on

metals and centrosomes have focused on arsenic. Both inorganic arsenic as well as organic species, such as dimethylarsinic acid, induce centrosome amplification and aneuploidy (Debec et al., 1990; Ochi, 2000; 2002a; Ochi et al., 1999a; 1999b; 2003; 2004; 2008; Yih et al., 2006; 2012; Liao et al., 2007; 2010; Wu et al., 2013). It appears that arsenic-induced centrosome amplification happens in cells during a prolonged mitotic arrest due to activation of the spindle checkpoint and involves fragmentation of the PCM, as centrosomes lack centrioles (Yih et al., 2006). Inorganic lead and mercury do not cause centrosome amplification but inorganic cadmium induces abnormal mitosis with scattered chromosomes (Debec et al., 1990; Ochi, 2002b; Holmes et al., 2006b). Interestingly, organic mercury, in the form of methylmercuric chloride, causes centrosome amplification and multipolar spindles but the mechanism is unknown (Ochi, 2002b). Metals in nanoparticle forms have also been considered. Titanium dioxide nanoparticles cause centrosome amplification in NIH/3T3 cells (Huang et al., 2009). The increase in the number of bi- and multinucleated cells suggests that failure of cytokinesis might be the underlying mechanism. Organic and inorganic forms of vanadium did not cause centrosome amplification but instead induced the formation of monopolar spindles which pinpoints to a lack of centrosome separation during mitosis (Navara et al., 2001). In summary, these studies emphasize that centrosome amplification is a common phenotype after exposure to metals. They also highlight differences in mechanisms, which is not surprising giving that these metals cause toxicity through very different mechanisms.

Table 1.1. Summary of Studies on Metal-Induced Centrosomal Defects.

Treatment	Co-Treatment	Assay	Cell Type	Summary of Effects	Reference
Arsenite 75 uM 0-42 h		Immunofluorescence for centrosomes and microtubules	Kc23 Drosophila embryonic cell line	Acentrosomal cells, disruption of microtubules (less quantity).	Debec et al., 1990
Arsenite 5-10 um 20-24 h		Acridine orange stain and immunofluorescence for microtubules	V79 chinese hamster lung fibroblasts	No effect on multinucleated cells or microtubule network.	Ochi et al., 1999a
Sodium arsenite 3-10 uM 48 h		Flow cytometry	Syrian hamster embryo cells	Hypo and hyperdiploidy.	Ochi et al., 2004
Sodium arsenite 2 uM 3-24 h		Immunofluorescence for centrosomes, microtubules, dynein and NuMA	CGL-2	Centrosome amplification in mitotic cells, acentriolar centrosomes or with abnormal number of centrioles, decreased dynein localization, increased NuMA expression.	Yih et al., 2006
Sodium arsenite 2 uM 1-16 h		Western blot for dynein and NuMA	CGL-2	Increased NuMA protein levels, no changes in dynein.	Yih et al. 2006
Sodium arsenite 2 uM 1-16 h		siRNA for BubR1 and Mad2	CGL-2	Spindle checkpoint is crucial for centrosome amplification, mitotic arrest leads to CA.	Yih et al. 2006
Sodium arsenite 1-10 uM 48 h	Pifithrin-alpha (p53 inhibitor) 20 uM	Immunofluorescence for centrosomes	BEAS-2B	Centrosome amplification in p53 compromised cells, cells grew in soft agar.	Liao et al., 2007

Table 1.1. Continued.

Treatment	Co-Treatment	Assay	Cell Type	Summary of Effects	Reference
Sodium arsenite 1-5 uM 48 h	NNK 1-5 uM	Immunofluorescence for microtubules	BEAS-2B	Centrosome amplification when cells are co-treated with As and NNK in a p53 compromised status (not seen if As or NNK are alone).	Liao et al., 2010
Sodium arsenite 1 uM 1-4 weeks		Immunofluorescence for microtubules and Aurora A	HaCaT	Multinucleated cells, aberrant chromosome segregation, multiple centrosomes, aberrant distribution of Aurora A.	Wu et al., 2013
Arsenic trioxide 3uM 40 h		Time lapse microscopy	EYP-tubulin HeLa	Disruption of the proper positioning of the spindle and induces centrosome and spindle abnormalities, in the form of multipolar spindles. These cells arrest at mitosis and undergo apoptosis.	Yih et al., 2012
Arsenic trioxide 1 uM 20-24 h	Y-27632 5-10 uM (ROCK inhibitor)	Immunofluorescence for microtubules	CGL-2	Spindle mis-positioning, ROCK inhibition reduces spindle abnormalities, arsenic may induce defects in mitotic spindles PIP4KIIγ-mediated activation of the Rho/ROCK pathway.	Yih et al., 2012
Dimethylarsinic acid 1-10 mM 6-12 h		Immunofluorescence for centrosomes and microtubules	V79 chinese hamster lung fibroblasts	Centrosome amplification and multipolar spindles, loss of microtubule network.	Ochi et al., 1999a

Table 1.1. Continued.

Treatment	Co-Treatment	Assay	Cell Type	Summary of Effects	Reference
Dimethylarsinic acid 2 mM 24 h		Videograph analysis	V79 chinese hamster lung fibroblasts	Cells become multinucleated without dividing into two daughter cells.	Ochi et al., 1999b
Dimethylarsinic acid 2 mM 24 h		Acridine orange stain	V79 chinese hamster lung fibroblasts	Multinucleated cells.	Ochi et al., 1999b
Dimethylarsinic acid 2-10 mM 6-20 h		Immunofluorescence for microtubules	V79 chinese hamster lung fibroblasts	Disappearance of microtubule network in interphase cells and aberrant mitotic spindles.	Ochi et al., 1999b
Dimethylarsinic acid 5-10 mM 6 h	1 um Nocodazole or 2 um Cyto-chalasin B	Immunofluorescence for centrosomes and microtubules	V79 chinese hamster lung fibroblasts	Multipolar spindles in mitotic cells, microtubule network required to induce centrosome amplification.	Ochi, 2000
Dimethylarsinic acid 8mM 6 h	0.5 mM Ortho-vanadate	Immunofluorescence for centrosomes and dynein	V79 chinese hamster lung fibroblasts	Multiple centrosomes, dynein not involved.	Ochi, 2002a
Dimethylarsinic acid 8mM 6 h	200 uM Monastrol	Immunofluorescence for centrosomes and microtubules	V79 chinese hamster lung fibroblasts	Kinesin might play a role in the induction of multiple centrosomes.	Ochi, 2002a

Table 1.1. Continued.

Treatment	Co-Treatment	Assay	Cell Type	Summary of Effects	Reference
Dimethylarsinic acid 0.1-2 mM 10-24 h		Immunofluorescence for centrosomes and microtubules	V79 chinese hamster lung fibroblasts	Centrosome amplification and multipolar division in telophase.	Ochi et al., 2003
Dimethylarsine iodide 0.125-0.5 mM 3-32 h		Immunofluorescence for centrosomes and microtubules, Giemsa staining and acridine orange staining	V79 chinese hamster lung fibroblasts	Centrosome amplification, multipolar mitosis, aneuploidy, multinucleate cells, disruption of microtubule network.	Ochi et al., 2003
Dimethylarsine iodide 0.25-1 uM 2-48 h	30 uM Nocodazole	Immunofluorescence for centrosomes and microtubules, flow cytometry	Syrian hamster embryo cells	Multipolar spindles, inhibition of microtubule re-growth, hypo and hyperdiploidy.	Ochi et al., 2004
Thio-dimethylarsenite 0.01-0.2 mM 48 h	1 mM BSO	Immunofluorescence for centrosomes, microtubules	HepG2	Centrosome amplification which may require GSH.	Ochi et al., 2008
Cadmium chloride 10-100 uM 0-24 h		Immunofluorescence for centrosomes and microtubules	Kc23 Drosophila embryonic cell line	Abnormal mitosis with scattered chromosomes.	Debec et al., 1990
Lead chromate 0.1-1 ug/cm^2 24-120h		Immunofluorescence for centrosomes, microtubules	WTHBF-6 human lung fibroblasts	Centrosome amplification caused by chromium, not lead.	Holmes et al., 2006b

Table 1.1. Continued.

Treatment	Co-Treatment	Assay	Cell Type	Summary of Effects	Reference
Lead chromate 1-10 ug/cm^2 120 h		Immunofluorescence for centrosomes, microtubules	BEP2D (foci derived cell lines)	3/10 foci had centrosome amplification in interphase cells; 7/10 foci had centrosome amplification in mitotic cells.	Xie et al., 2007
Zinc chromate 0.1-0.2 ug/cm^2 24-120 h		Immunofluorescence for centrosomes, centrioles and microtubules	WTHBF-6 human lung fibroblasts	Centrosome amplification in interphase and mitotic cells, caused by multiple mechanisms: multiple rounds of centrosome duplication, centriole splitting and acentriolar centrosome formation.	Holmes et al., 2010
Lead oxide 0.1-10 ug/cm^2 24-120 h		Immunofluorescence for centrosomes, microtubules	WTHBF-6 human lung fibroblasts	No centrosome amplification.	Holmes et al., 2006b
Mercuric chloride 0.5-10 uM 6-24 h		Immunofluorescence for centrosomes and microtubules	V79 chinese hamster lung fibroblasts	No effects on centrosome number or spindles.	Ochi, 2002b
Methylmercuric chloride 0.05-2.5 uM 6-30 h		Immunofluorescence for centrosomes and microtubules	V79 chinese hamster lung fibroblasts	Multinucleated cells and centrosome amplification with multipolar spindles.	Ochi, 2002b
Titanium dioxide nanoparticles 10 ug/ml 12 weeks	Nocodazole	Immunofluorescence for microtubules and Plk1	NIH/3T3	Centrosome amplification, bi- and multinucleated cells and aneuploidy, failure of cytokinesis due to misregulation of Plk1 might be a mechanism.	Huang et al., 2009

Table 1.1. Continued.

Treatment	Co-Treatment	Assay	Cell Type	Summary of Effects	Reference
Vanadocene acetylacetonate 0.3 uM 24 h		Immunofluorescence for centrosomes and microtubules	BT-20 breast cancer cell line	Monopolar spindles (did not count how many centrosomes).	Navara et al., 2001
Vanadocene dichloride 25 uM 24 h		Immunofluorescence for centrosomes and microtubules	BT-20 breast cancer cell line	Monopolar spindles formed by two centrosomes.	Navara et al., 2001

1.8.1. Cr(VI)-Induced Centrosome Amplification

An increase in the number of cells with extra centrosomes (i.e.: centrosome amplification) is observed after prolonged exposure (i.e.: 48-120 h) to particulate Cr(VI) compounds (Holmes et al., 2006b; Holmes et al., 2010). Centrosome amplification is present in both interphase and mitotic cells and is characterized by acentriolar centrosomes and cells with supernumerary centrioles (Holmes et al., 2010). The presence of different centrosome phenotypes suggests that multiple mechanisms underlie Cr(VI)-induced centrosome amplification. Lung epithelial cells neoplastically transformed by lead chromate also exhibit centrosome amplification (Xie et al., 2007). Moreover, centrosome amplification is also present in lung tumors from chromate workers that died of lung cancer (Holmes, 2011).

1.9. Summary

Cr(VI) is potent human lung carcinogen that most likely causes cancer through a genetic instability mechanism. Cr(VI) particles enter the lungs through inhalation and deposit at bifurcation sites where they persist. They slowly dissolve over time and as they do the chromate anions readily enter surrounding cells through generic anion transporters. Once inside the cells, Cr(VI) is reduced to Cr(III). Reduction forms Cr(V), Cr(IV) and reactive oxygen and carbon species. Reduction intermediates as well as Cr(III) are capable of reacting with DNA causing complex lesions such as adducts, crosslinks and DNA double strand breaks. These lesions lead to structural chromosome instability.

Cr(VI) also induces numerical chromosomal instability but the underlying mechanism is not known. Centrosomes have long been implicated in maintaining proper chromosome numbers due to their involvement in mitotic spindle formation and positioning. As a result, centrosome duplication is tightly regulated to ensure that the cell

only has two centrosomes at mitosis. Errors in centrosome duplication can lead to centrosome amplification (i.e.: extra centrosomes), causing chromosome missegregation which contributes to numerical chromosome instability. Centrosome amplification is very common in solid tumors, including those of the lung, and is considered a major driving force for tumorigenesis.

Centrosome amplification has also been observed in human lung cells exposed to Cr(VI). Cr(VI)-induced centrosome amplification appears to be complex, as it has been shown that multiple mechanisms might be involved in its formation. However, the centrosomal proteins and pathways affected by Cr(VI) remain elusive. Given that the centriole linkers are crucial for proper timing of centrosome cycle events and centrosome duplication, this project investigates Cr(VI) effects on the S-M linker and the G1-tether. Our hypothesis is that exposure to Cr(VI) causes premature splitting of the S-M linker and G1-G2 tether causing centrosome amplification.

CHAPTER 2

MATERIALS AND METHODS

2.1. Materials

2.1.1. Cell Culture

Dulbecco's Minimal Essential Medium and Ham's F-12 (DMEM/F-12) 50:50 mixture, Dulbecco's Phosphate Buffered Saline 1x (PBS), penicillin/streptomycin and glutaGRO were purchased from Mediatech, Inc. (Manassas, VA). Cosmic calf serum was purchased from HyClone (Logan, UT). 0.25% Trypsin/EDTA was purchased from Gibco (Grand Island, NY). Sodium pyruvate was purchased from Lonza (Walkersville, MD). Tissue culture dishes, flasks, and plasticware were purchased from BD (Franklin Lakes, NJ). MycoAlert mycoplasma detection kits were purchased from Lonza Rockland, Inc. (Rockland, ME). CO_2 tanks were purchased from Airgas (Salem, NH) and Matheson (South Portland, ME). Cloning cylinders were purchased from Scienceware (Wayne, NJ).

2.1.2. Particulate Cr(VI) Compounds

Zinc chromate ($ZnCrO_4$, CAS # 13530-65-9) was purchased from Sigma Aldrich (St. Louis, MO) and Pfaltz & Bauer, Inc. (Waterbury, CT). Lead chromate ($PbCrO_4$, CAS # 7758-97-6) was purchased from Sigma Aldrich (St. Louis, MO).

2.1.3. Numerical Chromosome Instability Assay

Demecolcine was purchased from Sigma Aldrich (St. Louis, MO). KCl and acetic acid were purchased from J.T. Baker (Phillipsburg, NJ). Methanol was purchased from BDH (Radnor, PA). Gurr's buffer was purchased from LifeTechnologies (Carslbad, CA). Giemsa stain was purchased from Ricca Chemical Co. (Arlington, TX). Richard Allan Scientific Super Up-Rite microscope slides and Cytoseal 60 slide mounting medium

were purchased from Thermo Scientific (Waltham, MA). Coverslips were purchased from VWR (Radnor, PA).

2.1.4. Immunocytochemistry

Lab Tek II glass chamber slides were purchased from Thermo Scientific (Waltham, MA). FNC coating mix was purchased from AthenaES (Baltimore, MD). Coverslips were purchased from VWR (Radnor, PA). Methanol was purchased from BDH (Radnor, PA). Acetone, $MgSO_4$, and KCl were purchased from J.T. Baker (Phillipsburg, NJ). 4% paraformaldehyde in PBS was purchased from Alfa Aesar (Ward Hill, MA). 10x PBS was purchased from Mediatech, Inc. (Manassas, VA). Goat serum was purchased from Life Technologies (Carslbad, CA). Glycerol, fish skin gelatin, Triton X-100, EDTA, PIPES and sodium azide were purchased from Sigma Aldrich (St. Louis, MO). BSA was purchased from EMD Millipore (Billerica, MA). ProLong Gold Antifade Reagent with DAPI and Alexa Fluor secondary antibodies were purchased Life Technologies (Carlsbad, CA). DyLight secondary antibodies were purchased from Jackson ImmunoResearch (West Grove, PA)

2.1.5. Western Blots

Glycine, NaCl, BSA, DTT and PMSF were purchased from EMD Millipore (Billerica, MA). Tris base was purchased from Amresco (Solon, OH). SDS and KCl were purchased from J.T. Baker (Phillipsburg, NJ). HCl was purchased from VWR (Radnor, PA). 30% acrylamide/BIS solution, ammonium persulfate, Tween-20, Quick Start BSA Standard, Quick Start Bradford Reagent, 0.45 um nitrocellulose membranes, 0.2 um ImmunBlot PVDF membranes, and HRP-conjugated goat anti-mouse and anti-rabbit IgG antibodies were purchased from BioRad (Hercules, CA). HEPES solution was purchased from American Bioanalytical (Natick, MA). EDTA, $MgCl_2$, $MnCl_2$, TEMED, 2-mercaptoethanol, and IGEPAL CA-630 were purchased from Sigma Aldrich (St. Louis, MO). PhosSTOP and cOmplete ULTRA phosphatase and protease inhibitor cocktail

tablets were purchased from Roche (Indianapolis, Indiana). Isopropyl alcohol was purchased from Avantor Performance Materials (Center Valley, PA). Odyssey blocking buffer was purchased from Li-Cor (Lincoln, NE). IRDye800 goat anti-mouse antibody was purchased from Rockland Inc. (Boyertown, PA). Alexa Fluor 680 goat anti-rabbit antibody and Tris-Glycine SDS 2x sample buffer were purchased from Life Technologies (Carlsbad, CA). RIPA Lysis Buffer System was purchased from Santa Cruz Biotechnology (Dallas, TX). Pierce ECL2 Western Blotting Substrate, PageRuler Plus Prestained Protein Ladder and PageRuler Prestained NIR Protein Ladder were purchased from Thermo Scientific (Waltham, MA).

2.2. Cells and Cell Culture

The majority of Cr(VI)-induced lung tumors are classified as squamous cell carcinomas (Ishikawa, 1994b), hence they are of epithelial origin. However, epithelial cells are difficult to culture and passage for extended periods of time. Fibroblasts are key components of the stroma underlying the epithelia (Kalluri and Zeisberg, 2006). They are associated with epithelial cells throughout all stages of the carcinogenic process and contribute to it by producing oncogenic signals, facilitating angiogenesis and potentially playing a role in metastasis (Kalluri and Zeisberg, 2006). Moreover, for Cr(VI)-induced lung tumors, Kondo et al. (2003) have shown that Cr(VI) accumulates in the bronchial stroma and not the epithelium. Hence, we used a fibroblast cell line, WTHBF-6 for all of our experiments. WTHBF-6 is an immortalized clonal cell line derived from primary human bronchial fibroblasts (PHBF) (Wise et al., 2004b). These cells have a stable and normal karyotype, normal growth parameters and respond similarly to Cr(VI) as the primary human cells that they are derived from. WTHBF-6 cells were maintained as adherent sub-confluent monolayers in DMEM/F-12 supplemented with 15% cosmic calf serum, 0.2 mM L-alanyl-L-glutamine, 0.1 mM sodium pyruvate, 100 IU/ml penicillin and

100 ug/ml streptomycin. Cells were fed three times a week, split at least once a week, and tested for mycoplasma contamination once a month. All cells and experiments were maintained in a 37°C, humidified incubator with 5% CO_2.

2.3. Zinc and Lead Chromate Preparation

Zinc and lead chromate were prepared according to our published methods (Wise et al., 2002). Briefly, zinc and lead chromate powders were washed twice in distilled water followed by two washes with acetone to remove soluble and organic impurities, respectively, and left to dry. The night before treatment, 0.042 g of either zinc or lead chromate were suspended in 10 ml of cold, filter-sterilized water. The suspension was stirred overnight at 4°C with a magnetic stir bar to break up large particles. The following day dilutions were made as needed. A vortex mixer was used to maintain particles in suspension while making dilutions.

2.4. Cell Treatments

Zinc and lead chromate were administered as a suspension of particles in cold sterile water according to our published methods (Wise et al., 2002). Logarithmically growing cells were seeded and allowed to rest for 48 hours. The media was changed and cells were treated for 24, 72 and 120 hours with a concentration range of 0.1, 0.15 and 0.2 ug/cm^2 of zinc chromate and 0.5 ug/cm^2 of lead chromate. A vortex mixer was used to maintain particles in suspension during treatments. Concentrations are expressed in ug/cm^2 to reflect treatment with a particulate compound and to account for undissolved particles. At the end of treatment time, cells were harvested as specified for each experiment type.

2.5. Clonal Expansion Assay

Our laboratory has also developed clonal cell lines that survived Cr(VI) exposure. These clones were treated with lead chromate for 24 h three times separated by one month intervals (Wise, 2013). Cells were seeded in 6-well plates, allowed to rest for 48 h and treated with 5 ug/cm^2 lead chromate for 24 h. At the end of treatment, cells were harvested and re-seeded at colony forming density (i.e.: 1000 cells per 100 mm dish). Once colonies formed (~2 weeks), they were ring-cloned and expanded into cell lines. These cell lines were treated for 24 h and cloned again. The resulting cell lines underwent treatment and cloning process one more time. A set of untreated cells were also expanded and cloned. Control and treated clonal cell lines were analyzed for centrosome amplification. These cell lines have also been karytyoped and characterized for their ability to growth in soft agar and their DNA repair efficiency (Wise, 2013). We used these clonal cell lines to assess the persistence of the centrosome amplification phenotype.

2.6. Numerical Chromosome Instability Assay

Numerical chromosome instability (CIN) was analyzed by staining metaphases and counting the number of chromosomes in 100 metaphases, as described in Holmes et al. (2006a). Briefly, cells seeded in 100 mm dishes were treated with 0, 0.1, 0.15 and 0.2 ug/cm^2 zinc chromate for 24, 72 and 120 h. An hour before the end of treatment, demecolcine, a microtubule depolymerizing agent, was added to arrest the cells in metaphase. At harvest, media was collected and cells were washed with PBS, trypsinized and spun down for 5 min at 1000 RPM in a 4°C centrifuge. The pellet was resuspended and incubated for 17 min in a 0.075 KCl hypotonic solution to swell cells. One ml of 3:1 methanol: acetic acid fix was added and cells were spun down. The pellet was resuspended in fix and incubated for 20 min at room temperature. The fix was

changed two more times and cells were dropped onto wet slides. Slides were dried overnight and stained for 5 minutes with 5% Giemsa stain. Dry slides were coverslipped using Cytoseal 60. Metaphases were observed under a 100x objective with an Olympus light microscope. At least three independent experiments were performed. Cells that deviated from the normal diploid number (i.e.: 2N=46 chromosomes) were classified as having numerical CIN.

2.7. Immunocytochemistry

2.7.1. Centrosome Amplification Analysis

To quantify the number of centrosomes in zinc chromate-treated cells, cells were treated and stained for γ-tubulin, a marker for the pericentriolar material, and α-tubulin, a component of microtubules, as described by Holmes et al. (2006b). Cells were seeded on 1-well glass chamber slides coated with FNC coating mix and treated with 0, 0.1, 0.15 and 0.2 ug/cm^2 zinc chromate for 24, 72 and 120 h. At harvest, cells were washed with a microtubule stabilizing buffer (3 mM EGTA, 50 mM PIPES, 1mM $MgSO_4$, 25 mM KCl), fixed with -20°C methanol for 10 minutes, air dried for 5 min, permeabilized with 0.05% Triton X-100 for 3 minutes and blocked for 30 minutes in centrosome blocking buffer (5% goat serum, 1% glycerol, 0.1% BSA, 0.1% fish skin gelatin and 0.04% sodium azide in 1x PBS). After blocking, cells were incubated for 1 h at room temperature with anti-γ-tubulin antibody (T6557, Sigma-Aldrich, St. Louis, MO), washed with PBS and incubated in the dark for 1 h at room temperature with Alexa Fluor 555 secondary antibody. This was followed by washing and incubation in the dark for 1 h at room temperature with anti-α-tubulin-FITC conjugated antibody (F2168, Sigma-Aldrich, St. Louis, MO). Cells were washed, left to dry and coverslips were mounted with DAPI. Centrosome numbers in 100 mitotic cells and 1000 interphase cells per

concentration/time point were analyzed under a 100x objective using an Olympus BX51 fluorescence microscope. Three independent experiments were performed.

2.7.2. Centrin Analysis

Multiple mechanisms can cause centrosome amplification (Fukasawa, 2005). These give rise to different phenotypes that can be visualized by staining centrioles with centrin, a protein found in the distal centriole lumen (Paoletti et al., 1996). Zinc chromate-treated cells were stained with centrin and γ-tubulin as described by Holmes et al. (2010). Cells were seeded on 1-well glass chamber slides coated with FNC coating mix and treated with 0 and 0.2 ug/cm^2 zinc chromate for 24, 72 and 120 h. At harvest, cells were washed with a microtubule stabilizing buffer, fixed with -20°C methanol for 10 minutes, air dried for 5 min, permeabilized with 0.05% Triton X-100 for 3 minutes and blocked for 30 minutes in centrosome blocking buffer. After blocking, cells were incubated for 1 h at room temperature with anti-γ-tubulin (T6557, Sigma-Aldrich, St. Louis, MO) and anti-centrin (gift from Dr. Jeffrey Salisbury, Mayo Clinic, Rochester, MN) antibodies, washed with 0.05% Triton X-100 and incubated in the dark for 1 h at room temperature with isotype-specific DyLight 488 and 549 secondary antibodies. Cells were washed, air-dried and coverslips were mounted with DAPI. Centrosome and centriole numbers in 50 mitotic cells and 200 interphase cells per concentration/time point were analyzed under a 100x objective using an Olympus BX51 fluorescent microscope. Centrosome and centriole numbers were used to assess the presence of supernumerary centrioles as well as quantify evidence for centriole disengagement. Three independent experiments were performed.

2.7.3. Centriole Disengagement Analysis

To confirm abnormal centriole disengagement in zinc chromate-treated cells, we used the ratio of centrin to C-Nap1 foci (Tsou and Stearns, 2006b). C-Nap1 is a protein present at the free, proximal end of centrioles. Engaged centrioles have a ratio of 2:1 of

centrin:C-Nap1, while disengaged centrioles exhibit a ratio of 1:1 (Tsou and Stearns, 2006b). Cells seeded on 4 well glass chamber slides coated with FNC coating mix were treated with 0, 0.1, 0.15 and 0.2 ug/cm^2 zinc chromate for 24, 72 and 120 h. After treatment, cells were washed with PBS and fixed with -20°C methanol and acetone for 10 and 1 min, respectively. Cells were re-hydrated with PBS and incubated with anti-centrin antibody (#04-1624, Millipore, Billerica, MA) overnight at 4°C. The following morning cells were washed with PBS and incubated with anti-C-Nap1 antibody (14498-1-AP, Proteintech, Chicago, IL) for 1 h at room temperature, followed by washing and incubation for 1 h at room temperature with anti-γ-tubulin antibody (T6557, Sigma-Aldrich, St. Louis, MO). Cells were washed and incubated in the dark with isotype-specific DyLight 488, Alexa Fluor 555 and Alexa Fluor 633 secondary antibodies. After washing and air-drying cells, coverslips were mounted with DAPI. A total of 100 interphase and 50 mitotic cells with a normal centrin number (2 centrin foci for G1 cells and 4 centrin foci for S/G2/mitotic cells) were analyzed per concentration/time point using a 100x objective and a BX51 Olympus fluorescence microscope equipped with a GenASIs Capture & Analysis System (Applied Spectral Imaging, Inc., Carlsbad, CA). Since Alexa 633 dyes are not visible to the human eye, we used the GenASIs camera and software to visualize the γ-tubulin signal on a computer screen. Three independent experiments were performed.

For the previous experiment, the assumption was made that all interphase cells with 4 centrioles were in S or G2 phase. To further confirm this data we measured centriole disengagement in zinc chromate-treated cells stained with cyclin D1. Cyclin D1 is expressed at high levels in G1 cells, where it localizes to the nucleus (Baldin et al., 1993). Thus, cyclin D1 nuclear staining is commonly used as a G1 phase marker. Cells were seeded on 2 well glass slides coated with FNC coating mix and treated with 0 and 0.2 ug/cm^2 zinc chromate for 24, 72 and 120 h. Cells were harvested and fixed as

above. After rehydration with PBS, they were incubated with anti-centrin antibody (#04-1624, Millipore, Billerica, MA) overnight at 4°C. The following morning cells were washed with PBS and incubated with anti-Cyclin D1 antibody (sc-8396, Santa Cruz Biotechnology, Inc., Dallas, TX) for 1 h at room temperature, followed by washing and incubation for 1 h at room temperature with anti-C-Nap1 antibody (14498-1-AP, Proteintech, Chicago, IL). Cells were washed and incubated in the dark with isotype-specific DyLight 488, Alexa Fluor 594 and Alexa Fluor 633 secondary antibodies. After washing and letting cells dry, coverslips were mounted with DAPI. Centrin numbers were analyzed in 100 interphase cells with nuclear cyclin D1 staining per concentration/time point. Three independent experiments were performed.

2.7.4. Centrosome Separation Measurements

Duplicated centrosomes formed in S-phase are normally held together by a protein linker. This linker is severed at the G2/M transition and allows for centrosomes to separate in prophase (Mardin and Schiebel, 2012). Depletion of linker proteins by siRNA caused increased centriole disengagement when cells were exposed to a DNA damaging agent (Conroy et al., 2012). This suggests that this linker may also help in protecting centriole engagement. Since zinc chromate is a strong DNA damaging agent (Xie et al., 2009) and causes centriole disengagement, we hypothesized that exposure might also disrupt this linker. Hence, we measured centrosome separation in interphase cells under the premise that if this linker is severed, centrosomes would prematurely separate in interphase. Cells were seeded on 1 well glass chamber slides coated with FNC coating mix and treated with 0, 0.1, 0.15 and 0.2 ug/cm^2 zinc chromate for 24, 72 and 120 h. At harvest, cells were washed with a microtubule stabilizing buffer, fixed with -20°C methanol for 10 minutes, air dried for 5 min, permeabilized with 0.05% Triton X-100 for 3 minutes and blocked for 30 minutes in centrosome blocking buffer. After blocking, cells were incubated for 1 h at room temperature with anti-γ-tubulin (T6557,

Sigma-Aldrich, St. Louis, MO), washed with PBS and incubated in the dark for 1 h at room temperature with Alexa Fluor 555 secondary antibody. Cells were washed, air-dried and coverslips were mounted with DAPI. Pictures of one hundred interphase cells per concentration/time point were taken using a Nikon Eclipse Ti confocal microscope. The distance between centrosomes was measured using the Nikon NIS Elements software. Centrosomes were classified as separated when the distance between them was >2 μm (Mayor et al., 2000).Three independent experiments were performed.

2.7.5. Nek2 Localization at Centrosomes

Disruption of the centrosome linker at the G2/M transition requires centrosomal localization and activity of the kinase Nek2A (Fry et al., 1998a; Fry et al., 1998b; Faragher and Fry, 2003; Bahe et al., 2005). Accordingly, we tested the effects of zinc chromate on Nek2 localization to the centrosomes. Cells were seeded on 1 well glass chamber slides coated with FNC coating mix and treated with 0, 0.1, 0.15 and 0.2 ug/cm^2 zinc chromate for 24, 72 and 120 h. At harvest, cells were washed with a microtubule stabilizing buffer, fixed with -20°C methanol for 10 minutes, air dried for 5 min, permeabilized with 0.05% Triton X-100 for 3 minutes and blocked for 30 minutes in centrosome blocking buffer. After blocking, cells were incubated overnight at 4°C with anti-Nek2 antibody (sc-55602, Santa Cruz Biotechnology Inc., Dallas, TX). The following day cell were washed with PBS and incubated at room temperature for 1 h with anti-γ-tubulin antibody (T6557, Sigma-Aldrich, St. Louis, MO). After washing, cells were incubated with Alexa 488 and 555 secondary antibodies for 1 h at room temperature. Cells were washed, air-dried and coverslips were mounted with DAPI. Nek2 localization to centrosomes was analyzed in one hundred interphase cells per concentration/time point using an Olympus BX51 fluorescence microscope. Three independent experiments were performed.

2.7.6. Eg5 Localization to Microtubules

Following disruption of the centrosome linker, centrosomes are separated from each other by a pushing force that is generated through the interaction of motor protein Eg5 with microtubules (Blangy et al., 1995). To further analyze centrosome separation, we tested the effects of zinc chromate on Eg5 localization to microtubules. Cells were seeded on 1 well glass chamber slides coated with FNC coating mix and treated with 0, 0.1, 0.15 and 0.2 ug/cm^2 zinc chromate for 24, 72 and 120 h. At harvest, cells were washed with a microtubule stabilizing buffer, fixed with -20°C methanol for 10 minutes, air dried for 5 min, permeabilized with 0.05% Triton X-100 for 3 minutes and blocked for 30 minutes in centrosome blocking buffer. After blocking, cells were incubated overnight at 4°C with anti-Eg5 antibody (sc-374212, Santa Cruz Biotechnology Inc., Dallas, TX). The following day cell were washed with PBS and incubated at room temperature for 1 h with Alexa 555 secondary antibody. This was followed by washing and incubation in the dark for 1 h at room temperature with anti-α-tubulin-FITC conjugated antibody (F2168, Sigma-Aldrich, St. Louis, MO). Cells were washed, air-dried and coverslips were mounted with DAPI. Eg5 localization to microtubules was analyzed in 50 mitotic cells and 100 interphase cells per concentration/time point under a 100x objective using an Olympus BX51 fluorescence microscope. Three independent experiments were performed.

2.8. Western Blots

2.8.1. Whole Cell Lysates for Analysis of Nek2

Nek2 protein levels were analyzed in whole cell lysates after zinc chromate treatment. Cells were seeded on 100 mm dishes and treated with 0, 0.1, 0.15 and 0.2 ug/cm^2 zinc chromate for 24, 72 and 120 h. At harvest, whole cell lysates were prepared by washing and collecting cells in cold PBS and centrifuging at 4°C and 14,000 RPM for

5 minutes. The pellet was resupended in RIPA Lysis Buffer System and incubated for 15 min on ice. After centrifugation at 4°C and 14,000 RPM for 10 min, supernatants were mixed with Tris-Glycine SDS Sample Buffer 2x with 5% 2-mercaptoethanol, and boiled for 5 min at 90-100°C. Protein concentrations were determined using a BSA standard curve and Synergy HT microplate reader (BioTek, Winooski, VT). Samples (10 µg) were resolved in 10% acrylamide/bis gels and electrophoresis buffer (25 mM Tris, 192 mM glycine, 0.1 % SDS) at 100V using a Mini-PROTEAN 3 Cell System (Bio-Rad, Hercules, CA). Proteins were transferred to nitrocellulose membranes for 2 h at 100 V with ice cold transfer buffer (25 mM Tris, 192 mM glycine, 20 % methanol) using a Mini Trans-Blot Cell (Bio-Rad, Hercules, CA). Membranes were blocked with 5% milk and incubated overnight at 4°C with anti-Nek2 antibody (610594, BD, Franklin Lakes, NJ). The following day they were washed with 1X TBS/0.1% Tween-20 and incubated for 1 h at room temperature with an HRP-conjugated secondary antibody (170-6516, Bio Rad, Hercules, CA). After washing, membranes were incubated with Pierce ECL2 Western Blotting Substrate and scanned with a Storm 840 Imaging System (GE Healthcare Life Sciences, Piscataway, NJ). Bands were quantified using ImageQuant TL software (GE Healthcare Life Sciences, Piscataway, NJ). Equal protein loading was confirmed by blotting for GAPDH (ab8245, Abcam, Cambridge, MA). Normalized values were calculated by dividing Nek2 values over GAPDH values for each concentration/time point. Final protein levels were calculated by dividing the normalized values from treatments over those from the control. Two independent experiments were performed.

2.8.2. Cell Fractionation for Analysis of Plk1, Eg5, Securin, and Separase

2.8.2.1. Mitotic Shakeoff

Proteins involved in centriole disengagement and centrosome separation are usually found at high levels during mitosis. These high levels could potentially mask the effects of zinc chromate in interphase cells. In order to better assess the effects of zinc

chromate on centriole disengagement proteins, we separated mitotic from interphase cells. Cells were seeded in T150 cell culture flasks and treated with 0 and 0.2 ug/cm^2 zinc chromate for 24, 72 and 120 h. At the end of treatment, the media was saved and PBS was added to each flask. Flasks were shaken vigorously by hand during 10 minutes each. Mitotic cells are rounded-up and loosely attached to the bottom of the flask, so when shaking they detach and float. Floating cells were recovered and mixed with previously saved media and centrifuged at 4°C and 1000 RPM for 5 min. After centrifuging, cells were washed once with PBS and centrifuged again. Pellets were resupended in 1 ml of PBS, transferred to microcentrifuge tubes and centrifuged at 4°C for 5 min at 14,000 RPM. Cell pellets were stored at -80°C until lysis. Before centrifuging, a 20 ul sample of the cell suspension in PBS was used to count the number of cells. These samples were loaded in Cellometer Cell Counting Chambers and counted using a Cellometer Vision Image Cytometer and Software (Nexcelom Bioscience LLC, Lawrence, MA). Cell numbers are used to estimate the amount of lysis buffer added for protein extraction.

The remaining attached cells in the flasks (interphase cells) were detached using 0.25% trypsin/EDTA. The trypsin was quenched with cell culture media and cells were centrifuged as above. Pellets were washed with PBS twice, resupended in 2 ml of PBS and transferred to microcentrifuge tubes. Cell suspensions were centrifuged at 4°C for 5 min at 14,000 RPM. Cell pellets were stored at -80°C until lysis. Before centrifugation, a 20 ul sample of the suspensions were used for cell number quantification, as explained for mitotic cells.

2.8.2.2. Lysis of Interphase and Mitotic Fractions

Mitotic and interphase cell pellets were thawed on ice and resuspended in a mild lysis buffer (modified from Fry et al., 1997) (50 mM HEPES-KOH, pH 7.4, 5 mM MnCl2, 10 mM MgCl2, 2mM EDTA, 100 mM NaCl, 5 mM KCl and 0.1% (v/v) IGEPAL with

protease and phosphatase inhibitors). Suspensions were incubated on ice for 30 min and sheared through a 27½ G needle seven times. This was done while tubes were on ice to dissipate the heat produced by the shearing. After shearing, the lysates were centrifuged at 4°C and 14,000 RPM for 10 min. After centrifugation supernatants were mixed with Tris-Glycine SDS Sample Buffer 2x with 5% 2-mercaptoethanol, and boiled for 5 min at 90-100°C. Protein concentrations were determined using a BSA standard curve and Synergy HT microplate reader (BioTek, Winooski, VT).

2.8.3. Plk1 and phospho-Plk1 Western Blots

Mitotic and interphase whole cell lysates (5 ug-10 ug) were resolved in 10% acrylamide/bis gels and electrophoresis buffer (25 mM Tris, 192 mM glycine, 0.1 % SDS) at 100V using a Mini-PROTEAN 3 Cell System (Bio-Rad, Hercules, CA). Proteins were transferred to PVDF membranes for 2 h at 100 V with ice cold transfer buffer (25 mM Tris, 192 mM glycine, 20 % methanol) using a Mini Trans-Blot Cell (Bio-Rad, Hercules, CA). Membranes were blocked with Odyssey blocking buffer and incubated overnight at 4°C with anti-Plk1 (ab14210, abcam, Cambridge, MA) and anti-phospho-Plk1 (T210) (KAP-CC107, Stressgen, Ann Arbor, MI) antibodies. The following day they were washed with 1X TBS/0.1% Tween-20 and incubated for 1 h at room temperature with Alexa Fluor 680 and IRDye800 secondary antibodies for 1 h at room temperature in the dark. After washing, membranes were scanned with an Odyssey Infrared Imaging System (Li-Cor Biosciences, Lincoln, NE). Bands were quantified using Odyssey software (Li-Cor Biosciences, Lincoln, NE). Equal protein loading was confirmed by blotting for B-actin (GT5412, GeneTex Inc., Irvine, CA). Normalized values were calculated by dividing Plk1 and phospho-Plk1 values over B-actin values for each concentration/time point. Final protein levels were calculated by dividing the normalized values from treatments over those from the control. Phospho-Plk1 to Plk1 ratios were

calculated by dividing final protein levels for each concentration/time point. Three independent experiments were performed.

2.8.4. Eg5 and phospho-Eg5 Western Blots

Mitotic and interphase whole cell lysates (5-10 ug) were resolved in 10% acrylamide/bis gels and electrophoresis buffer (25 mM Tris, 192 mM glycine, 0.1 % SDS) at 100V using a Mini-PROTEAN 3 Cell System (Bio-Rad, Hercules, CA). Proteins were transferred to PVDF membranes for 2 h at 300 V with ice cold transfer buffer (25 mM Tris, 192 mM glycine, 20 % methanol) using a Mini Trans-Blot Cell (Bio-Rad, Hercules, CA). Membranes were blocked with Odyssey blocking buffer and incubated overnight at 4°C with anti-Eg5 antibody (sc374212, Santa Cruz Biotechnology, Inc., Dallas, TX) and anti-phospho-Eg5 (T927) (ab61104, abcam, Cambridge, MA) antibodies. The following day they were washed with 1X TBS/0.1% Tween-20 and incubated for 1 h at room temperature with Alexa Fluor 680 and IRDye800 secondary antibodies for 1 h at room temperature in the dark. After washing, membranes were scanned with an Odyssey Infrared Imaging System (Li-Cor Biosciences, Lincoln, NE). Bands were quantified using Odyssey software (Li-Cor Biosciences, Lincoln, NE). Equal protein loading was confirmed by blotting for B-actin (GT5412, GeneTex, Inc., Irvine, CA). Normalized values were calculated by dividing Eg5 and phospho-Eg5 values over B-actin values for each concentration/time point. Final protein levels were calculated by dividing the normalized values from treatments over those from the control. Three independent experiments were performed.

2.8.5. Separase and Securin Western Blots

Mitotic and interphase whole cell lysates (15-20 ug) were resolved in 8% acrylamide/bis gels and electrophoresis buffer (25 mM Tris, 192 mM glycine, 0.1 % SDS) at 100V using a Mini-PROTEAN 3 Cell System (Bio-Rad, Hercules, CA). The top portions of the membranes (proteins above the 55 kDa marker) were transferred to

nitrocellulose membranes overnight at 30 V with ice cold transfer buffer (25 mM Tris, 192 mM glycine, 10 % methanol) using a Mini Trans-Blot Cell (Bio-Rad, Hercules, CA). The bottom portions of the membranes (proteins below the 55 kDa marker) were transferred to nitrocellulose membranes for 2 h at 100 V with ice cold transfer buffer (same as above but with 20% methanol). Top and bottom portions of membranes were blocked with Odyssey blocking buffer and incubated overnight at 4°C with anti-separase (MA1-16595, Thermo Fisher Scientific, Rockford, IL) and anti-securin (ab3305, abcam, Cambridge, MA) antibodies. The following day they were washed with 1X TBS/0.1% Tween-20 and incubated for 1 h at room temperature with IRDye800 secondary antibodies for 1 h at room temperature in the dark. After washing, membranes were scanned with an Odyssey Infrared Imaging System (Li-Cor Biosciences, Lincoln, NE). Bands were quantified using Odyssey software (Li-Cor Biosciences, Lincoln, NE). Equal protein loading was confirmed by blotting for B-actin (GT5412, GeneTex Inc., Irvine, CA). Normalized values were calculated by dividing separase and securin values over B-actin values for each concentration/time point. Final protein levels were calculated by dividing the normalized values from treatments over those from the control. Three independent experiments were performed.

2.9. Statistics

Values were expressed as the mean ± SEM (standard error of the mean) of triplicate experiments. The student's t-test was used to calculate p-values to determine the statistical significance of difference in means for each pair of concentrations. A 95% confidence interval for the difference in means of each pair of concentrations was constructed based on the Student's t distribution.

CHAPTER 3

RESULTS

3.1. Overview

Cr(VI) causes centrosome amplification, a phenotype that contributes to chromosome instability and is commonly observed in tumors. However, how Cr(VI) affects centrosomes is not known. Moreover, whether centrosome amplification is a transient or permanent phenotype after Cr(VI) exposure is also unknown. Centrosomes duplicate once and only once during a cell cycle but deregulation of the mechanisms that control centrosome duplication can lead to centrosome amplification. A key event in centrosome cycle control is the formation of the centrosome linkers, the G1-G2 thether and the S-M linker. The disruption of these protein linkers controls centrosome duplication control and contributes to the coordination of the centrosome and cell cycles.

This study has two main objectives. The first objective is to address whether **centrosome amplification after particulate Cr(VI) exposure is a permanent phenotype**. We will test this by analyzing centrosome amplification in a set of clonal cell lines developed after repeated exposure to Cr(VI). The second objective is to analyze if disruption of the centriole linkers is part of Cr(VI) toxicity. For this, we propose that **particulate Cr(VI) induces premature disruption of the centriole linkers by activating Plk1**. We will test this hypothesis with three specific aims: 1) Particulate Cr(VI) induces premature disruption of the centriole linkers, 2) Particulate Cr(VI) activates the securin-separase and Nek2/Eg5 pathways, and 3) Particulate Cr(VI) induces Plk1 activity.

The results are presented in three parts (Figure 3.1). Part 1 shows that centrosome amplification after Cr(VI) exposure is a permanent phenotype. Part 2 demonstrates that particulate Cr(VI) causes premature disruption of the S-M and G1-G2

tethers. Part 3 shows that after Cr(VI) exposure the p-Plk1/Plk1 ratio increases. It also shows that Cr(VI) decreases securin protein levels while increasing the levels of active separase. Moreover, we also show that Cr(VI) decreases Nek2 and Eg5 protein levels and centrosomal and microtubule localization, respectively. All three parts are presented in detail below.

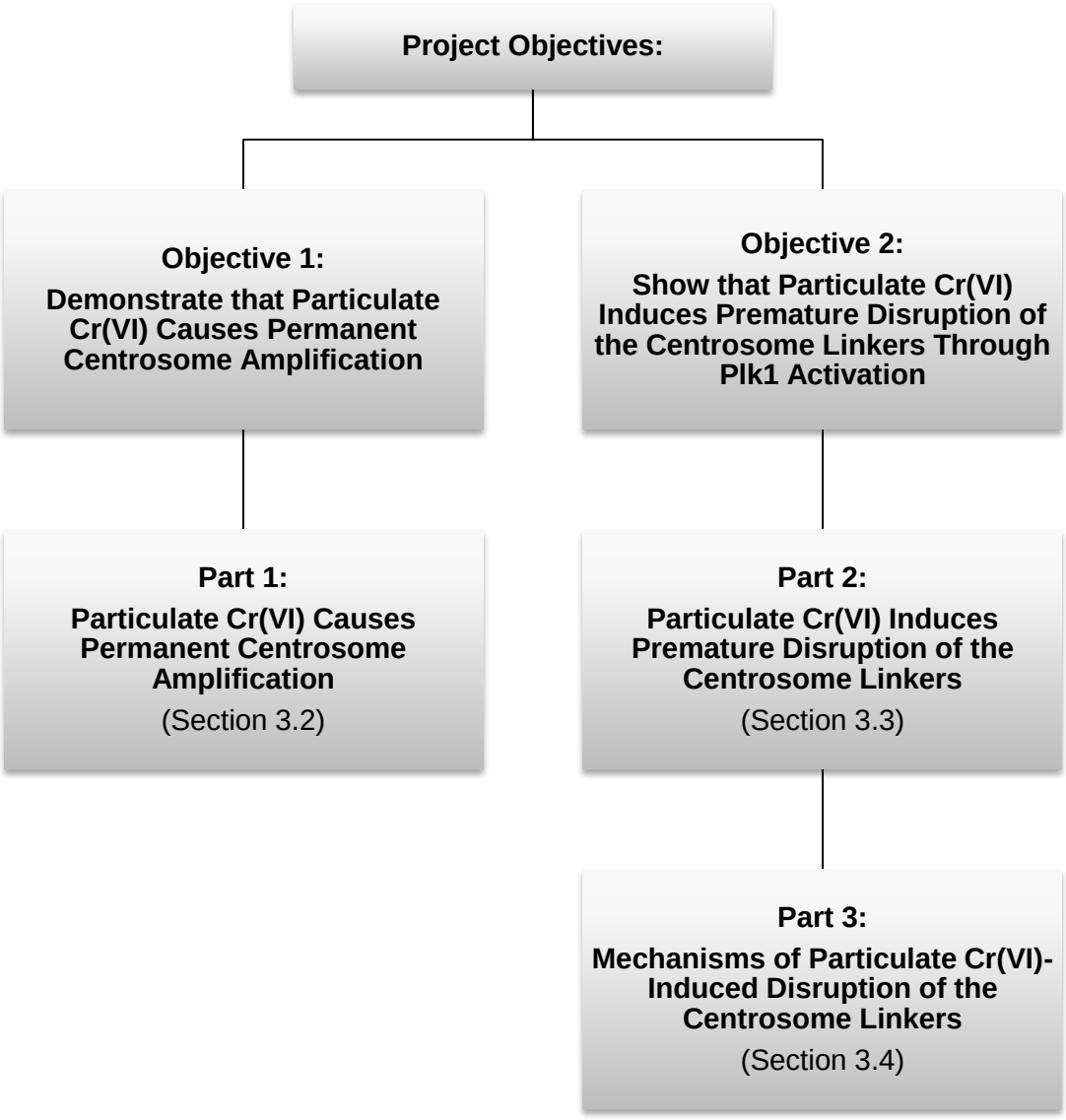

Figure 3.1. Organizational Flow Chart of the Project.

3.2. Part 1: Particulate Cr(VI) Induces Permanent Centrosome Amplification

The first part of this study addresses whether centrosome amplification induced by Cr(VI) is a permanent phenotypic change (Figure 3.2). For this, centrosome amplification was analyzed in a set of clonal cell lines derived from repeated exposure to Cr(VI). The data show that particulate Cr(VI)-induced centrosome amplification is a permanent phenotype that persists even in the absence of Cr(VI) exposure. Centrosome amplification appeared after the initial treatment in the 1st generation cell lines and remained after multiple Cr(VI) treatments and throughout all clonal generations.

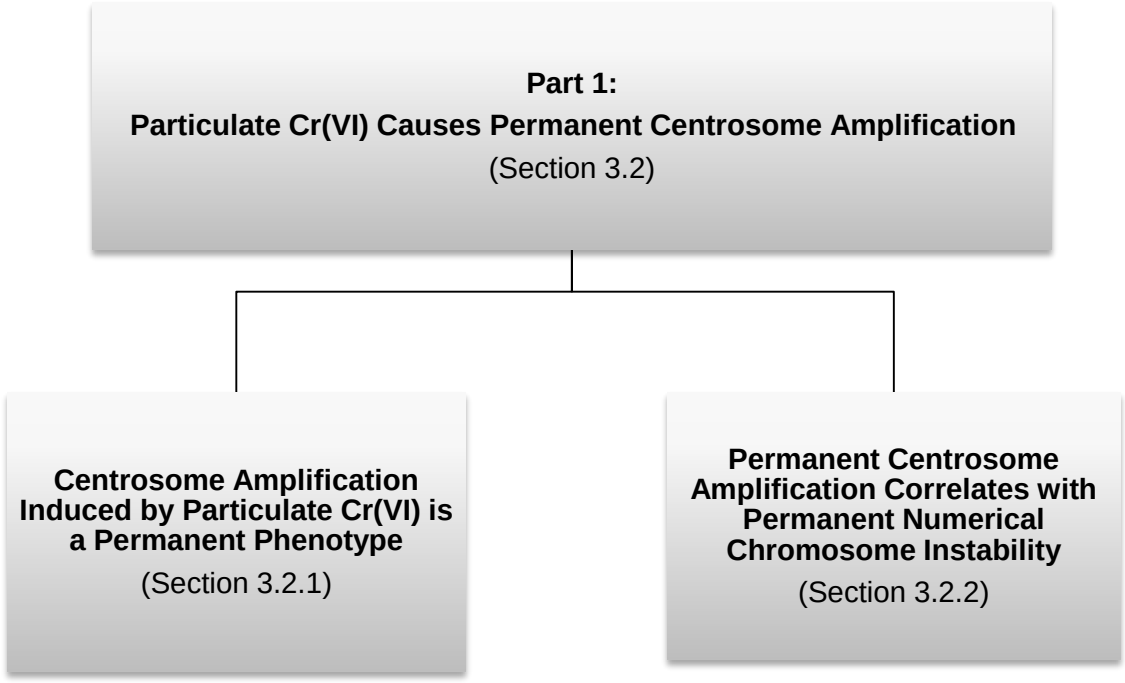

Figure 3.2. Organizational Flow Chart of Part 1: Particulate Cr(VI) Causes Permanent Centrosome Amplification.

3.2.1. Centrosome Amplification Induced by Particulate Cr(VI) is a Permanent Phenotype

Clonal cell lines were developed by treating WTHBF-6 cells with particulate Cr(VI) for 24 h in three separate treatments (Wise, 2013) (Figure 3.3). After each treatment, cells were seeded at colony forming density, cloned, expanded into cell lines and retreated. Untreated cells were also seeded at colony forming density, cloned and expanded three times. Overall, there were 91 control clones and 63 treated clones. Centrosome amplification was analyzed in all clones except one treated clone (T2-1) which was lost before the analysis. Karyotypes and numerical chromosome instability were also analyzed (Wise, 2013). The analysis of these clones allows us to identify permanent phenotypic changes, cellular heritability and temporal patterns of effects (i.e. do effects happen after 1, 2 or 3 exposures) in living cells.

Figure 3.4 shows the distribution of centrosome amplification in untreated clones. The percent of mitotic cells with centrosome amplification ranged from 0-6%, while the parental cell line, WTHBF-6, had a background level of 3% of cells with centrosome amplification. In contrast, in treated clones the values ranged from 0-22%. Clones with 7% or greater percent of cells with centrosome amplification were classified as having centrosome amplification as a permanent phenotype. The threshold value was based on the range of values observed in untreated clones (0-6%) which are likely due to effects of the cloning process. As a result, any value above 6% was classified as centrosome amplification. Considering all generations, 29% of Cr(VI)-treated clones have permanent centrosome amplification (Figure 3.6A). Considering the results by generation, in the first generation, 43% of treated clones had centrosome amplification while the second and third generations had 44 and 21%, respectively (Figure 3.6B).

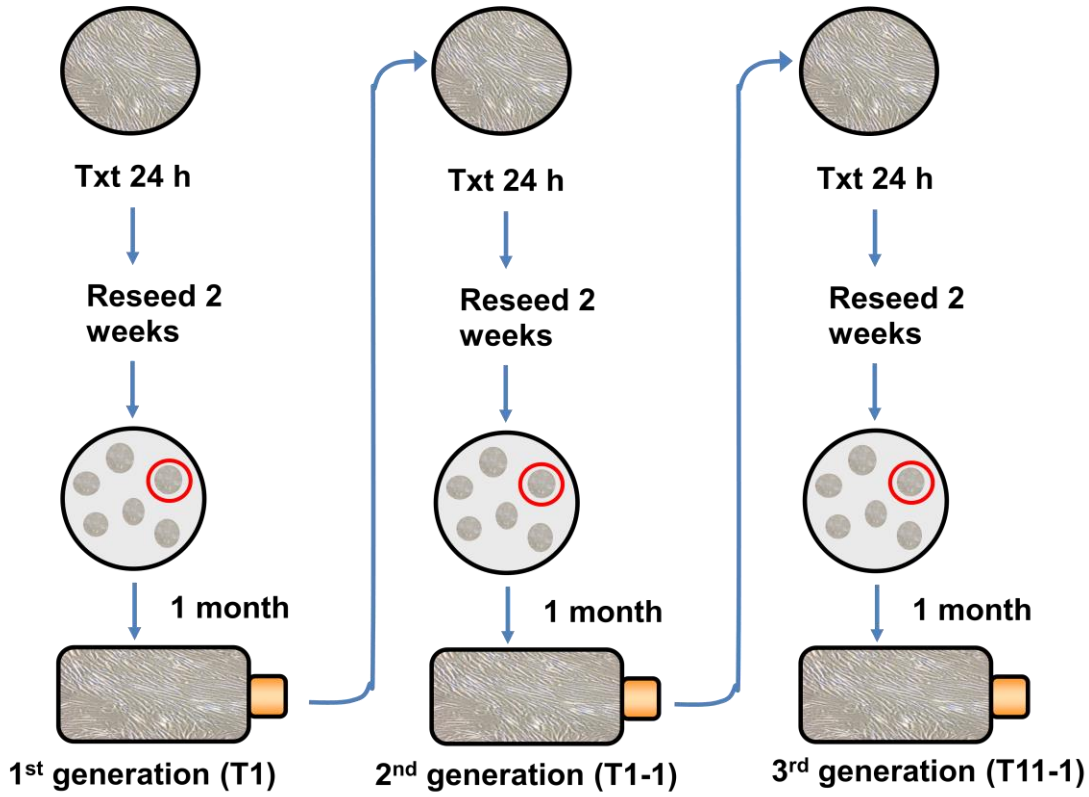

Figure 3.3. Experimental Design of the Clonal Expansion. This figure shows the experimental design for the clonal expansion (Wise, 2013). Cells were exposed to lead chromate for 24 h in three separate treatments. After each treatment, cells were seeded at colony forming density and allowed to grow for two weeks. Colonies were isolated, expanded into cell lines and retreated. At each stage, cell lines were karyotyped and analyzed for numerical chromosome instability as well as centrosome amplification.

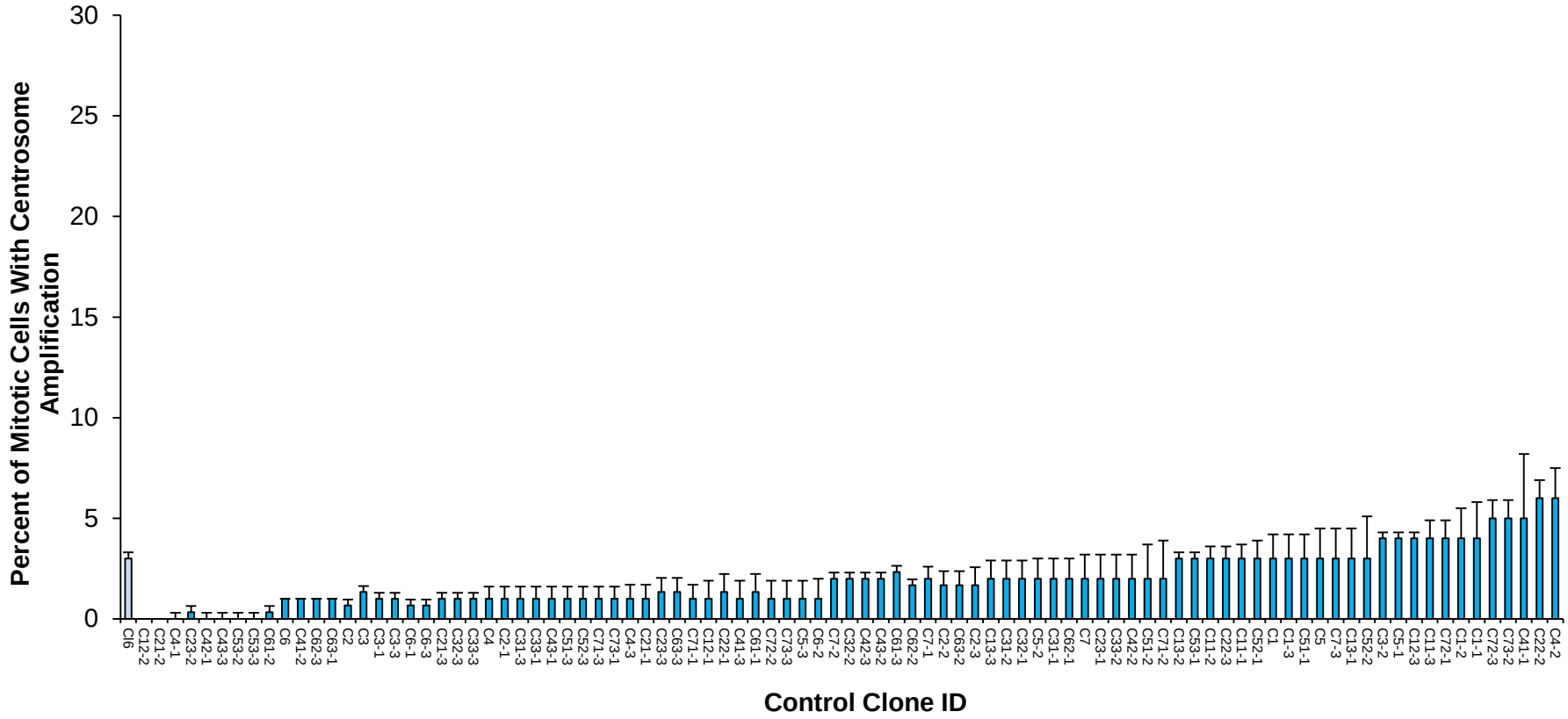

Figure 3.4. Distribution of Centrosome Amplification in Untreated Clones. This figure shows the distribution of centrosome amplification in untreated clones. The parental cell line WTHBF-6 (Clone 6), with 3% of mitotic cells with centrosome amplification, is shown as a reference (light blue bar). The percent of mitotic cells with centrosome amplification in untreated clones (dark blue bars) ranged from 0 to 6%. Data represent an average of three independent experiments ± the standard error of the mean.

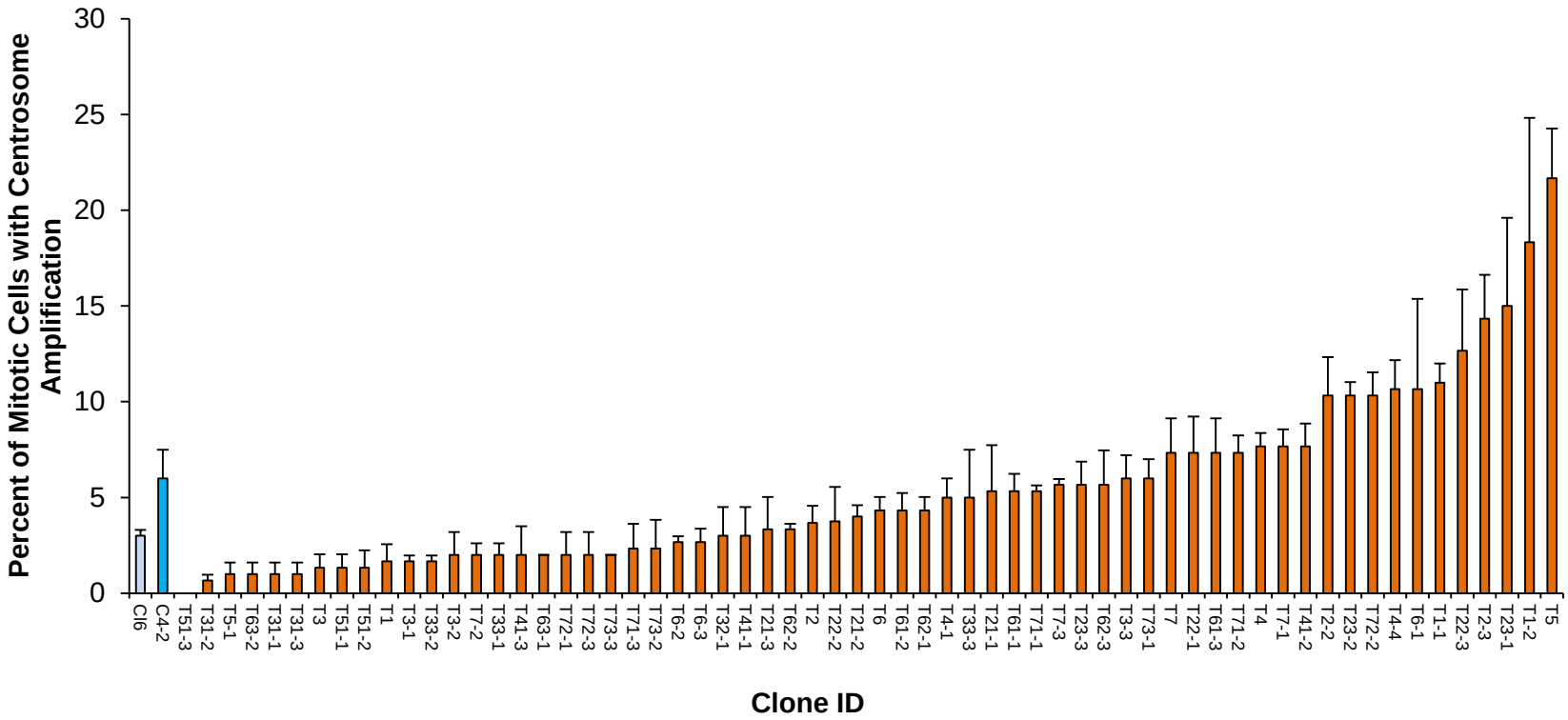

Figure 3.5. Distribution of Centrosome Amplification in Treated Clones. This figure shows the distribution of the percent of mitotic cells with centrosome amplification in treated clones. The parental cell line WTHBF-6 (Clone 6) and the untreated clone with the highest value are shown as references (blue bars). The percent of mitotic cells with centrosome amplification in treated clones ranged from 0 to 22% (orange bars). Data represent an average of three independent experiments ± the standard error of the mean.

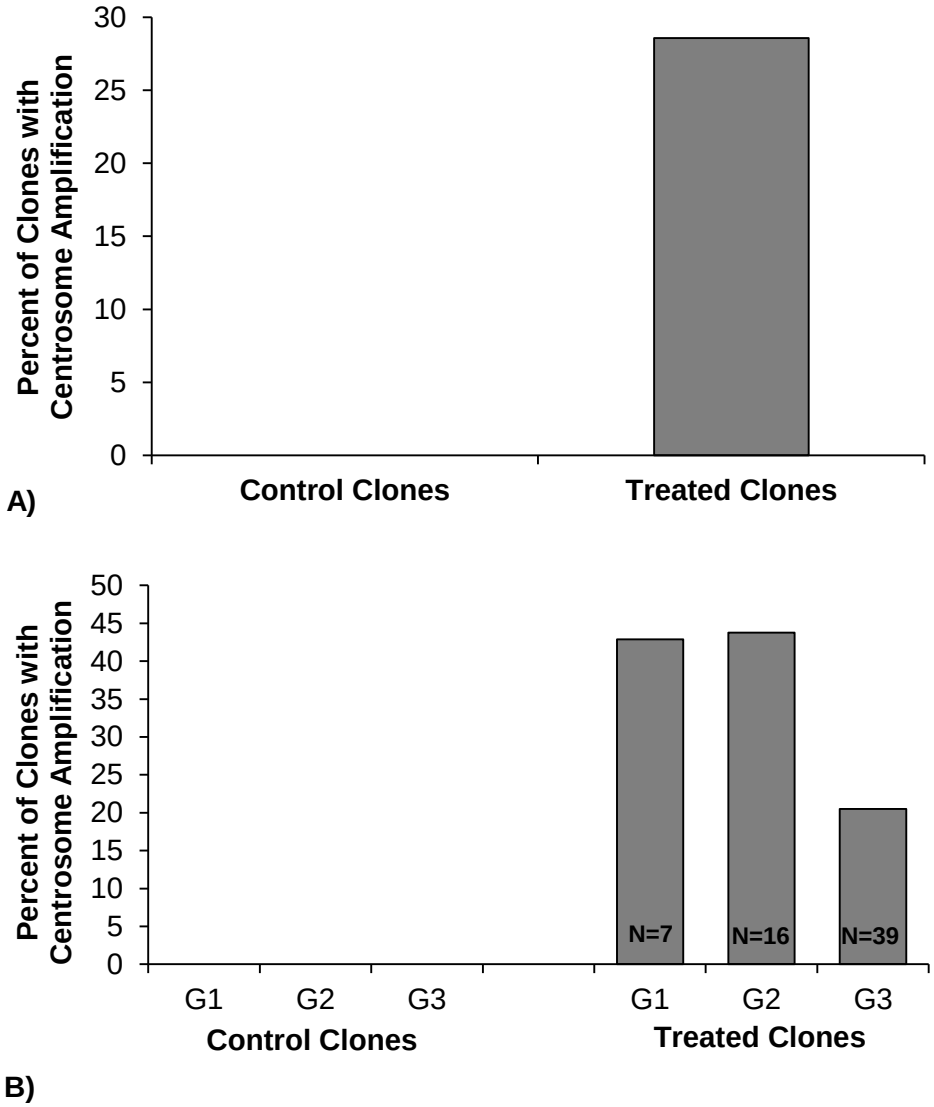

Figure 3.6. Cr(VI)-Treated Clones Exhibit Permanent Centrosome Amplification. This figure shows the percent of treated clones with centrosome amplification. **A)** This panel shows that 29% of treated clones have permanent centrosome amplification. **B)** This panel shows that permanent centrosome amplification is present across all generations of treated clones. In the first generation (G1), 43% of treated clones had centrosome amplification while the second (G2) and third (G3) generations had 44 and 21%, respectively. N=number of clones analyzed in each generation.

3.2.2. Permanent Centrosome Amplification Correlates with Permanent Numerical Chromosome Instability

Next, we compared the centrosome amplification phenotype with data on numerical chromosome instability (CIN) for each clone (Wise, 2013). Numerical CIN can be assessed by analyzing the karyotypes of each clone and whether it deviates from the expected 46X,Y complement. Figure 3.7A shows that, when all generations are taken into account, 56% of treated clones have numerical CIN compared to only 5% of control clones. This shows that Cr(VI) treatment induces numerical CIN, which correlates with the induction of centrosome amplification (Figure 3.7A). When analyzed by generation, numerical CIN was present in 14% of treated clones from the 1st generation. Numerical CIN increases with subsequent Cr(VI) treatments. The 2nd and 3rd generations had 65 and 59% of clones with numerical CIN, respectively (Figure 3.7B). When the numerical chromosome instability phenotype is compared to the centrosome amplification phenotype, we observe that after the first Cr(VI) treatment there is a significant increase in centrosome amplification and a slight increase in numerical CIN. Numerical CIN increases significantly after 2nd and 3rd treatments and correlates with the increase in centrosome amplification in the previous generation. This is consistent with centrosome amplification being a causative mechanism that leads to induction of numerical CIN.

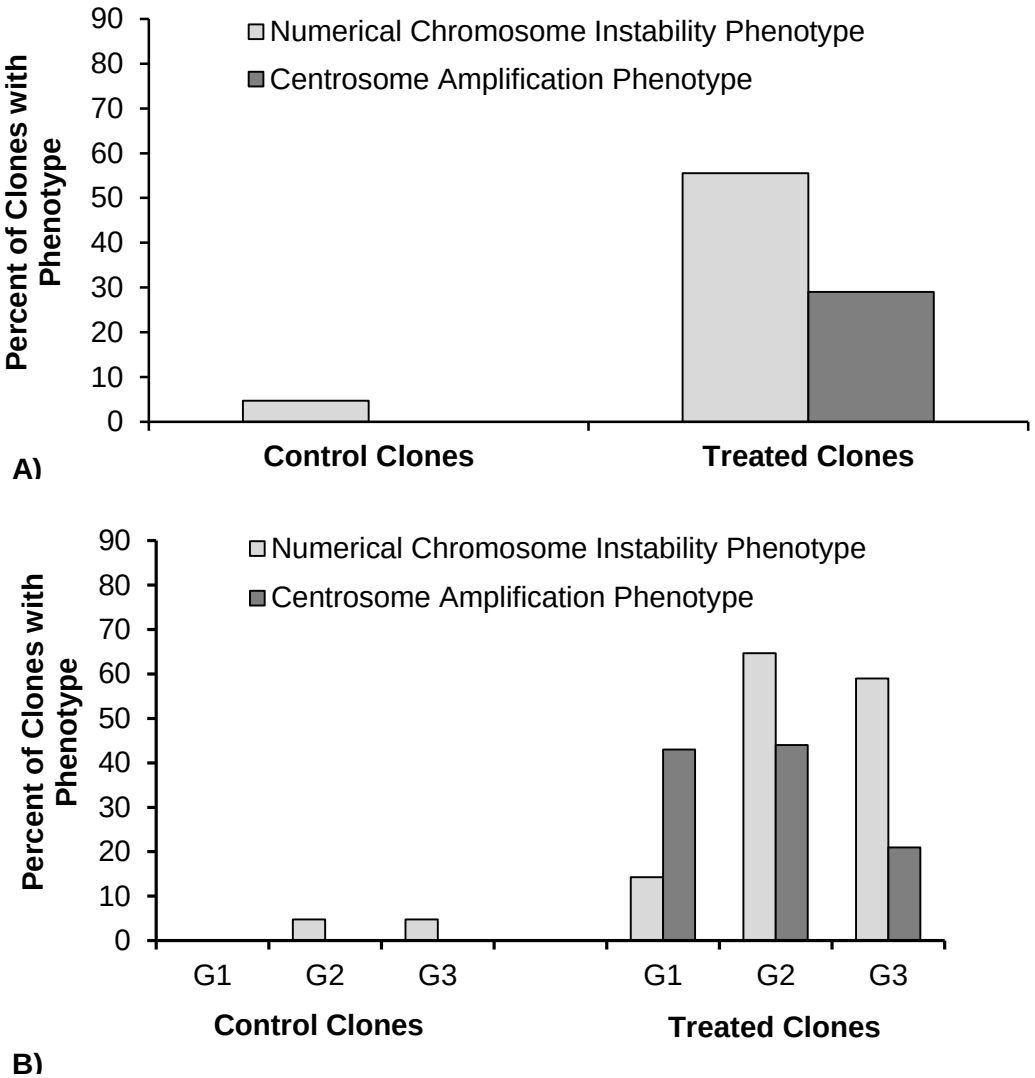

Figure 3.7. Correlation of Centrosome Amplification and Numerical Chromosome Instability Phenotypes in Cr(VI)-treated Clones. This figure shows that an increase in centrosome amplification correlates with an increase in numerical chromosome instability in Cr(VI)-treated clones. **A)** This panel shows the correlation considering the totality of the clones. **B)** This panel shows the correlation for each generation of clones. Centrosome amplification precedes the appearance of numerical chromosome instability.

The above analysis shows the overall effects of repeated exposure to Cr(VI) on clonally expanded cells. However, it does not take into account that clones are related to each other. To analyze whether this relationship affects centrosome amplification, clones were organized in pedigrees that show each 1st treatment clone (1st generation) with its two subsequent clone generations (2nd and 3rd generations) (Figures 3.8-3.14). Pedigrees also show the overlap between centrosome amplification and numerical CIN phenotypes.

Analyzing the pedigrees, we can see that 44% of clones classified as having permanent centrosome amplification also exhibit numerical CIN (T1-1, T1-2, T2-3, T23-1, T23-2, T4-2, T41-2 and T7-1). Moreover, these clones belong to families that, as a whole, also have high percentage of clones with either numerical CIN or centrosome amplification supporting the relatedness of these two phenotypes. All first generation clones (i.e.: T1 through T7) had normal karyotypes (46, XY) and hence, did not have numerical CIN. However, 43% had centrosome amplification. This is consistent with centrosome amplification being an earlier phenotype that contributes to numerical CIN.

Clone T5 had the highest centrosome amplification value (21.7%). Interestingly, this clone's family was very small because only one colony survived the clonal expansion. This colony was normal and gave rise to normal daughter clones. In contrast, T4 and T7 had 7.7 and 7.3% centrosome amplification, respectively, and gave rise to clones that had centrosome amplification and/or numerical CIN. Furthermore, some of these clones had daughter clones with these phenotypes as well. Similar results are observed between 2nd and 3rd generation clones of other families (i.e.: T2-2, T2-3, T6-1). This indicates that the degree of centrosome amplification might determine the viability of the cells and that at a certain level cells with amplified centrosome do not survive. This is in agreement with centrosome amplification being a deleterious phenotype for cells. However, at lower levels of centrosome amplification cells not only survive, but

also develop numerical CIN. Overall, the clonal analysis suggest that centrosome amplification and numerical CIN are persistent phenotypes after Cr(VI) exposure and that cells that possess them have the ability to survive and give rise to daughter cells.

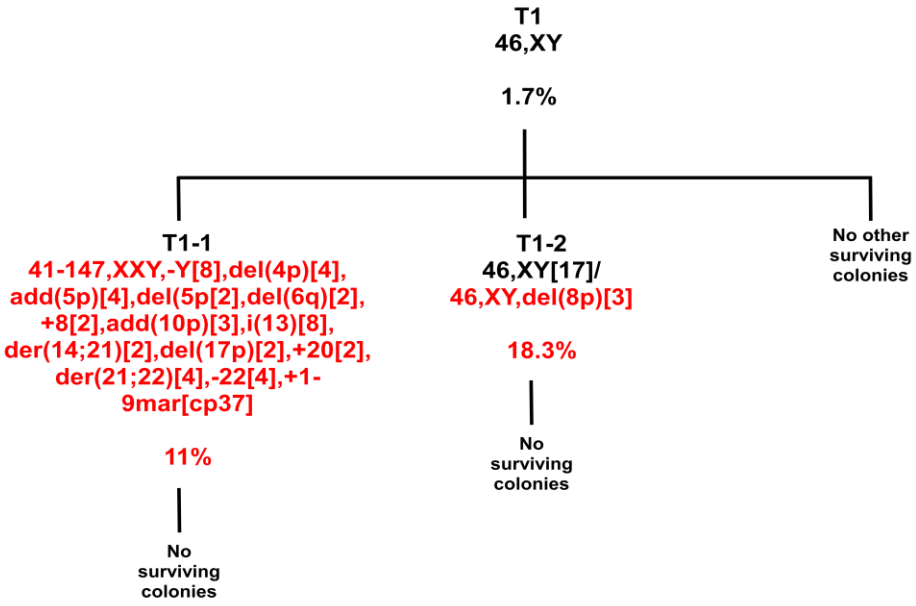

Figure 3.8. Pedigree of T1 Family. This figure shows individual clones of the T1 family with their corresponding karyotype and percent of centrosome amplification. Red letters represent abnormal karyotypes and/or the presence of centrosome amplification.

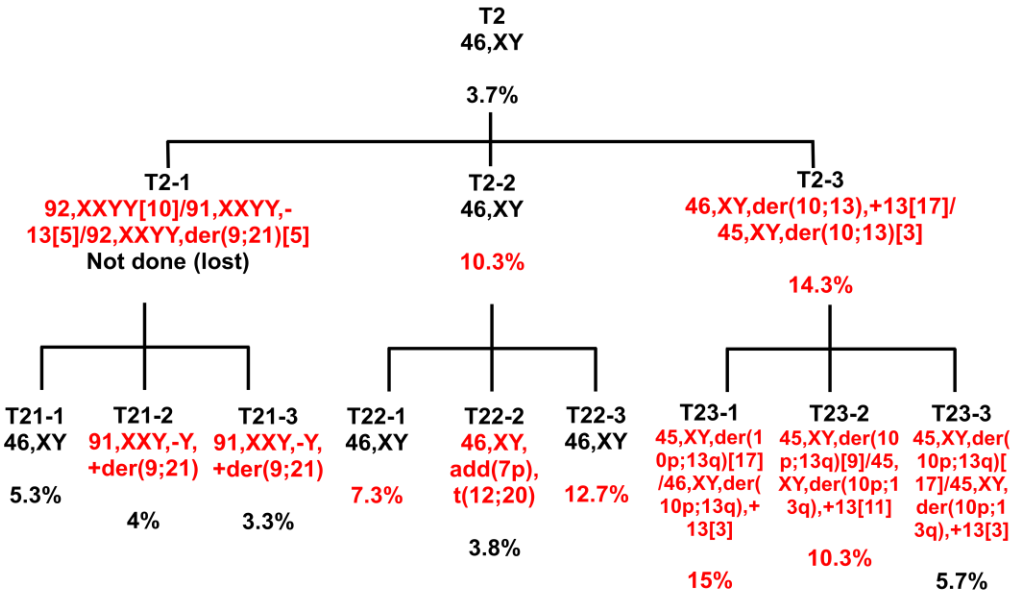

Figure 3.9. Pedigree of T2 Family. This figure shows individual clones of the T2 family with their corresponding karyotype and percent of centrosome amplification. Red letters represent abnormal karyotypes and/or the presence of centrosome amplification.

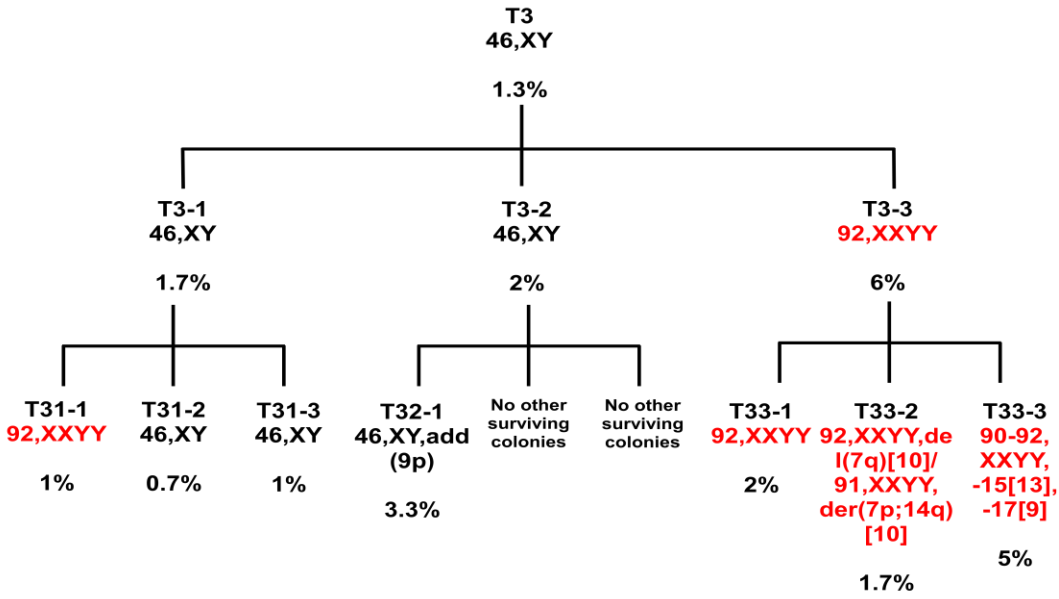

Figure 3.10. Pedigree of T3 Family. This figure shows individual clones of the T3 family with their corresponding karyotype and percent of centrosome amplification. Red letters represent abnormal karyotypes and/or the presence of centrosome amplification.

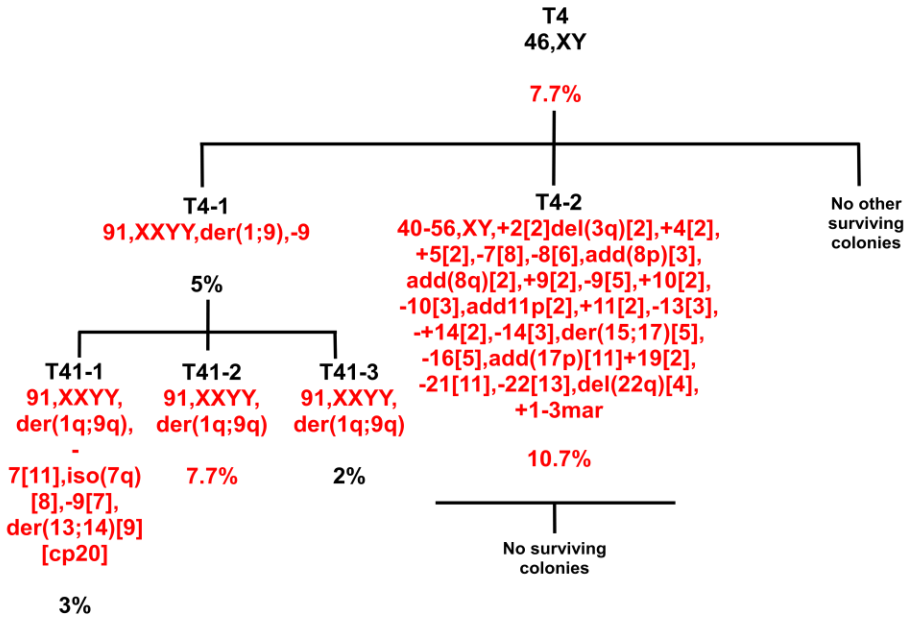

Figure 3.11. Pedigree of T4 Family. This figure shows individual clones of the T4 family with their corresponding karyotype and percent of centrosome amplification. Red letters represent abnormal karyotypes and/or the presence of centrosome amplification.

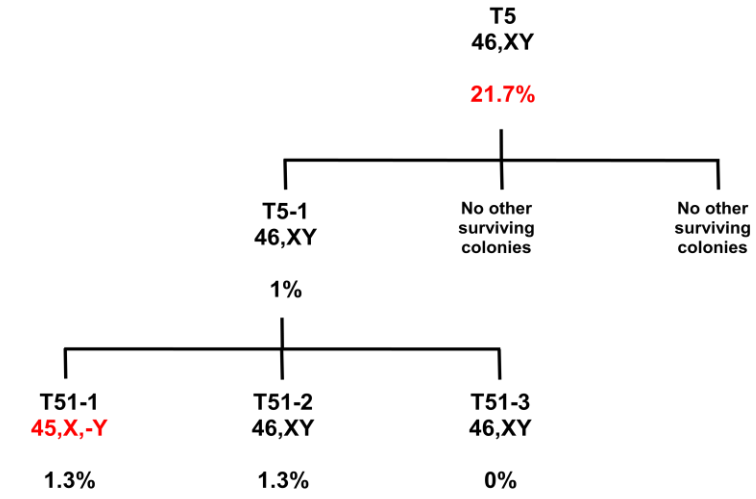

Figure 3.12. Pedigree of T5 Family. This figure shows individual clones of the T5 family with their corresponding karyotype and percent of centrosome amplification. Red letters represent abnormal karyotypes and/or the presence of centrosome amplification.

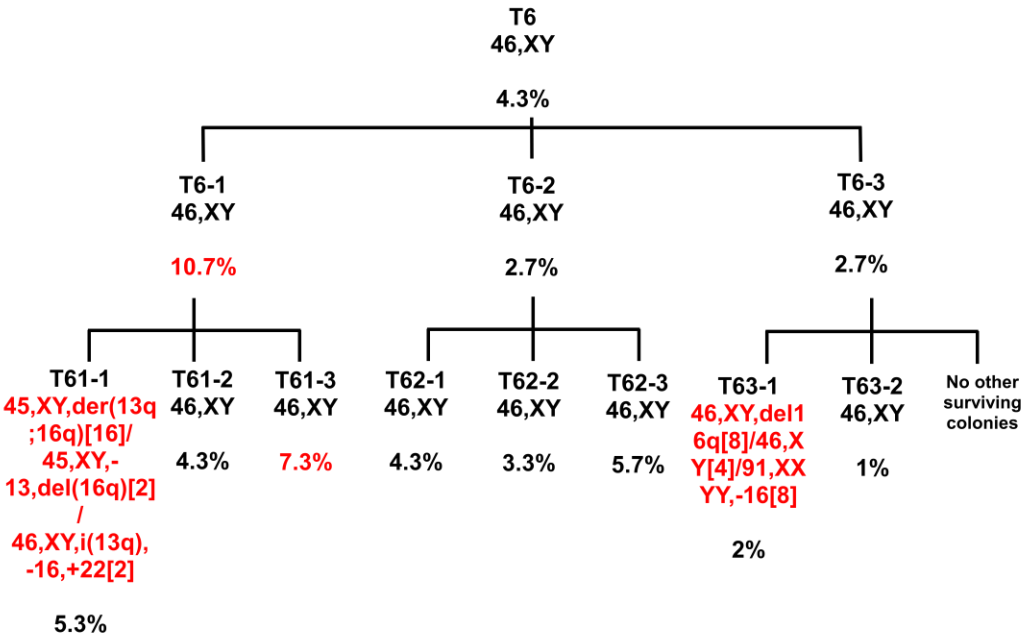

Figure 3.13. Pedigree of T6 Family. This figure shows individual clones of the T6 family with their corresponding karyotype and percent of centrosome amplification. Red letters represent abnormal karyotypes and/or the presence of centrosome amplification.

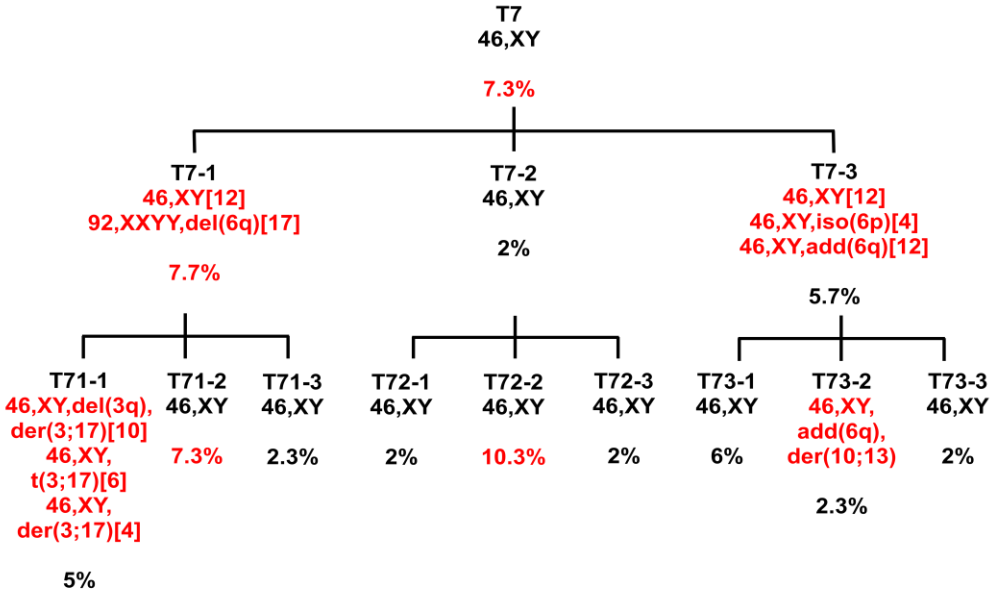

Figure 3.14. Pedigree of T7 Family. This figure shows individual clones of the T7 family with their corresponding karyotype and percent of centrosome amplification. Red letters represent abnormal karyotypes and/or the presence of centrosome amplification.

3.2.3. Part 1 Summary

The analysis of Cr(VI)-treated clonal cell lines shows that cells exposed to Cr(VI) develop permanent centrosome amplification. Moreover, these cells also develop numerical CIN. In many of the clones, centrosome amplification and numerical CIN both occur. Given that centrosome amplification was analyzed in several independent experiments for each clone, this further supports that these phenotypes are stable and permanent. That is, a clone that has centrosome amplification and/or numerical CIN will continue to have these phenotypes.

3.3. Part 2: Particulate Cr(VI) Induces Premature Disruption of the Centriole Linkers

Given that Cr(VI) causes permanent centrosome amplification and that this phenotype is implicated in tumorigenesis, it is important to understand the underlying mechanisms that contribute to its appearance. The second part of this project addresses a potential mechanism for Cr(VI)-induced centrosome amplification which involves the premature disruption of the centriole linkers (Figure 3.15). For this, we measured two phenotypes associated with centriole linker disruption in Cr(VI)-treated cells: centriole disengagement and centrosome separation. The data show that particulate Cr(VI) induces premature centriole disengagement and centrosome separation in interphase cells, consistent with a disruption of the centriole linkers and/or the mechanisms that regulate them.

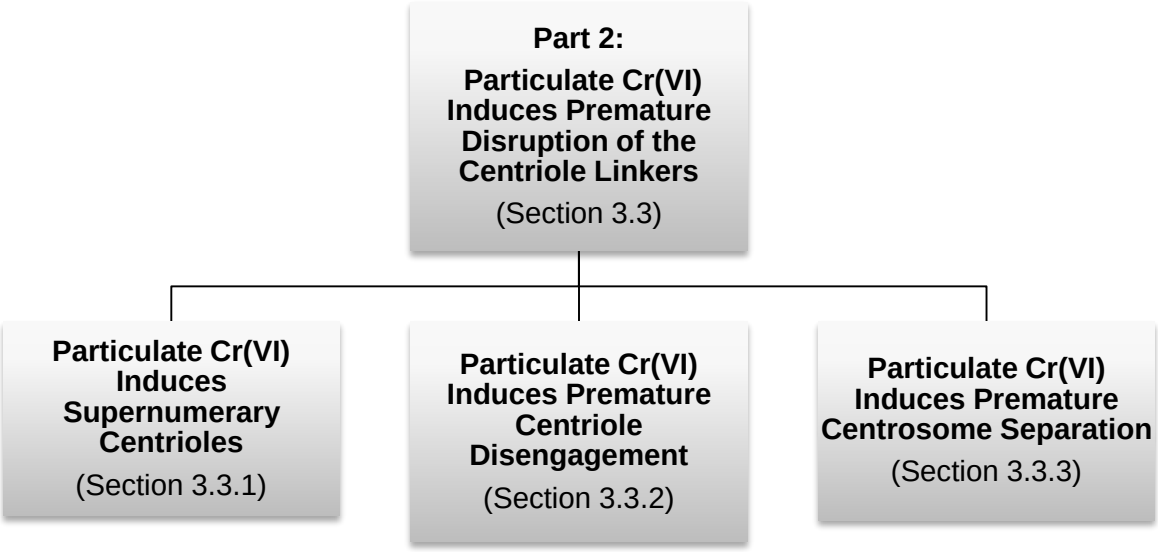

Figure 3.15. Organizational Flow Chart of Part 2: Particulate Cr(VI) Induces Premature Disruption of the Centriole Linkers.

3.3.1. Particulate Cr(VI) Induces Supernumerary Centrioles

As shown in Part 1, Cr(VI) causes centrosome amplification and numerical CIN. In order to study the mechanisms underlying centrosome amplification, we exposed human lung cells for 24, 72 and 120 h to 0, 0.1, 0.15 and 0.2 ug/cm^2 zinc chromate, a particulate form of Cr(VI). These concentrations have been previously shown to induce centrosome amplification after chronic exposures (i.e.: >24 h) (Holmes et al., 2010).

Figure 3.16A shows the centrosome amplification data from Holmes et al. (2010) arranged in a side-by-side comparison of interphase versus mitotic cells. This figure shows that after 24 h exposure human lung cells exposed to zinc chromate do not show centrosome amplification. In contrast, chronic exposure (i.e.: 72 and 120 h) to zinc chromate caused a statistically significant time- and concentration-dependent increase in centrosome amplification in both interphase and mitotic cells ($p<0.05$). In interphase cells, a 24 h exposure to 0.1, 0.15 and 0.2 ug/cm^2 zinc chromate induced 2.9, 2.2 and 2.6 percent of cells with centrosome amplification, respectively; while after 120 h

exposure the same concentrations induced 13.9, 18 and 21.3 percent of cells with centrosome amplification. The same pattern was observed in mitotic cells. After 24 h exposure to 0.1, 0.15 and 0.2 ug/cm^2 zinc chromate, there were 1, 1 and 1 percent of cells with centrosome amplification, respectively; while after 120 h exposure the same concentrations induced 21, 33 and 46 percent of cells with centrosome amplification.

In Cr(VI)-treated clones we observed a correlation between centrosome amplification and numerical CIN. However, Holmes et al. (2010) did not show the correlations between the centrosome amplification and numerical CIN phenotypes in cells exposed to Cr(VI) for 24, 72 and 120 h. The correlations for their data are shown in Figure 3.16B. Chromosome numbers were analyzed in solid stained metaphases after 24, 72 and 120 h exposure to 0.1, 0.15 and 0.2 ug/cm^2 zinc chromate. The data show that after 24 h exposure there is no increase in the percent of cells with numerical CIN, while after 72 and 120 h there is a statistically significant time- and dose-dependent increase in the percent of cells with numerical CIN ($p<0.05$). A 24 h exposure to 0.1, 0.15 and 0.2 ug/cm^2 zinc chromate induced 13, 13, 13.7 and 14.3 percent of cells with numerical CIN, respectively, while after 120 h exposure, the same concentrations induced 28, 40.3 and 44.3 percent of cells with numerical CIN.

Most importantly, the time- and concentration-dependent increase observed in numerical CIN correlated with the time- and concentration-dependent increase in centrosome amplification in mitotic cells (Figure 3.16B). We used mitotic cells as a comparison because numerical CIN was assessed in metaphases, which correspond to a mitotic phase. After 24 h exposure to 0.1, 0.15 and 0.2 ug/cm^2 zinc chromate, there is no increase in numerical CIN or centrosome amplification, while after 72 and 120 h exposure to the same concentrations, both numerical CIN and centrosome amplification increase proportionally with time and concentration.

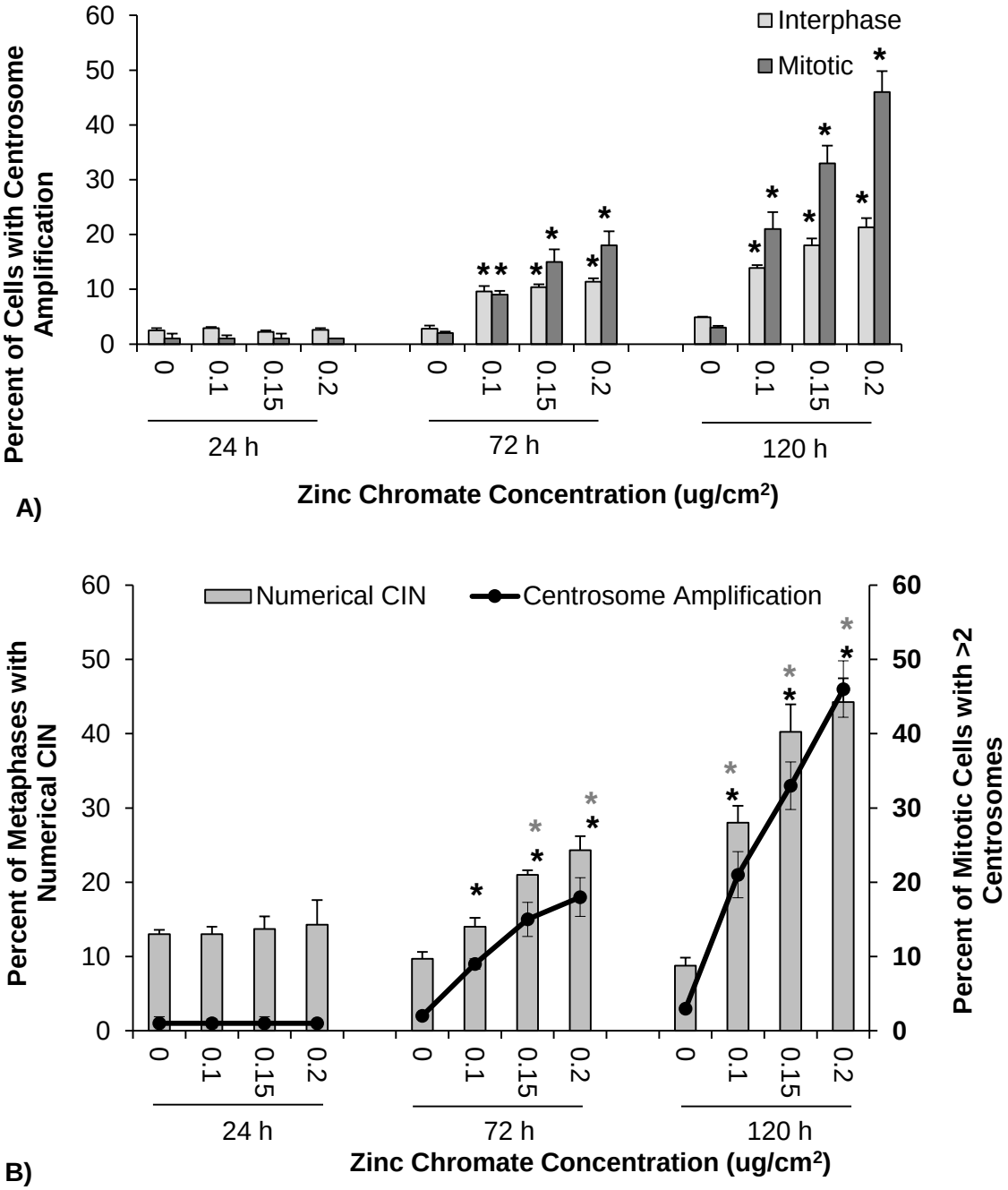

Figure 3.16. Chronic Exposure to Cr(VI) Induces Numerical CIN and Centrosome Amplification in Human Lung Cells. This figure shows that chronic exposure to zinc chromate induces a time- and concentration-dependent increase in numerical CIN and centrosome amplification. A) Percent of cells with centrosome amplification in interphase and mitotic cells. B) Percent of metaphases with numerical CIN and its correlation with percent of cells with centrosome amplification in mitosis. Both phenotypes show a similar increase. *Statistically different from the control ($p<0.05$). Data represent an average of three independent experiments ± the standard error of the mean.

Centrosome amplification can be caused by different mechanisms which include multiple rounds of centrosome duplication within one cell cycle, centriole disengagement, formation of acentriolar centrosomes and failure of cytokinesis (Fukasawa, 2005). The analysis of centrioles, the microtubule-based structures within each centrosome, can be used to distinguish some of these phenotypes (Fukasawa, 2005). To gain a better understanding of Cr(VI)-induced centrosome amplification, we used the centriole marker centrin to stain and count centrioles after Cr(VI) treatment

Figure 3.17A shows the effects of Cr(VI) on centriole numbers in interphase cells. In interphase, normal G1 phase cells have two centrioles while normal S and G2 phase cells have four centrioles. Chronic exposure to zinc chromate induced a time-dependent increase in the percent of cells that had supernumerary centrioles in both interphase and mitotic cells. In interphase cells, the percent of G1 cells (i.e.: with two centrioles) remained constant with increased exposure time and concentration. For example, after a 24 h exposure to 0.2 ug/cm^2 zinc chromate the percent of cells with 2 centrioles was 54%, while after 120 h exposure, it was 52%. The percent of cells with three centrioles also remained constant with treatment and increased exposure time. After 24 h exposure to 0.2 ug/cm^2 zinc chromate there was 1% of interphase cells with 3 centrioles, while after 120 h the percent of cells was 4%.

In contrast, after exposure to zinc chromate there was a time-dependent decrease in the percent of cells with 4 centrioles (i.e.: S or G2 phase cells). After 24 h exposure to 0.2 ug/cm^2 zinc chromate the percent of cells with 4 centrioles was 45%, while after 120 h exposure, it was 36%. This decrease was not statistically significant but shows a clear trend. In parallel, the percent of cells with supernumerary centrioles also increased with exposure time and concentration. After 24 h exposure to 0.2 ug/cm^2 zinc chromate the percent of cells greater than 4 centrioles was 1%, while after 120 h

exposure, it was 8%. This increase was not statistically significant but also shows a clear trend.

Figure 3.17B shows the effects of Cr(VI) exposure on centriole number in mitotic cells. Normal mitotic cells have four centrioles at any mitotic phase. In mitotic cells, there was a statistically significant decrease ($p<0.05$) in the percent of cells with four centrioles. After 24 h exposure to 0.2 ug/cm^2 zinc chromate there were 94% of mitotic cells with 4 centrioles, while after 120 h exposure, the percent of cells decreased to 67%. In parallel, there was a statistically significant increase ($p<0.05$) in the percent of mitotic cells with supernumerary centrioles. After 24 h exposure to 0.2 ug/cm^2 zinc chromate, the percent of mitotic cells with supernumerary centrioles was 6%, while after 120 h exposure the percent of cells increased to 30%. No changes were observed in the percent of mitotic cells with 3 centrioles. After 24 h exposure to 0.2 ug/cm^2 zinc chromate there were 0% interphase cells with 3 centrioles, while after 120 h the percent of cells was 3%.

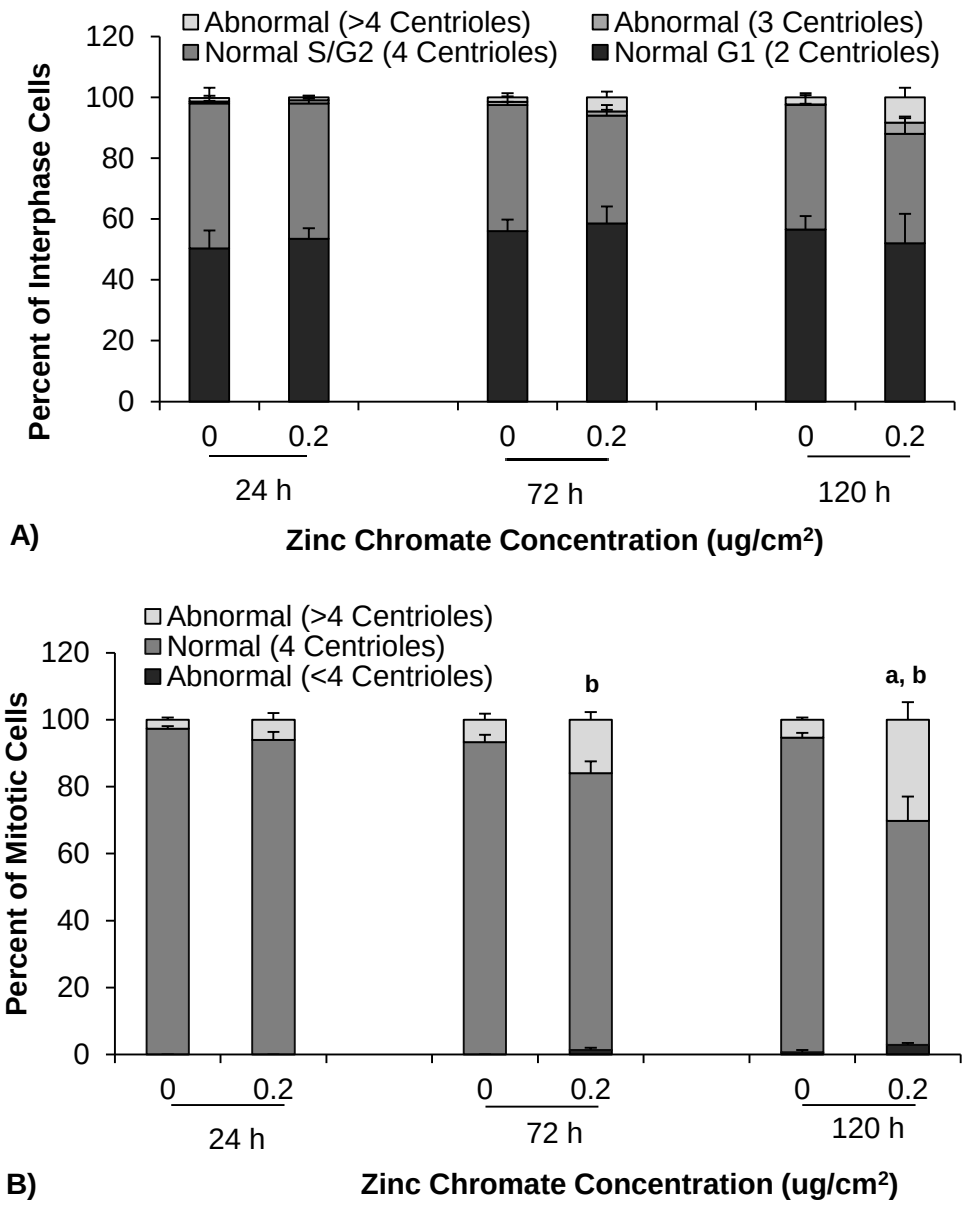

Figure 3.17. Chronic Exposure to Cr(VI) Induces Supernumerary Centrioles in Interphase and Mitotic Cells. This figure shows that Cr(VI) exposure induces an increase in centriole numbers in interphase and mitotic cells. **A)** Interphase cells exposed to Cr(VI) show a time-dependent decrease in the percent of cells with 4 centrioles and an increase in the percent of cells with greater than four centrioles. **B)** Mitotic cells exposed to Cr(VI) show a time-dependent decrease in the percent of cells with 4 centrioles and an increase in the percent of cells with greater than 4 centrioles. **a**, Cells with supernumerary centrioles are statistically different from the control ($p<0.05$); **b**, Cells with normal number of centrioles are statistically different from the control ($p<0.05$). Data represent an average of three independent experiments ± the standard error of the mean.

3.3.2. Particulate Cr(VI) Induces Premature Centriole Disengagement

When cells divide, each daughter cell inherits one centrosome with two centrioles. Each centriole will duplicate once during the following S phase in order to maintain a correct number of centrioles for the future two daughter cells. Centriole duplication is regulated through the engagement of the inherited centrioles. While engaged, centriole duplication is inhibited. However, when centrioles disengage, centrioles can undergo duplication. The increase in centriole numbers observed in cells exposed to Cr(VI) suggests that some Cr(VI)-treated cells are undergoing multiple rounds of centriole duplication. Given that centriole disengagement is the licensing factor for centriole duplication, we analyzed centriole disengagement after Cr(VI) exposure.

Normal centriole disengagement usually occurs as cells exit mitosis or very early in G1 phase (Agircan et al., 2014). Hence, we hypothesized that Cr(VI)-treated cells might exhibit premature centriole disengagement (i.e.: occurring in S or G2 phase or in mitosis before anaphase). This could result in centrosome amplification because disengaged centrioles can undergo re-duplication thus increasing centriole and centrosome numbers (Tsou and Stearns, 2006a). Since Cr(VI) exposure induces increases in both centriole and centrosome numbers, premature centriole disengagement seems a feasible mechanism for Cr(VI)-induced centrosome amplification.

To quantify centriole disengagement we analyzed the ratios of centriolar proteins centrin and C-Nap1. Centrin is a core component of centrioles while C-Nap1 localizes to the free proximal end of centrioles. When two centrioles are engaged, they have two centrin foci (one from each centriole) and one C-Nap1 foci at the free proximal end of the mother centriole (Tsou and Stearns, 2006b). Thus, engaged centrioles have a 2:1 centrin:C-Nap1 foci ratio. By contrast, disengaged centrioles have two free proximal

ends, one from the mother centriole and one from the now disengaged daughter centriole creating a 1:1 centrin:C-Nap1 foci ratio (Figure 3.18).

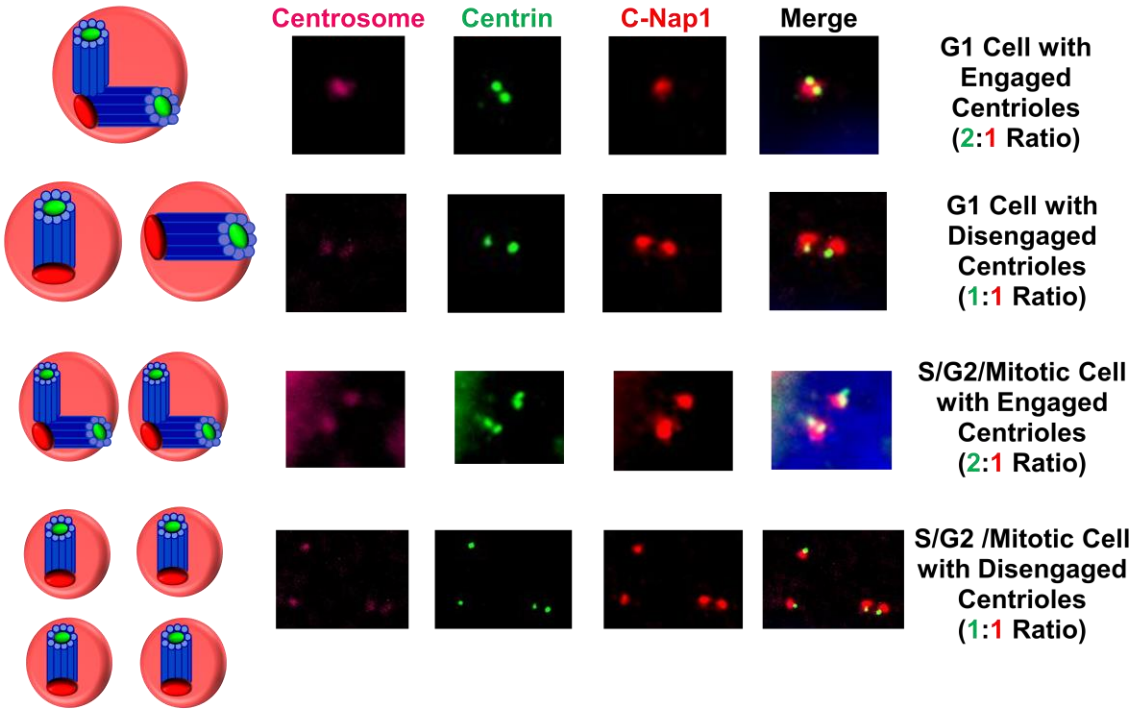

Figure 3.18. Centriole Disengagement and Centrin/C-Nap1 Ratios. This figure shows schematics and representative images of cells with engaged and disengaged centrioles and their corresponding centrin/C-Nap1 ratio. Pink circles represents centrosomes, blue cylinders represent centrioles with centrin shown in green, while red circles represent C-Nap foci. G1 cells with engaged centrioles have one centrosome with 2 centrioles and one C-Nap1 focus, while G1 cells with disengaged centrioles have two centrosomes, each with one centriole and one C-Nap1 focus. Cells in S, G2 or mitosis with engaged centrioles have two centrosomes, each with two centrioles and one C-Nap1 focus, while cells with disengaged centrioles have four centrosomes, each with an individual centriole and C-Nap1 focus.

Figure 3.19 shows the effects of Cr(VI) on centriole disengagement in G1, S/G2 and mitotic cells. For this analysis we quantified centrin/C-Nap1 ratios in interphase and mitotic cells focusing the analysis in cells that have a normal number of centrioles. Normal G1 cells have two centrioles and normal S, G2 and mitotic cells have four centrioles. Cells with supernumerary centrioles display centrosomes with more than 2 centrioles as well as centriolar defects such as centrosomes without centrioles, which

make centrin/C-Nap1 ratios very difficult to determine. Moreover, because centriole numbers are abnormal it is impossible to determine the original centrioles which underwent disengagement. In cells with normal number of centrioles, these limitations are not present.

First, we analyzed centriole disengagement in interphase cells with two centrioles which are considered G1 cells. Figure 3.19A shows that Cr(VI) exposure induces a time-dependent increase in centriole disengagement in G1 cells. This increase was not found to be statistically significant but the data show a strong trend. After 24 h exposure to 0.1, 0.15 and 0.2 ug/cm^2 zinc chromate, centriole disengagement was present in 49, 45 and 37% of interphase cells with two centrioles, respectively; while after 120 h exposure the percent of cells with centriole disengagement was 72, 75 and 88%, respectively. It is worth mentioning that centriole disengagement can occur in early G1 and as such this increase observed after Cr(VI) exposure cannot be considered abnormal.

Next, we analyzed centriole disengagement in interphase cells with 4 centrioles, which can either be S or G2 phase cells. Figure 3.19B shows that in this population of cells Cr(VI) induced a statistically significant time- and concentration-dependent increase in centriole disengagement ($p<0.05$). After 24 h exposure to 0.1, 0.15 and 0.2 ug/cm^2 zinc chromate, centriole disengagement was present in 1, 5 and 4% of interphase cells with 4 centrioles, respectively; while after 120 h exposure the percent of cells with centriole disengagement was 25, 40 and 51%, respectively. This increase in disengagement is abnormal and premature with respect to the following cell cycle, which is when centrioles from previous cycle should disengage. Thus, the data show that chronic exposure to Cr(VI) causes premature centriole disengagement in interphase cells.

Last, we analyzed centriole disengagement in mitotic cells whose normal centriole number is four. Figure 3.19C shows that in normal mitotic cells Cr(VI) does not

cause centriole disengagement. After 24 h exposure to 0.2 ug/cm^2 zinc chromate, centriole disengagement was not present in any mitotic cells, while after 120 h exposure the percent of mitotic cells with centriole disengagement was 3%. This slight increase was not statistically significant.

Figure 3.19. Chronic Exposure to Cr(VI) Induces Premature Centriole Disengagement in Interphase Cells with 4 Centrioles. This figure shows that chronic exposure to zinc chromate induces premature centriole disengagement in S/G2 cells. **A)** Centriole disengagement in G1 cells (i.e.: interphase cells with 2 centrioles) **B)** Centriole disengagement in S/G2 cells (i.e.: interphase cells with 4 centrioles) **C)** Centriole disengagement in mitotic cells. *Statistically significant difference from the control ($p<0.05$). Data represent an average of three independent experiments ± the standard error of the mean.

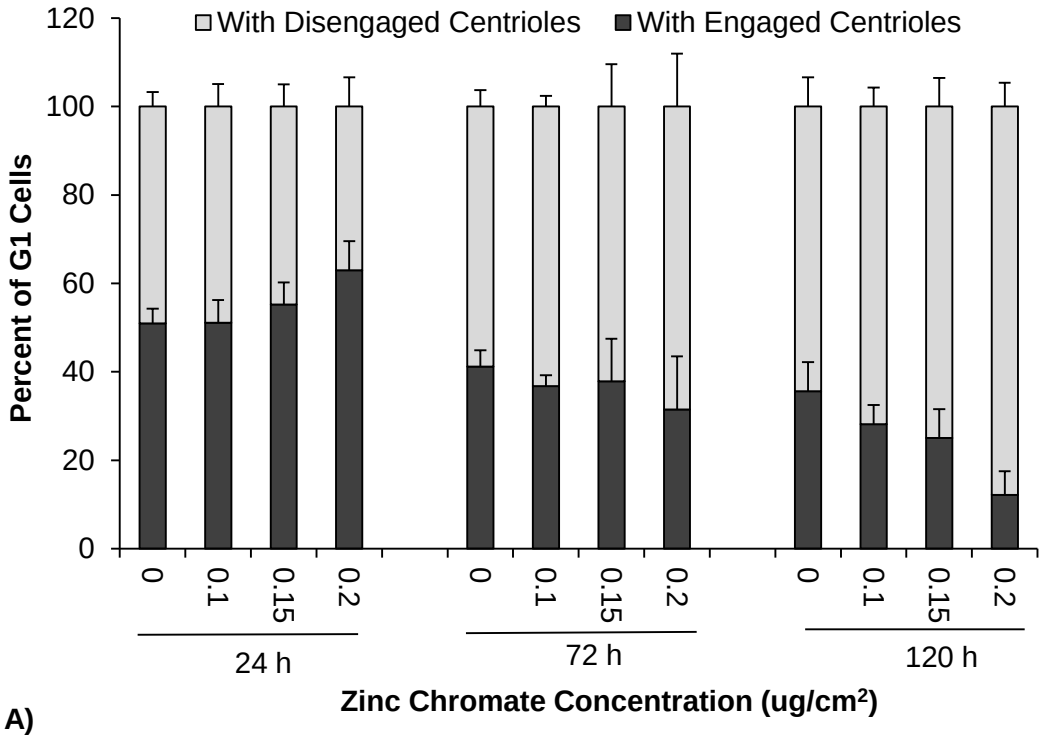

A)

Figure 3.19. Continued.

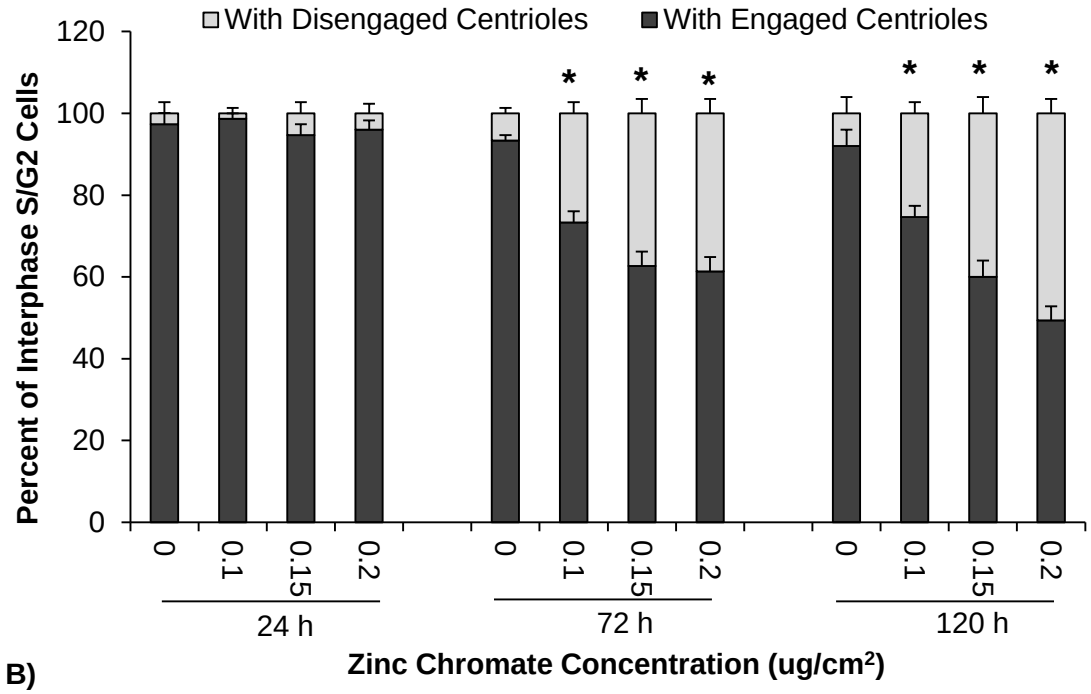

B)

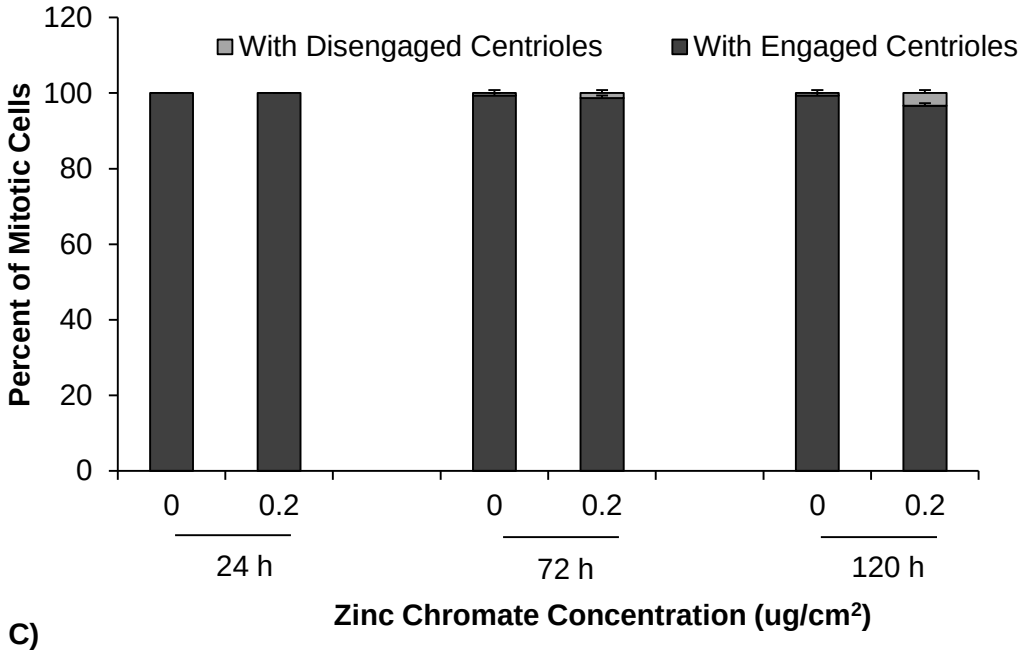

C)

For the centriole disengagement analysis, we made the assumption that cells with two centrioles were in G1 phase, and that cells with four centrioles were in either S or G2 phase. To support the notion that Cr(VI) causes premature centriole disengagement in S/G2 cells we stained cells with cyclin D1, a G1 phase cell cycle marker. We quantified centrioles in cyclin D1-positive cells and found that indeed, cells with two centrioles are in G1 phase (Figure 3.20). Moreover, exposure to 0.2 ug/cm^2 zinc chromate for 24 and 72 h did not change the percent of cyclin D1-positive cells with two centrioles. There was a slight and statistically significant increase in the percent of cells in G1 phase with four centrioles at 120 h, but this small increase (6%) cannot account for all of the centriole disengagement observed in cells with four centrioles after 120 h exposure (Figure 3.19B). This data confirms that interphase cells with two centrioles are in G1 phase and interphase cells with four centrioles are not, and as such, they must be in S or G2 phase, and supports that premature centriole disengagement after Cr(VI) exposure is in S/G2 cells as shown in Figure 3.19B.

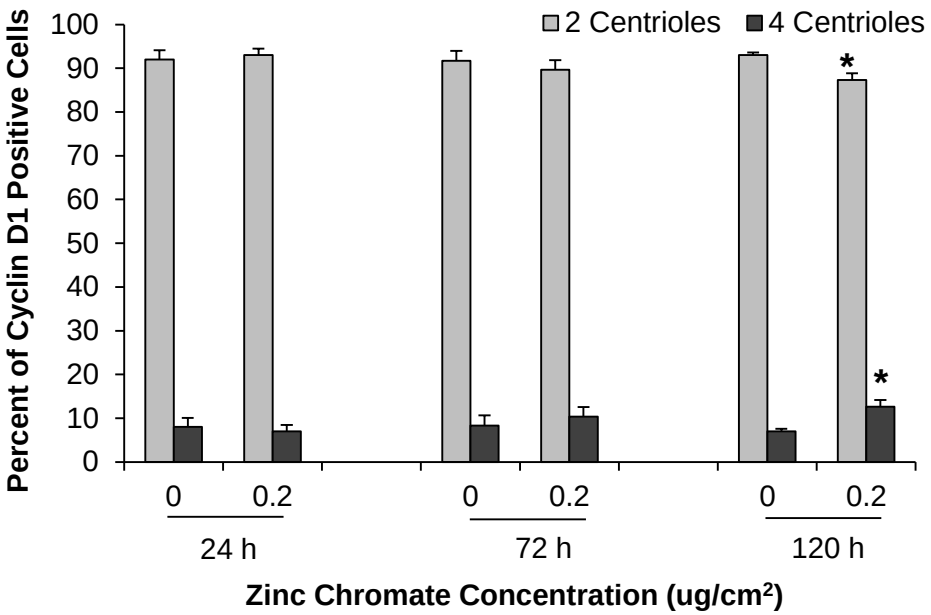

Figure 3.20. Number of Centrioles in G1 cells After Cr(VI) Exposure. This figure shows the number of centrioles in cells stained with cyclin D1, a G1 phase marker. The majority of cyclin D1 positive cells have two centrioles. There is a small increase in the percent of G1 cells that have four centrioles after 120 h exposure to Cr(VI). *Statistically significant difference from the control ($p<0.05$). Data represent an average of three independent experiments ± the standard error of the mean.

3.3.3. Particulate Cr(VI) Induces Premature Centrosome Separation

Duplicated centrosomes formed in S phase are normally held together by the G1-G2 tether. This linker is severed at the G2/M transition and allows centrosomes to separate in prophase so that they can be positioned in a bipolar fashion. Interestingly, depletion of G1-G2 tether proteins by siRNA caused increased centriole disengagement when cells were exposed to a DNA damaging agent (Conroy et al., 2012). This suggests that the G1-G2 tether may be involved in protecting centriole engagement. Since Cr(VI) is a strong DNA damaging agent and causes centriole disengagement, we hypothesized that Cr(VI) exposure might also disrupt this linker. Hence, we measured centrosome separation in interphase cells under the premise that if this linker is severed, centrosomes would prematurely separate in interphase (Mayor et al. 2000; Faragher and Fry, 2003; Bahe et al., 2005; Mardin and Schiebel, 2012). Using γ-tubulin as a marker

for centrosomes, we measured the distance between pairs of centrosomes. Centrosomes were classified as separated if the distance between them was greater than 2 um (Mayor et al., 2000) (Figure 3.21).

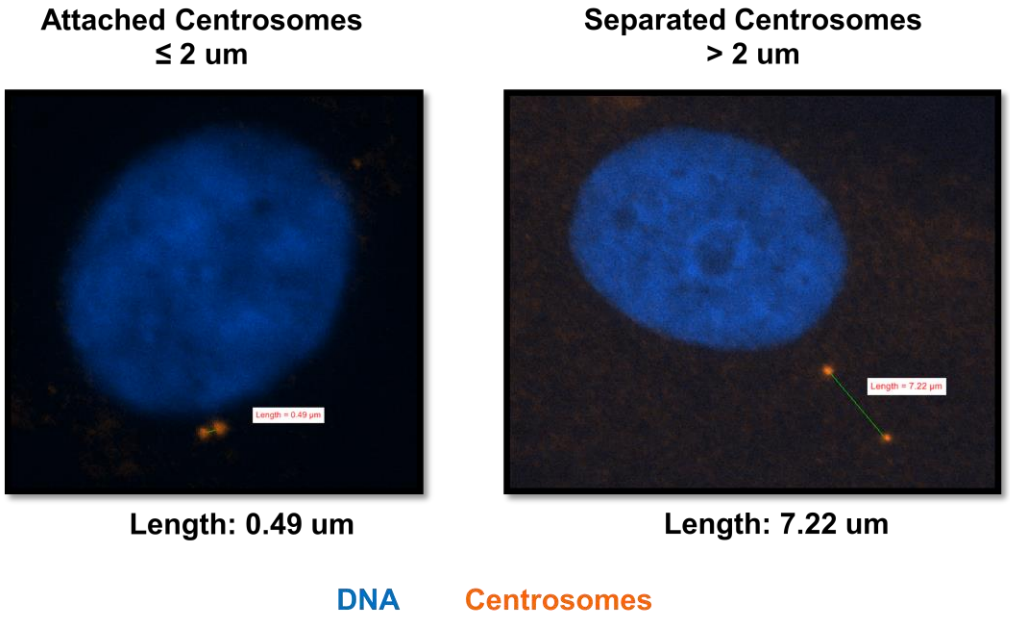

Figure 3.21. Representative Images of Centrosome Separation Analysis. This figure shows an interphase cell with centrosomes that are still attached to each other (left) and an interphase cell with separated centrosomes (right). Blue staining corresponds to DNA and orange staining to centrosomes. Green lines are used to measure the distance between each pair of centrosomes. Centrosomes with distances >2 um are considered separated.

Figure 3.22 shows that chronic exposure to Cr(VI) induced a statistically significant ($p<0.05$) time- and dose-dependent increase in the percent of interphase cells with separated centrosomes. After 24 h exposure to 0.1, 0.15 and 0.2 ug/cm^2 zinc chromate the percent of interphase cells with separated centrosomes was 15, 15 and 13%, while after 120 h exposure the percent of cells increased to 30, 33 and 36%, respectively. Given that the centrosome separation analysis was done in interphase cells and that centrosomes normally separate in prophase of mitosis, centrosome separation induced by Cr(VI) is premature.

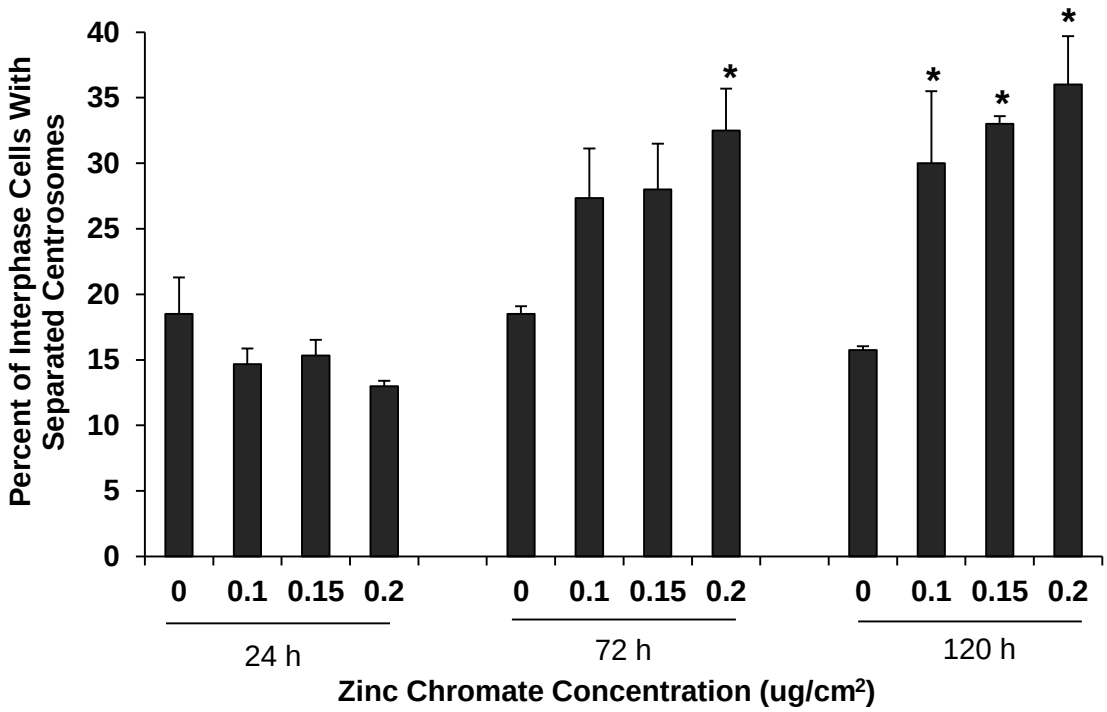

Figure 3.22. Chronic Exposure to Cr(VI) Induces Premature Centrosome Separation. This figure shows that chronic exposure to zinc chromate induces a time- and concentration-dependent increase in premature centrosome separation in interphase cells. *Statistically significant difference from the control ($p<0.05$). Data represent an average of three independent experiments ± the standard error of the mean.

Moreover, this time- and dose-dependent increase in premature centrosome separation in interphase cells correlates with the time- and dose-dependent increase in premature centriole disengagement observed in S/G2 cells (Figure 3.23A). More importantly, both premature centriole disengagement and premature centrosome separation also correlate with the increased centrosome separation observed in interphase cells after Cr(VI) exposure (Figure 3.23B and 3.23C).

Figure 3.23. Correlations between Centrosome Separation, Centriole Disengagement, and Centrosome Amplification. This figure shows that premature centriole disengagement and premature centrosome separation correlate with each other as well as with centrosome amplification in interphase cells. After chronic exposure to Cr(VI), all phenotypes show a similar increase. **A)** Correlation between premature centriole disengagement (left y axis) and premature centrosome separation (right y axis). **B)** Correlation between premature centriole disengagement (left y axis) and centrosome amplification (right y axis). **C)** Correlation between premature centrosome separation (left y axis) and centrosome amplification (right y axis). Data represent an average of three independent experiments ± the standard error of the mean.

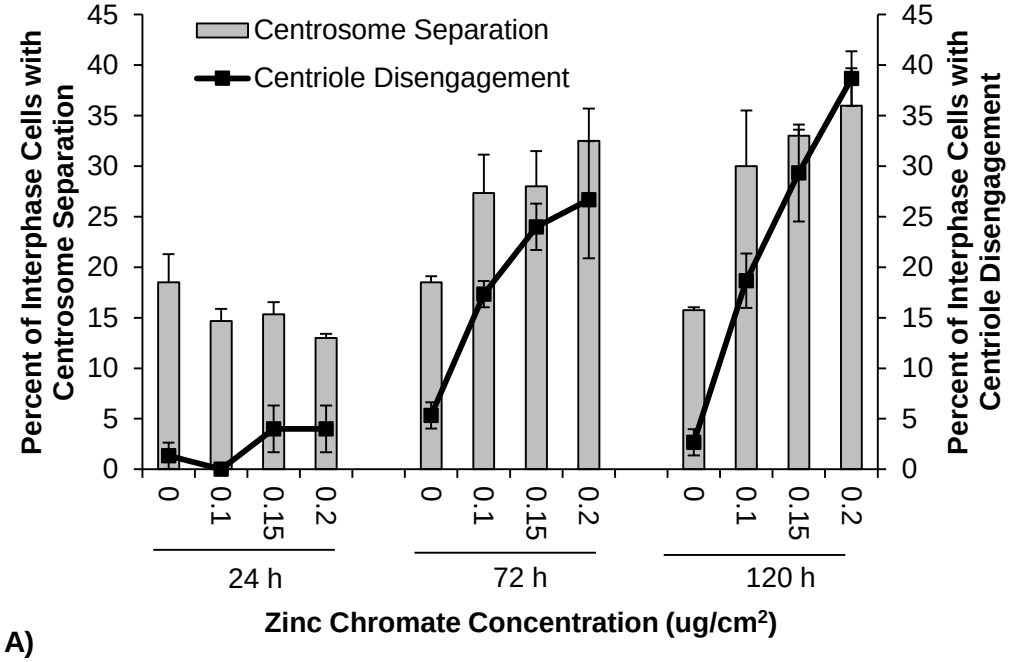

A)

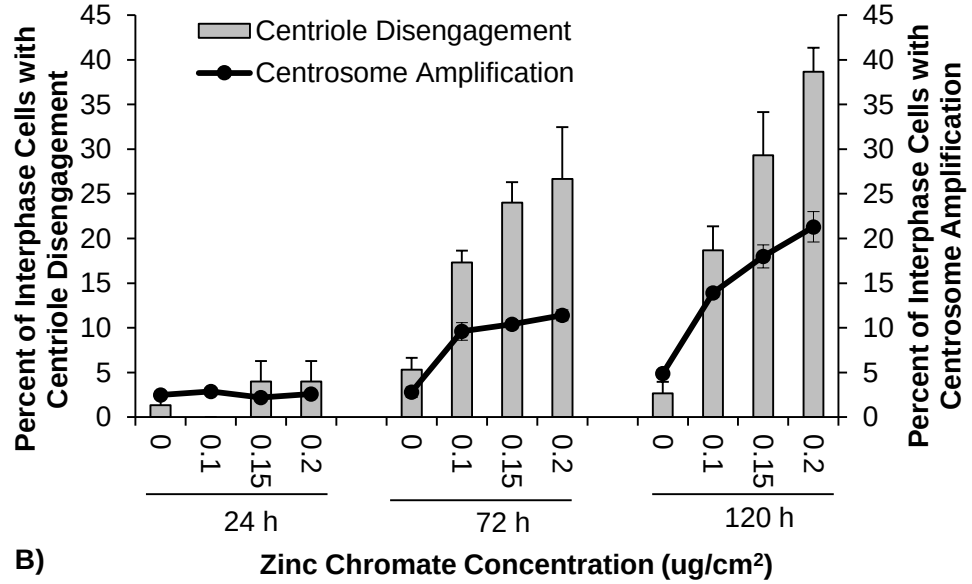

B)

Figure 3.23. Continued.

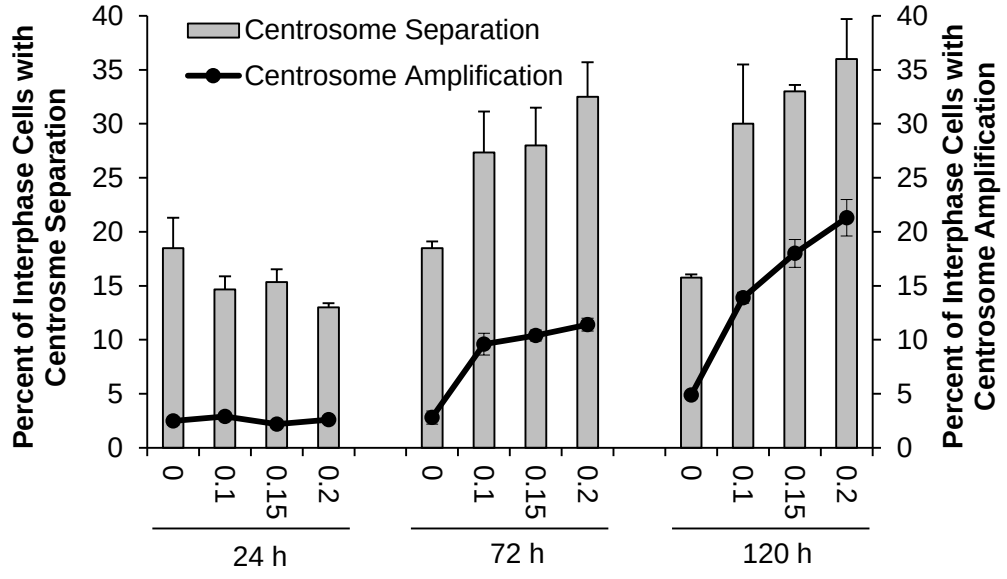

C)

3.3.4. Part 2 Summary

In Part 2 we have begun to elucidate some of the mechanism that may underlie the centrosome amplification observed after Cr(VI) exposure. The analysis of centrioles and centrosomes in interphase and mitotic cells after Cr(VI) exposure shows that chronic exposure to Cr(VI) causes a slight increase in supernumerary centrioles in interphase cells and a significant increase in supernumerary centrioles in mitotic cells. This suggests that centriole overduplication might play a role in Cr(VI)-induced centrosome amplification. The licensing step for centriole duplication is centriole disengagement. Consistent with the increase in supernumerary centrioles, chronic exposure to Cr(VI) induces a time- and dose- dependent increase in premature centriole disengagement in interphase cells during S/G2 phase. In addition, premature centrosome separation is also observed in interphase cells exposed chronically to Cr(VI). Both centriole engagement and centrosome attachment are possible due to protein linkers that link

centrioles and centrosomes together. Our data suggest that Cr(VI) is affecting these linkers proteins or their regulation causing the linkers to disrupt prematurely.

3.4. Part 3: Mechanisms of Particulate Cr(VI)-Induced Disruption of the Centriole Linkers

The formation and disruption of the centriole linkers are important aspects of centrosome cycle regulation. As such, they are tightly regulated by different proteins. In Part 3, we explore the effects of chronic exposure to particulate Cr(VI) on proteins involved in linker disruption. We analyzed protein levels and localization of proteins involved in centriole disengagement and centrosome separation, as well as their upstream regulator, Plk1 (Figure 3.24). The data show that particulate Cr(VI) increases the ratio of p-Plk1/Plk1. The separase-securin pathway that causes centriole disengagement is also affected by Cr(VI) through increased levels of active separase and decreased levels of securin, which are consistent with the observed centriole disengagement. The Nek2-Eg5 pathway involved in centrosome separation has decreased protein levels and decreased centrosome and microtubule localization after Cr(VI) exposure, suggesting that parallel mechanisms separate centrosomes after Cr(VI) exposure.

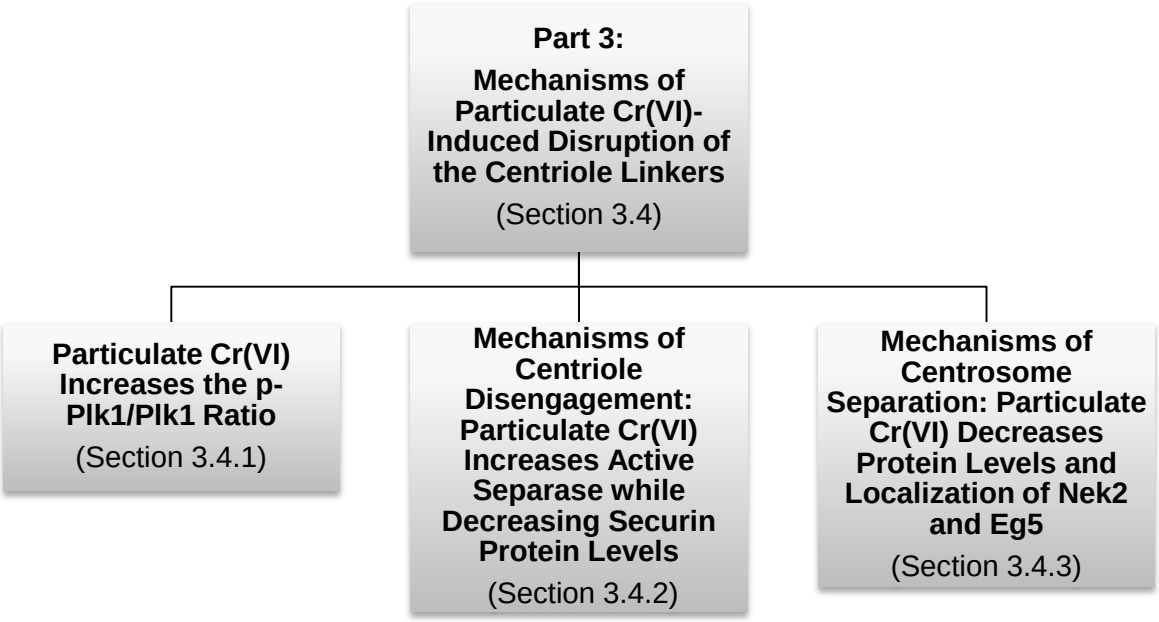

Figure 3.24. Organizational Flow Chart of Part 3: Mechanisms of Particulate Cr(VI)-Induced Disruption of the Centriole Linkers.

3.4.1. Particulate Cr(VI) Increases the p-Plk1/Plk1 Ratio

The disruption of the centriole linkers is a key event in the centrosome cycle. As such, it is tightly regulated by numerous proteins. Upstream of the regulation cascade is Polo-like kinase 1 (Plk1), a serine-threonine kinase involved in many aspects of the cell and centrosome cycles. Plk1 is activated by phosphorylation of its catalytic loop in threonine 210 (T210) during late G2 phase and remains active throughout mitosis.

Because of its pivotal role in centrosome linker disruption and given that Cr(VI) causes premature centriole disengagement and centrosome separation, we investigated the effects of Cr(VI) on the levels of active Plk1. Active Plk1 (p-Plk1) is phosphorylated on T210 and can be recognized by multiple commercially available antibodies. Hence, quantitative western blotting can be used to measure the levels of active protein. Also, because the overall activity of Plk1 in a cell is determined by the balance between its active and inactive states, we also measured levels of inactive Plk1. Furthermore, since

premature centriole disengagement and premature centrosome separation after Cr(VI) exposure were observed in interphase, we separated interphase cells from mitotic cells by doing a mitotic shake-off. This allowed us to analyze p-Plk1 and Plk1 protein levels in interphase and mitotic cells separately.

Figure 3.25A shows representative images of p-Plk1 and Plk1 western blots after 24 and 120 h exposure to 0.2 ug/cm^2 zinc chromate. The data show that in interphase cells (Figure 3.25B), Plk1 levels decrease significantly after Cr(VI) exposure ($p<0.05$). After 24 h exposure to 0.2 ug/cm^2 zinc chromate, Plk1 protein levels were 0.78 relative to control (set as 1), while after 72 and 120 h exposures, Plk1 protein levels were 0.33 and 0.32 relative to control. In contrast, p-Plk1 levels remain constant after Cr(VI) exposure. After 24 h exposure to 0.2 ug/cm^2 zinc chromate, p-Plk1 protein levels were 0.86 relative to control (set as 1), while after 72 and 120 h exposures, p-Plk1 protein levels were 0.77 and 0.90 relative to control.

In mitotic cells, both p-Plk1 and Plk1 decreased significantly after Cr(VI) exposure ($p <0.05$) (Figure 3.25C). Exposure to 0.2 ug/cm^2 zinc chromate for 24, 72 and 120 h decreased Plk1 levels to 0.97, 0.47 and 0.17 relative to control value, respectively. p-Plk1 levels also significantly decreased after Cr(VI) exposure ($p<0.05$). After 24, 72 and 120 h exposure to 0.2 ug/cm^2 zinc chromate, Plk1 levels were to 0.87, 0.82 and 0.52 relative to control, respectively.

Overall kinase activity in cells depends on a fine balance between active versus inactive forms (Domingo-Sananes et al., 2011). Hence, we calculated ratios of p-Plk1 versus Plk1 after Cr(VI) exposure (Figure 3.25D). A p-Plk1/Plk1 ratio greater than 1 indicates the balance is tilted towards an excess of active Plk1, while a ratio lower than 1 indicates the balance is tilted towards an excess of inactive Plk1. The data show that after chronic exposure to Cr(VI) the p-Plk1/Plk1 ratio is greatly increased. In interphase cells, after 24, 72 and 120 h exposure to 0.2 ug/cm^2 zinc chromate the p-Plk1/Plk1 ratio

increased to 1.2, 2.8 and 5.4, respectively. In mitotic cells, a similar increase was observed. After 24, 72 and 120 h exposure to 0.2 ug/cm^2 zinc chromate the p-Plk1/Plk1 ratios were 1, 2 and 3.9, respectively. The data indicate that chronic exposure to Cr(VI) increases p-Plk1 levels 4-6 fold over inactive Plk1. This suggest that Plk1 activity is increased after Cr(VI) treatment.

Figure 3.25. Cr(VI) Exposure Increases the p-Plk1/Plk1 Ratio. This figure shows that chronic exposure to Cr(VI) causes an overall increase in p-Plk1 levels. **A)** Representative images of western blots for p-Plk1 (red) and Plk1 (green), the merged images and loading control (B-actin, green). **B)** Protein levels of Plk1 (dark gray bars) and p-Plk1 (light grey bars) in interphase cells after Cr(VI) exposure. **C)** Protein levels of Plk1 (dark gray bars) and p-Plk1 (light grey bars) in mitotic cells after Cr(VI) exposure. **D)** Ratios of p-Plk1/Plk1 protein levels in interphase (dark grey bars) and mitotic cells (light grey bars). *Statistically significant difference from the control ($p<0.05$). Data represent an average of three independent experiments ± the standard error of the mean.

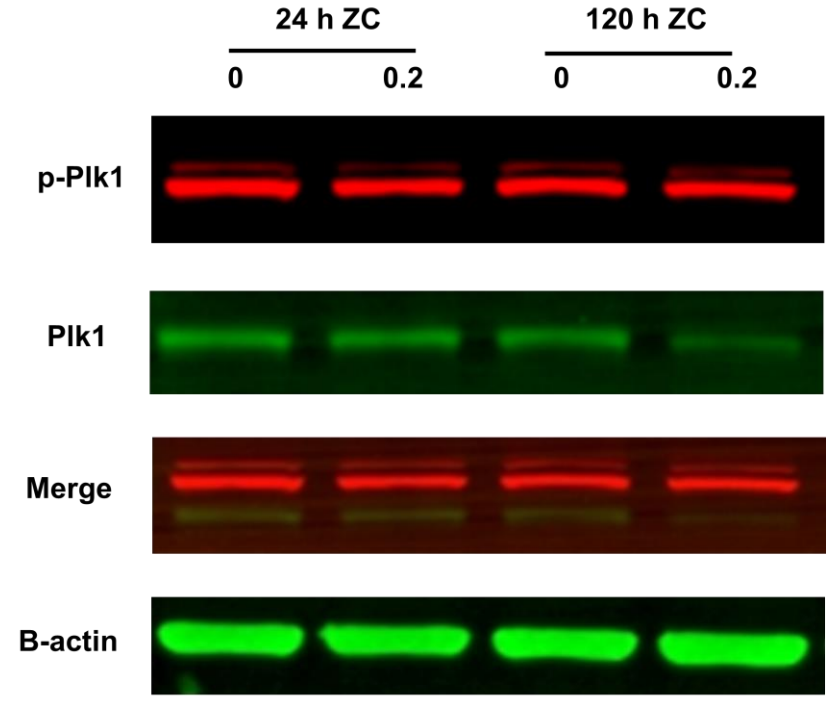

A)

Figure 3.25. Continued.

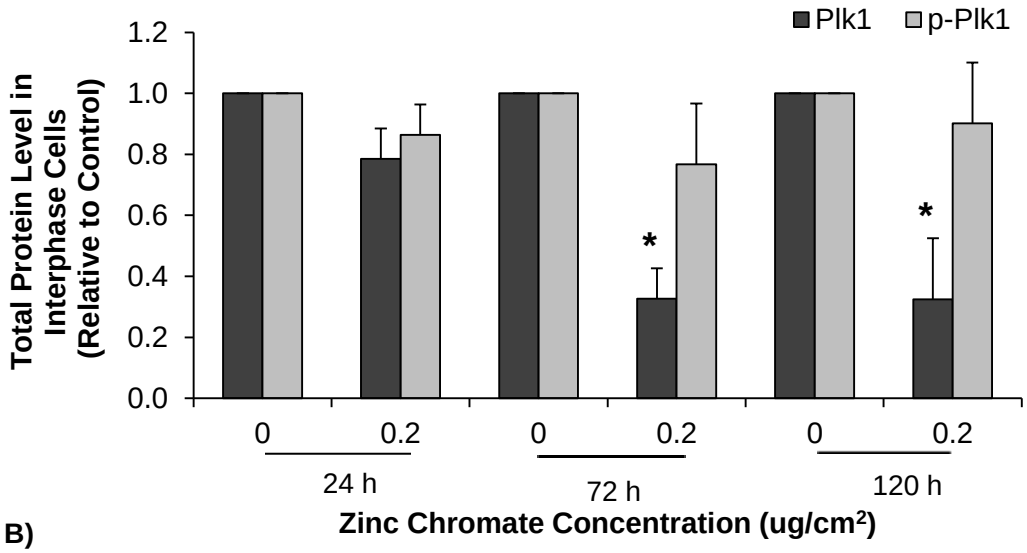

B)

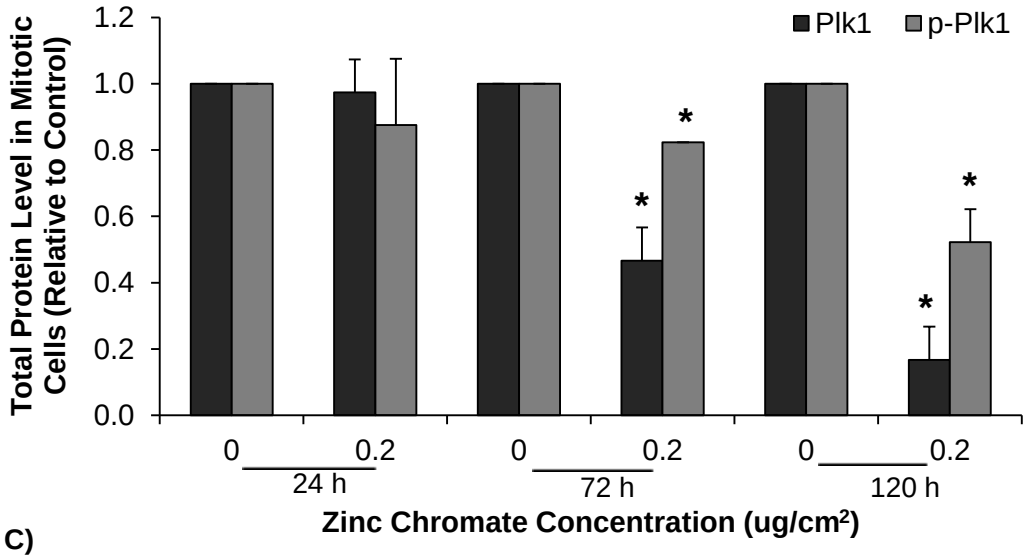

C)

Figure 3.25. Continued.

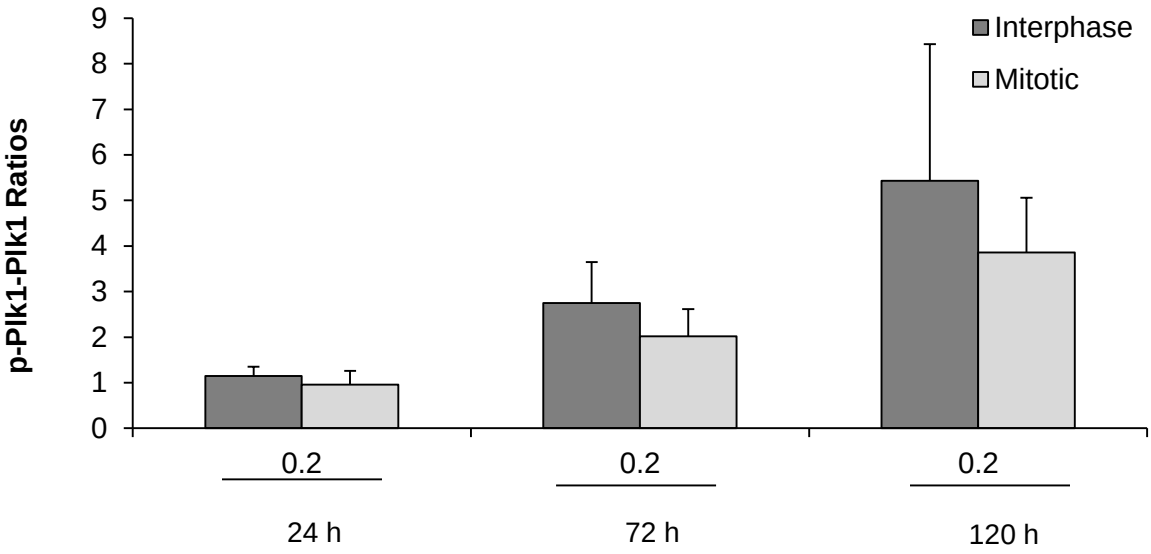

D)

3.4.2. Mechanisms of Centriole Disengagement: Particulate Cr(VI) Increases Active Separase while Decreasing Securin Protein Levels

Centriole disengagement is dependent on the activity of the protease separase (Figure 3.26). Separase activity is inhibited by securin, its binding partner. Plk1 activation activates the anaphase promoting complex/cyclosome (APC/C) which ubiquitinates proteins targeting them for degradation. One of the APC/C's main targets is securin. Upon securin degradation, separase becomes active and cleaves the proteins cohesin and pericentrin B involved in centriole engagement. In normal cells, this happens at the end of mitosis or early G1. Since our data show that chronic exposure to Cr(VI) causes premature centriole disengagement in interphase cells and that p-Plk1 levels are increased after Cr(VI) exposure, we analyzed separase and securin levels. For this, we used western blots to measure separase and securin protein levels in interphase cells. Because premature centriole disengagement is observed in interphase, our analysis was limited to interphase cells.

Figure 3.27A shows representative images of separase and securin western blots. For separase analysis, we quantified two separate bands. The 220 kDa band corresponding to full-length separase, which is the inactive form bound to securin. We also quantified the 65 kDa band, which is a product of separase autocleavage upon its activation following securin degradation. Quantifying these bands allows us to indirectly assess separase activity after Cr(VI) exposure. Figure 3.27B shows the effects of Cr(VI) on separase protein levels. Full-length separase levels significantly decreased ($p<0.05$) after chronic exposure to Cr(VI). After 24 h exposure to 0.2 ug/cm^2 zinc chromate separase protein levels was 1.12 relative to control, while after 72 and 120 h exposures protein levels decreased to 0.44 and 0.07 relative to control, respectively. In contrast, protein levels of cleaved separase significantly increased after chronic Cr(VI) treatment ($p<0.05$). At 24 h exposure to 0.2 ug/cm^2 zinc chromate, cleaved separase levels were 1.2 relative to control, while after 120 h exposure protein levels increased to 1.6 relative to control.

Figure 3.27B also shows the effects of Cr(VI) on securin protein levels. Securin protein levels significantly decreased after Cr(VI) treatment ($p<0.05$). After 24 h exposure to 0.2 ug/cm^2 zinc chromate, securin protein levels were 0.89 relative to control while after 72 and 120 h exposures, protein levels were 0.36 and 0.17 relative to control, respectively.

Overall, our data show that chronic exposure to particulate Cr(VI) decreases securin protein levels. Consistent with this decrease, protein levels of full-length separase (inactive form) also decrease after Cr(VI) exposure. Because protein levels of cleaved separase (active form) increase after Cr(VI) treatment, the decrease in full-length separase can be partially attributed to separase activation and autocleavage after securin degradation.

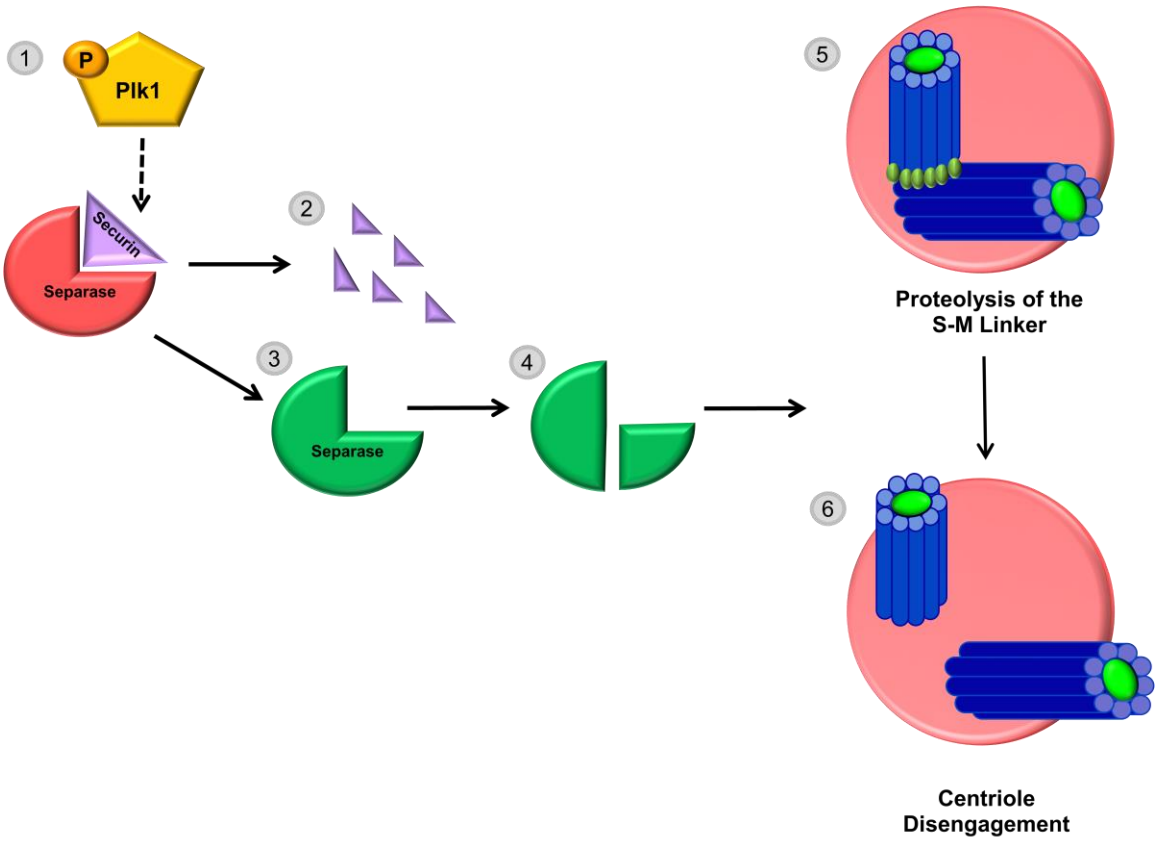

Figure 3.26. Centriole Disengagement Mechanism. This figure shows the molecular mechanism underlying centriole disengagement. 1) Plk1 activation in mitosis causes a signaling cascade that acts upon many substrates, including securin. 2) Securin is degraded by the proteasome during anaphase. 3) Securin degradation frees separase which becomes active. 4) Separase activation leads to auto-cleavage. 5) Active separase acts on proteins forming the S-M linker leading to its proteolysis. 6) S-M linker proteolysis causes centriole disengagement in late mitosis/early G1.

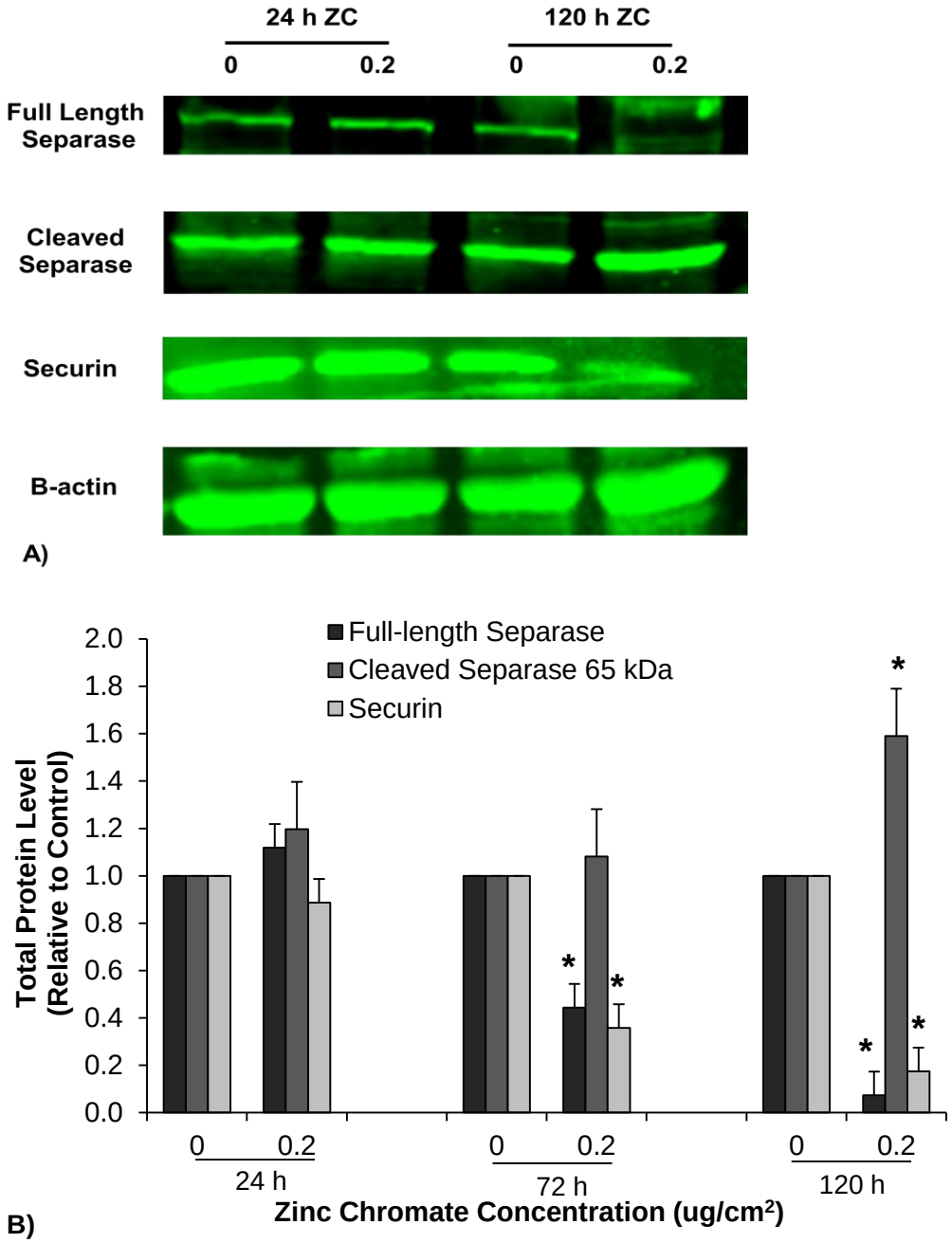

Figure 3.27. Cr(VI) Induces an Increase in Active Separase and Decreases Securin. This figure shows that chronic exposure to particulate Cr(VI) decreases securin and full-length separase protein levels while increasing levels of autocleaved separase. **A)** Representative images of western blots showing bands corresponding to full-length separase, cleaved separase, securing and B-actin (loading control). B) Quantification of full-length separase (light black bars), cleaved separase (dark grey bars) and securin (light grey bars). *Statistically significant difference from the control ($p<0.05$). Data represent an average of three independent experiments ± the standard error of the mean.

3.4.3. Mechanisms of Centrosome Separation: Particulate Cr(VI) Decreases Protein Levels and Localization of Nek2 and Eg5

Given that Cr(VI) causes premature centrosome separation, we examined the effects of Cr(VI) on proteins that control centrosome separation. As with centriole disengagement, centrosome separation is also regulated via Plk1 activation and the Nek2A-Mst1-PP1 complex (Figure 3.28). Nek2A is a kinase that can undergo autophosphorylation. However, phosphate groups on Nek2A are removed by the phosphatase PP1, keeping the complex inactive. Upon Plk1 activation, Plk1 phosphorylates Mst2 inducing a conformational change that prevents binding of PP1. As a result, PP1 can no longer dephosphorylate Nek2A and Nek2A remains phosphorylated, increasing its kinase activity. Kinase activity reaches a peak during the G2/M transition and Nek2A phosphorylates linker proteins C-Nap1, Rootletin and LRRC45 leading to their removal and releasing centrosomes from each other so that they can separate in prophase.

To study the effects of Cr(VI) on Nek2A, we analyzed protein levels with western blots as well as its centrosomal localization using immunofluorescence. Figure 3.29A shows representative images of Nek2 western blots. Nek2 exists in isoforms A and B with 48 and 46 kDa, respectively. Because of their molecular weight difference, these isoforms are separated during electrophoresis and appear as two distinct bands on blots. We only quantified the Nek2A band since this is the isoform involved in centrosome separation. Figure 3.29B shows that chronic exposure to particulate Cr(VI) causes a statistically significant decrease in Nek2A protein levels ($p<0.05$). After 24 h exposure to 0.1, 0.15 and 0.2 ug/cm^2 zinc chromate, Nek2A protein levels were 97, 93 and 76 percent of control, respectively; while after 120 h exposure protein levels decreased to 57, 69 and 23 percent of control, respectively.

Since Nek2A activity is required at the centrosome, we also analyzed its centrosomal localization after Cr(VI) exposure. Figure 3.30A shows representative images of cells with Nek2 localized at the centrosomes. Currently, isoform-specific antibodies for Nek2 are not available so we could not narrow the localization analysis to solely Nek2A. Figure 3.30B shows that chronic exposure to Cr(VI) decreases centrosomal localization of Nek2 ($p<0.05$). After 24 h exposure to 0.1, 0.15 and 0.2 ug/cm^2 zinc chromate, the percent of cells with Nek2 localized to the centrosomes was 97, 93 and 76 percent, respectively; while after 120 h exposure the percent of cells with Nek2 localized to the centrosome was 28, 11 and 10 percent of control, respectively. In normal cells, Nek2 activity and centrosomal localization are required in late G2 phase. Hence, we also analyzed Nek2 localization in G2 phase cells using cyclin B1 as a G2 phase marker (Figure 3.31A). Interestingly, chronic exposure to Cr(VI) did not change centrosomal localization of Nek (Figure 3.31B). After 24, 72 and 120 h exposure to 0.2 ug/cm zinc chromate the percent of G2 phase cells with centrosomal localization of Nek2 was 95, 93 and 94%, respectively.

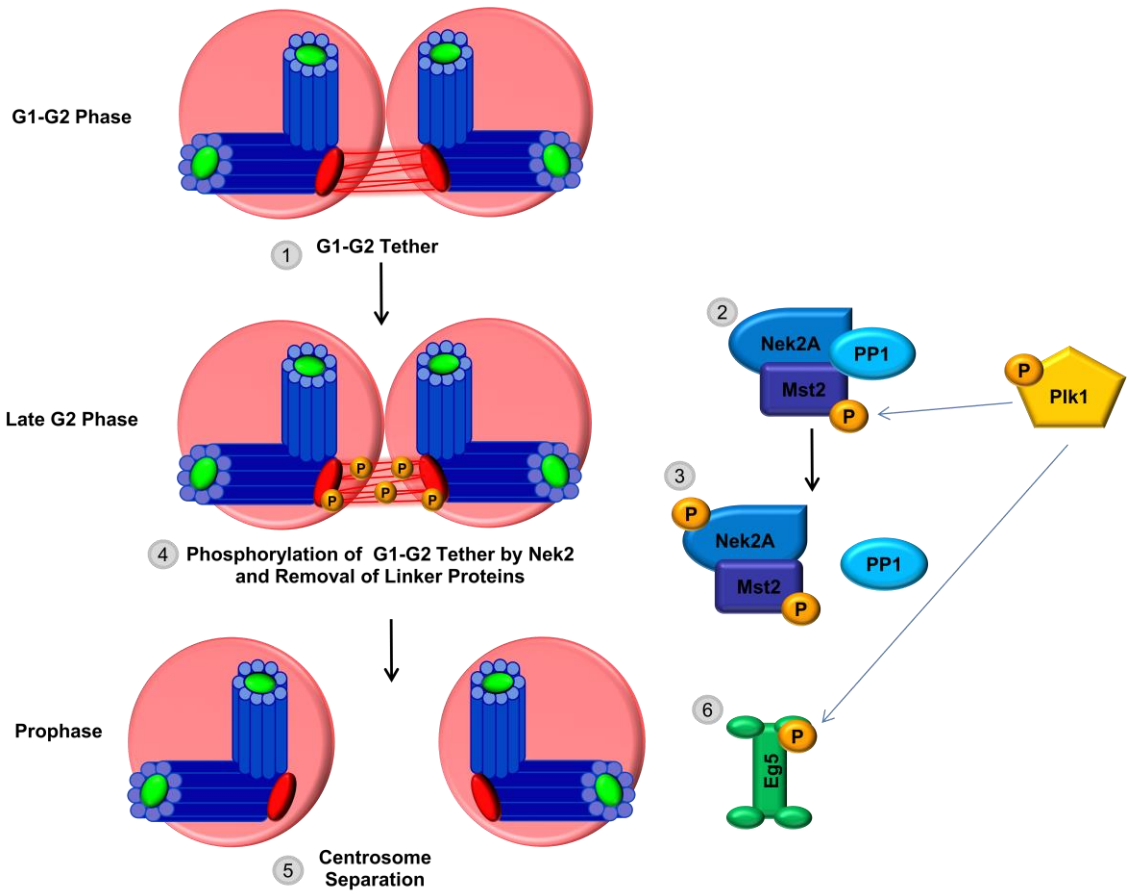

Figure 3.28. Centrosome Separation Mechanism. This figure shows the mechanism of centrosome separation. 1) The G1-G2 tether holds centrosomes together. 2) The kinases Nek2 and Mst2 form a complex with phosphatase PP1. Mst2 is phosphorylated by active Plk1 at the end of the G2/M transtition. 3) Mst2 phosphorylation induces a conformational change that prevents PP1 binding. This allows Nek2 to become active and autophosphorylate. 4) Active Nek2 phosphorylates G1-G2 tether proteins leading to their removal from centrosomes. 5) In prophase, the absence of the G1-G2 tether allows for centrosome separation. This is achieved through microtubule movements produced by the motor protein Eg5. 6) Plk1 phosphorylation contributes to Eg5 activation.

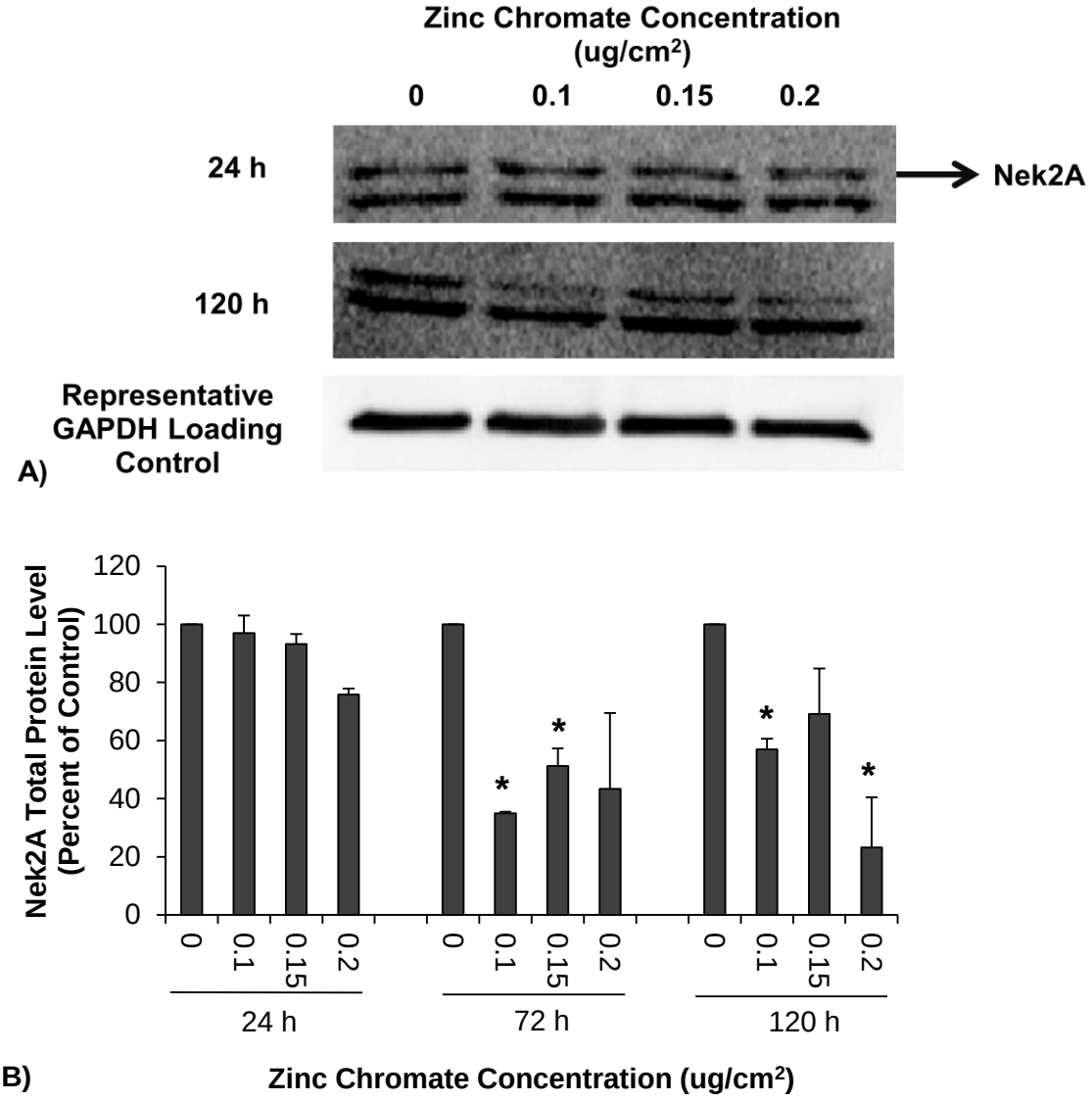

Figure 3.29. Cr(VI) Decreases Nek2A Protein Levels. This figure shows that chronic exposure to Cr(VI) decreases Nek2A protein levels. **A)** Representative images of Nek2 western blots. The two bands correspond to two isoforms: Nek2A and Nek2B. Nek2A is the top band. **B)** Total protein levels of Nek2A after Cr(VI) exposure. *Statistically significant difference from the control ($p<0.05$). Data represent an average of two independent experiments ± the standard error of the mean.

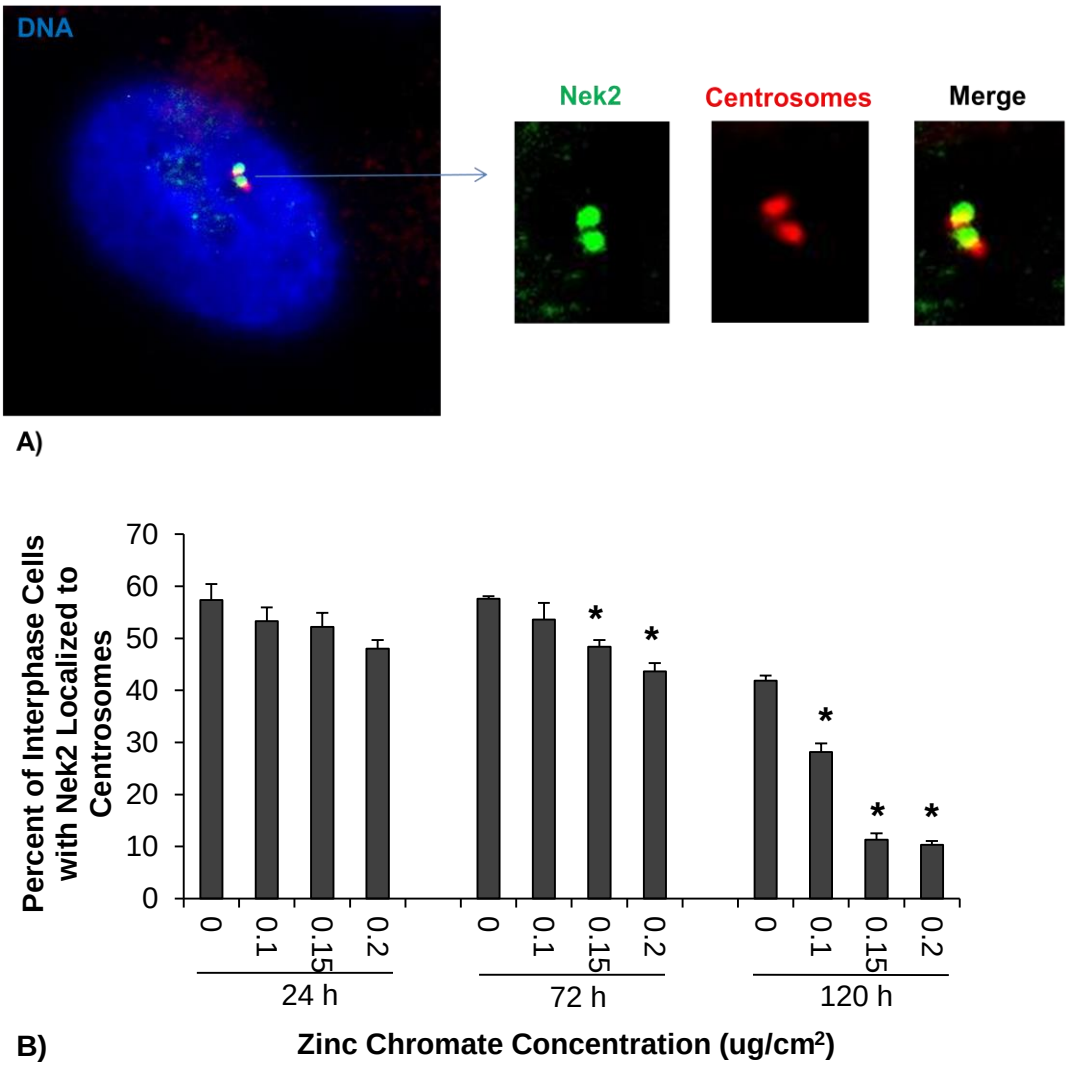

Figure 3.30. Nek2 Centrosomal Localization in Interphase Cells after Cr(VI) Exposure. This figure shows that chronic exposure to Cr(VI) decreases Nek2A centrosomal localization in interphase cells. **A)** Representative images of an interphase cell with Nek2 localization to the centrosomes. Blue, green and red represent DNA, Nek2, and centrosomes, respectively. **B)** Nek2 centrosomal localization after Cr(VI) exposure. *Statistically significant difference from the control ($p<0.05$). Data represent an average of three independent experiments ± the standard error of the mean.

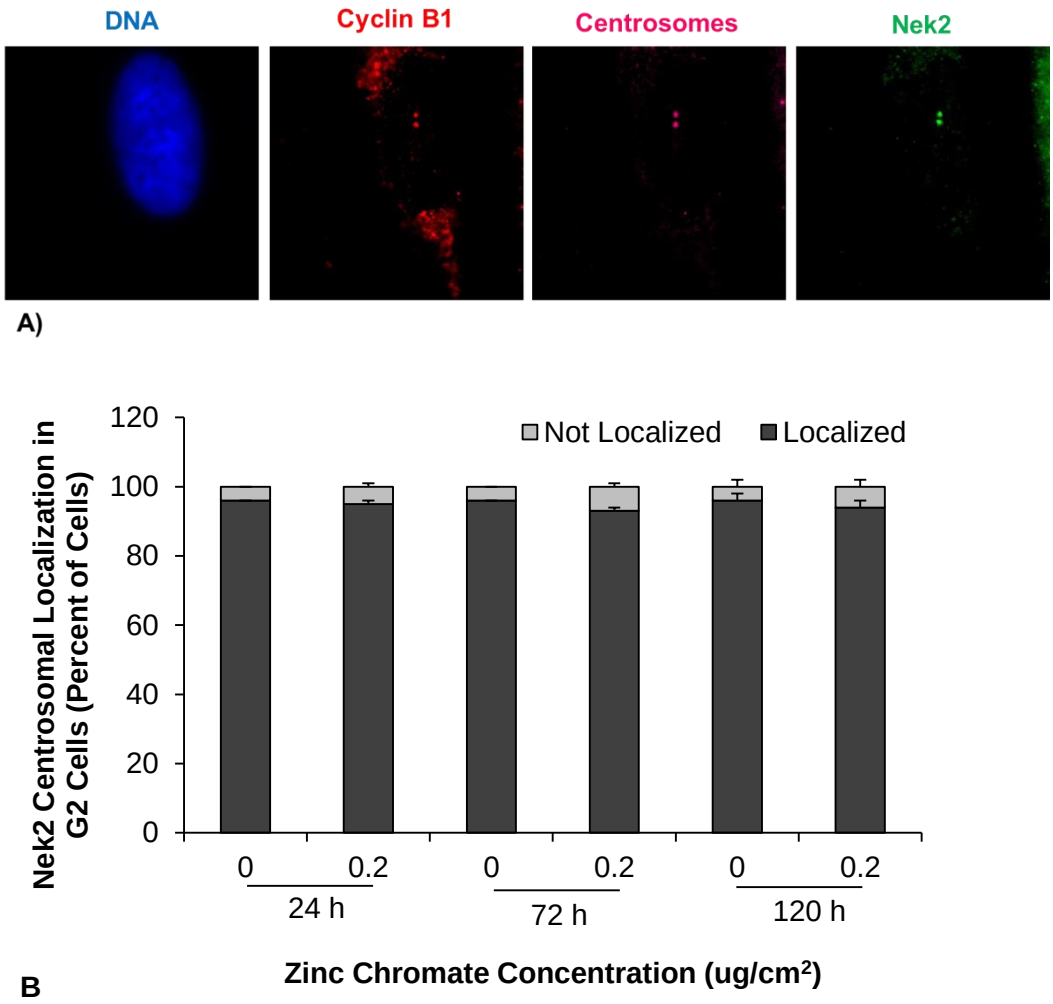

Figure 3.31. Nek2 Centrosomal Localization in G2 Phase Cells after Cr(VI) Exposure. This figure shows that chronic exposure to Cr(VI) does not affect Nek2 centrosomal localization in G2 phase cells. **A)** Representative images of a G2 cell with Nek2 localization to centrosomes. Blue, red, pink and green represent DNA, cyclin D1, centrosomes and Nek2, respectively. **B)** Nek2 centrosomal localization in G2 phase cells after Cr(VI) exposure. Data represent an average of two independent experiments ± the standard error of the mean.

Cr(VI) exposure decreases Nek2 protein levels and localization which are in disagreement with the premature centrosome separation observed in interphase cells. However, lack of Nek2 can be compensated by Eg5, the motor protein responsible for microtubule movements involved in centrosome separation (Mardin et al., 2010). Consequently, we analyzed protein levels of Eg5 in interphase cells after Cr(VI) exposure. Binding of Eg5 to microtubules is dependent on Cdk1-dependent phosphorylation on threonine 927 (Blangy et al., 1995). Since there are antibodies that recognize this phosphorlyated site, we also measured phosphorylated Eg5 (p-Eg5) protein levels. Because Eg5 activity is restricted to microtubules, we also analyzed the effects of Cr(VI) on its microtubule localization.

Figure 3.32A shows representative images of western blots for Eg5 and p-Eg5, the merged images and B-actin which was used as a loading control. Western blots were performed with interphase cell lysates, following the same procedures to remove mitotic cells used for the Plk1 and p-Plk1 western blots. Chronic exposure to Cr(VI) significantly decreased Eg5 and p-Eg5 protein levels ($p<0.05$) (Figure 3.32B). After 24, 72 and 120 h exposure to 0.2 ug/cm^2 zinc chromate, Eg5 protein levels were 0.89, 0.26 and 0.11 relative to control, respectively; while p-Eg5 levels were 1.25, 0.24 and 0.22, respectively. Microtubule localization of Eg5 in interphase cells was also significantly decreased after chronic exposure to Cr(VI) treatment ($p<0.05$) (Figure 3.33B). Figure 3.33A shows representative images of cells with and without Eg5 localized to microtubules. After exposure to 0.1, 0.15 and 0.2 ug/cm^2 zinc chromate, there were 64, 62 and 69% of cells with Eg5 localized to microtubules, while after 120 h exposure there were 26, 15 and 8% of cells, respectively.

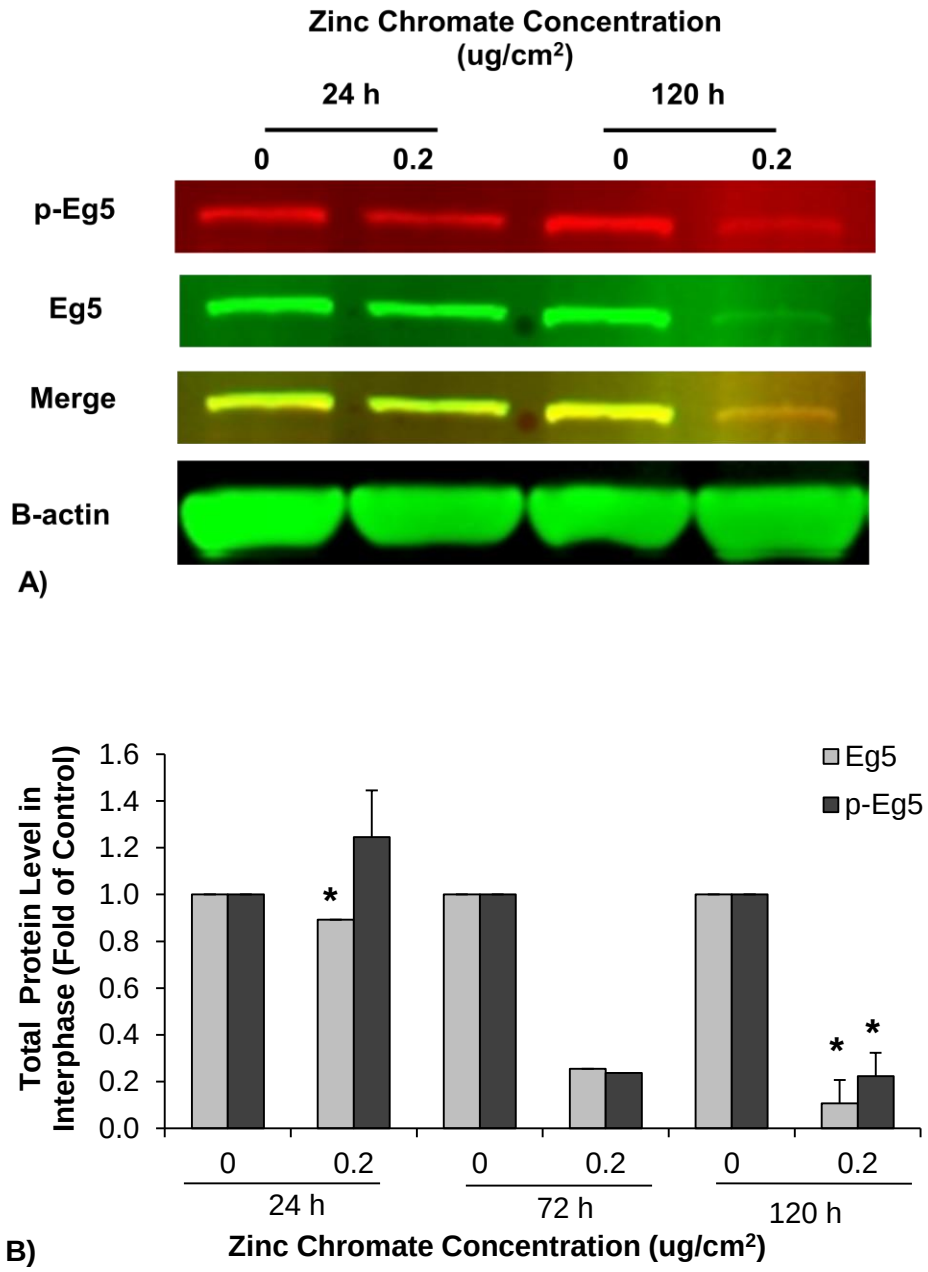

Figure 3.32. Eg5 Protein Levels in Interphase Cells after Cr(VI) Exposure. This figure shows that chronic exposure to Cr(VI) decreases protein levels of Eg5 and p-Eg5 (p-Eg5). **A)** Representative images of Eg5 western blots showing p-Eg5 in red, Eg5 in green, the merged images and B-actin as a loading control. **B)** Eg5 and p-Eg5 protein levels in interphase cells decrease after Cr(VI) exposure. *Statistically significant difference from the control ($p<0.05$). Data represent an average of three independent experiments ± the standard error of the mean.

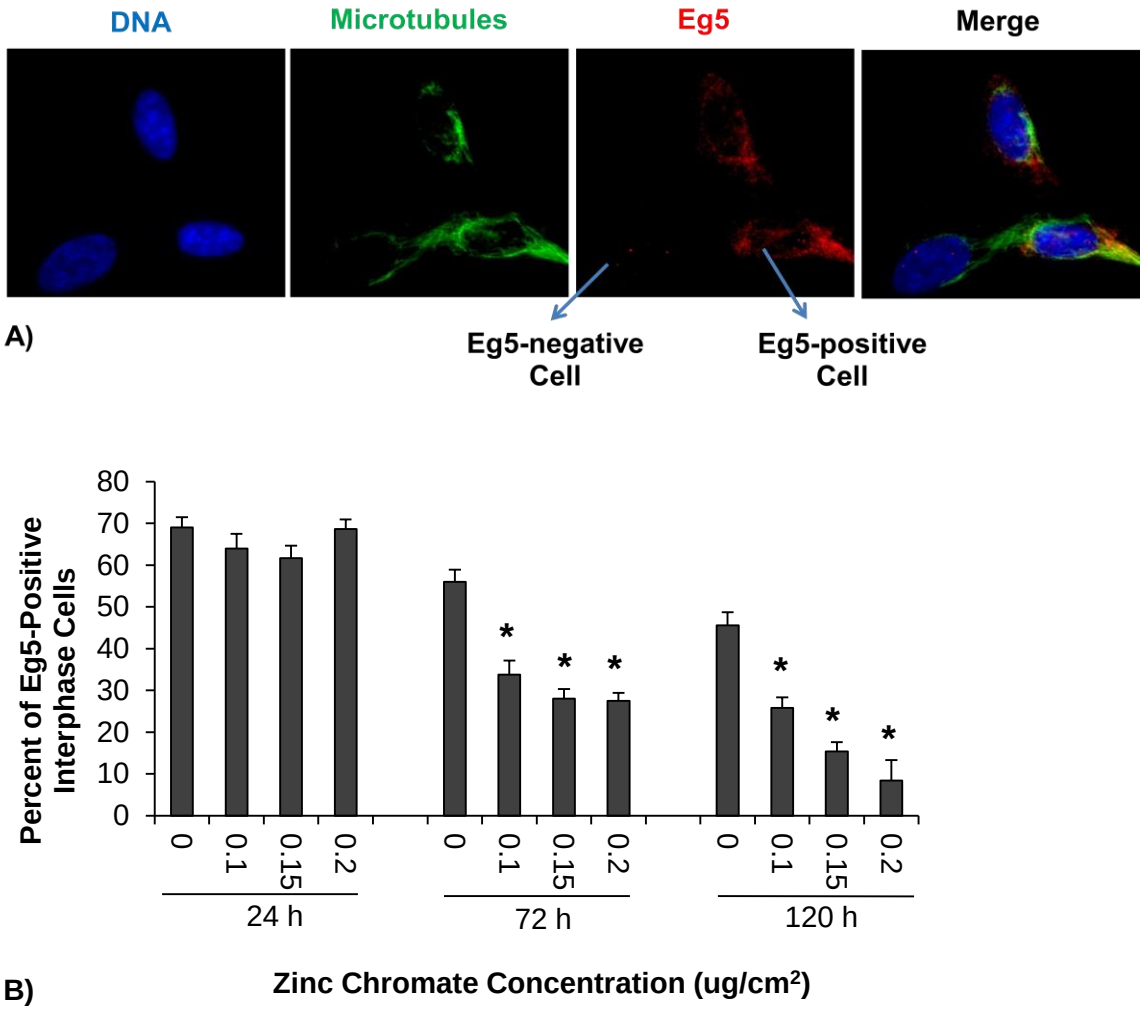

Figure 3.33. Eg5 Localization to Microtubules in Interphase Cells after Cr(VI) Exposure. This figure shows that chronic exposure to Cr(VI) decreases Eg5 localization to microtubules in interphase cells. **A)** Representative images of cells with and without Eg5 localization to microtubules. Blue, green and red represent DNA, microtubules and Eg5, respectively. **B)** Eg5 localization to microtubules in interphase cells decreasaes after Cr(VI) exposure. *Statistically significant difference from the control ($p<0.05$). Data represent an average of three independent experiments ± the standard error of the mean.

Because both centrosome separation pathways appear to be downregulated after Cr(VI) exposure, we hypothesized that premature centrosome separation after Cr(VI) treatment might be due to a failure of the G1-G2 tether to form. If this were the case, centrosome separation would still be possible even without Nek2 and Eg5 activity and localization. To determine if Cr(VI) affects the formation of the G1-G2 tether we

analyzed centrosomal localization of C-Nap1 and Rootletin, two key linker proteins. Rootletin forms fiber-like structures that connect both centrosomes, while C-Nap1 serves as a docking site for Rootletin. Even though other proteins also form fibers and provide alternative docking sites, depletion of C-Nap1 and Rootletin alone can cause centrosome separation because they serve as the structural basis for the rest of the linker (Mayor et al., 2000; Bahe et al., 2005).

Figure 3.34A shows representative images of an interphase cell with C-Nap1 and Rootletin localization to centrosomes. Chronic exposure to Cr(VI) did not affect C-Nap1 localization to centrosomes and we did not find any control or treated cell without C-Nap1 at centrosomes (Figure 3.34B). As for Rootletin, there seems to be a slight increase in its centrosomal localization after Cr(VI) exposure (Figure 3.34B). Approximately 90% of untreated cells have Rootletin at centrosomes, and this increases to 92, 95 and 100% after 24h exposure to 0.1, 0.15 and 0.2 ug/cm^2 zinc chromate, respectively and to 100, 100 and 100% after 120 h exposure, respectively. We only performed one experiment so statistical analysis on these data can not be performed. However, the data strongly suggest that C-Nap1 and Rootletin are still present at the centrosomes after Cr(VI) treatment.

Interestingly, cells with Cr(VI)-induced premature centrosome separation also have C-Nap1 and Rootletin localized to centrosomes (Figure 3.34C). C-Nap1 was localized to centrosomes in 100% of untreated and treated cells, while Rootletin localization to centrosomes was 96, 96 and 100% after 24, 72 and 120 h exposure to 0.2 ug/cm^2 zinc chromate, respectively (Figure 3.34D). In summary, the analysis of C-Nap1 and Rootletin localization to centrosomes shows that centrosome separation after Cr(VI) exposure occurs despite the presence of C-Nap1 and Rootletin.

Figure 3.34. C-Nap1 and Rootletin Localization at Centrosomes after Cr(VI) Exposure. This figure shows that Cr(VI) does not affect C-Nap1 and Rootletin localization to centrosomes. **A)** Representative images of an nterphase cell (DNA in blue) showing C-Nap1 (red) and Rootletin (green) localization to centrosomes. **B)** Percent of interphase cells with C-Nap1 and Rootletin localization to centrosomes after Cr(VI) exposure. **C)** Representative images of an interphase cell (DNA in blue) with separated centrosomes and C-Nap1 (red) and Rootletin (green) localization to centrosomes. **D)** Percent of interphase cells with separated centrosomes with C-Nap1 and Rootletin localization to centrosomes after Cr(VI) exposure. Data represent one experiment.

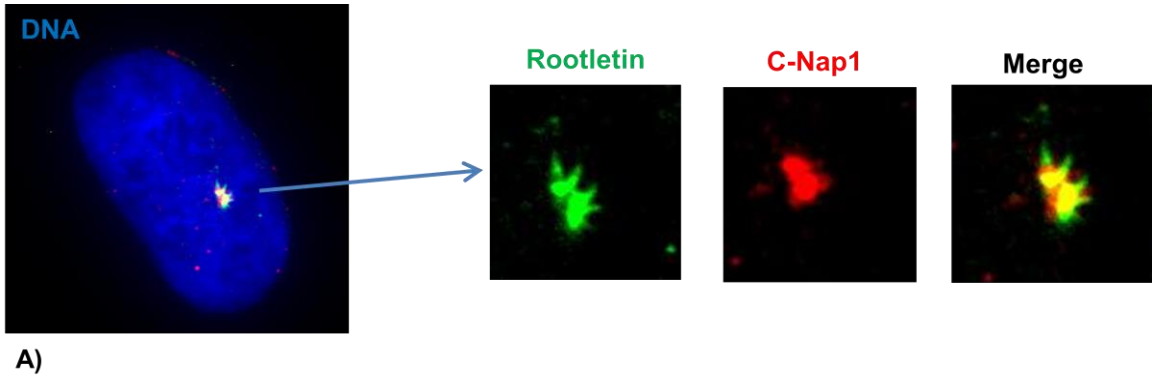

A)

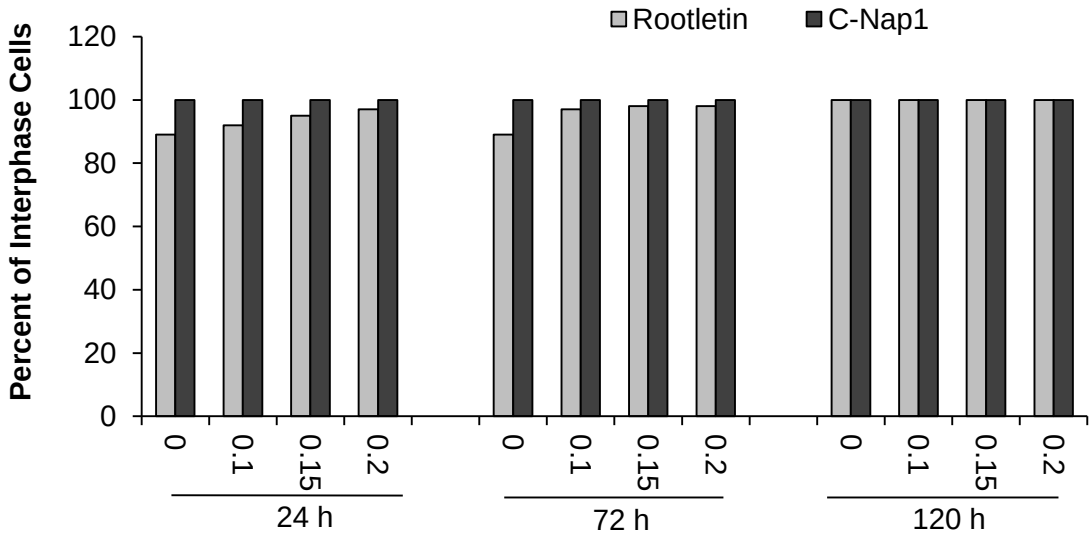

B)

Figure 3.34. Continued.

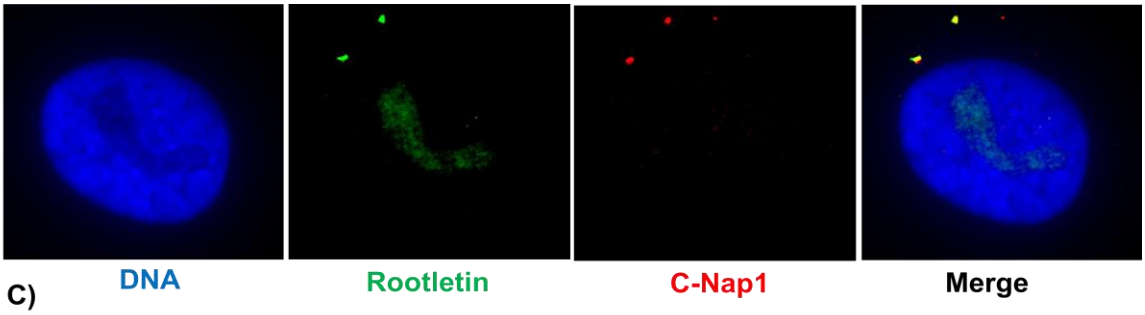

C)

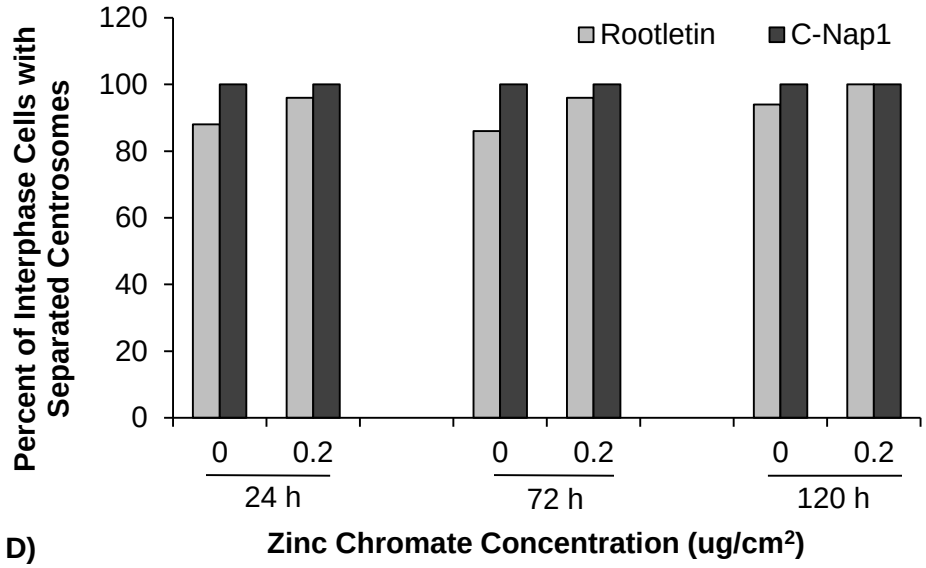

D)

3.4.4. Part 3 Summary

In Part 3 we demonstrate that chronic exposure to particulate Cr(VI) affects multiple proteins involved in the regulation of the centriole linkers. Specifically, Cr(VI) increases the levels of active Plk1 in interphase cells. We also found that after Cr(VI) exposure cells securin as well as inactive separase levels are decreased, while active separase levels are increased. These changes are consistent with the premature centriole disengagement observed in interphase cells after Cr(VI) treatment.

In contrast, we show that Nek2 and Eg5 protein levels and their centrosome and microtubule localization, respectively, are decreased after chronic exposure to Cr(VI).

We also show that the localization of key G1-G2 tether proteins is not affected by Cr(VI). These results are not consistent with the premature centrosome separation caused by Cr(VI).

3.5. Overall Summary of Results

Part 1 demonstrates that centrosome amplification induced by Cr(VI) is a permanent phenotype and that it correlates with permanent numerical chromosome instability. Part 2 shows that exposure to Cr(VI) causes premature centriole disengagement and premature centriole separation in interphase cells. Part 3 shows that Cr(VI) activates the proteins that regulate centriole disengagement. It also suggests that centrosome separation after Cr(VI) exposure may be mediated through novel mechanisms. In summary, the data show that centrosome amplification after Cr(VI) exposure is permanent and that Cr(VI) affects the protein linkers that regulate the centrosome, providing a feasible mechanism for centrosome amplification.

CHAPTER 4

DISCUSSSION

4.1. Overview

In general, lung tumors are characterized by very complex karyotypes with numerical chromosome instability (Balsara and Testa., 2002; Haruki et al., 2001, Masuda et al., 2002). Multiple cellular mechanisms contribute to changes in chromosome numbers. This work focuses on one of those mechanisms: centrosome amplification. Centrosome amplification is prevalent in solid tumors, including those of the lung (Pihan et al., 1998). Centrosomes are key players because one of their main roles is to form the bipolar spindle that evenly divides the genetic material during mitosis. Therefore, supernumerary centrosomes (i.e. centrosome amplification) can lead to numerical chromosome instability.

Cr(VI) is a metal widely used in industry and a common environmental pollutant. It is also a well-established human lung carcinogen. However, its carcinogenicity remains poorly understood. Cr(VI) induces centrosome amplification in human lung cells as well as numerical chromosome instability (Holmes et al., 2010). But the mechanisms underlying Cr(VI)-induced centrosome amplification are unknown. It is also unknown whether this phenotype is transiently induced or persists after Cr(VI) exposure.

In normal cells, centrosomes duplicate once and only once per cell cycle. Duplication is triggered by the disengagement of their underlying structures, the centrioles. Thus, centriole disengagement is considered the licensing step for centrosome duplication (Tsou and Stearns, 2006a; 2006b). Centrioles are kept engaged by a group of proteins collectively referred to as the S-M linker because the linker forms in S phase and is normally degraded during late mitosis or very early in G1 (Nigg and Stearns, 2011). Then, after centrosomes duplicate, they are kept together by another

group of proteins referred to as the G1-G2 tether (Nigg and Stearns, 2011). This tether is split at the G2/M transition and allows for centrosome separation in prophase (Mardin and Schiebel, 2012). Moreover, Plk1 activation is involved in both centriole disengagement and centrosome separation, suggesting common upstream regulatory mechanisms. Overall, it appears that the linkers are involved in preventing centrosome duplication until is the proper time to do so.

This project investigated the hypothesis that particulate Cr(VI) causes premature disruption of these two centrosome linkers and whether centrosome amplification after Cr(VI) exposure is a permanent phenotypic change. We demonstrate for the first time that Cr(VI) induces premature centriole disengagement and premature centrosome separation in interphase cells. Moreover, Cr(VI) causes Plk1 activation consistent with the premature centriole disengagement and centrosome separation observed in interphase. For centriole disengagement, we demonstrate the securin/separase pathway is activated after Cr(VI) exposure. We also show the Nek2/Eg5 pathway might not be responsible for Cr(VI)-induced premature centrosome separation. This project also confirms centrosome amplification after Cr(VI) exposure is a permanent phenotypic change.

In the following sections we discuss the data that show that particulate Cr(VI): 1) causes a permanent centrosome amplification phenotype (Section 4.2), 2) induces premature centriole disengagement through Plk1, separase and securin deregulation (Section 4.3) and 3) promotes premature centrosome separation independent of Nek2 and Eg5 (Section 4.4).

4.2. Part 1: Particulate Cr(VI) Causes Permanent Centrosome Amplification

Centrosome amplification is considered a deleterious phenotype because extremely uneven cell divisions likely lead to unviable daughter cells. However, tumors harbor cells with centrosome amplification and their presence correlates with numerical chromosome instability and tumor progression (Pihan et al., 2001; Lingle et al., 2002; Pihan et al., 2003). This outcome suggests that cells with amplified centrosomes do survive and play a role in carcinogenesis. A longstanding debate regarding cells with multiple centrosomes is whether they survive or not because it is expected that cells that undergo multipolar division will have such an abnormal genetic content that they will be unviable. Consequently, we investigated whether centrosome amplification is a permanent phenotypic change after Cr(VI) exposure.

In order to address this, we analyzed centrosome amplification in a set of clonal cell lines that were developed after one, two or three exposures to Cr(VI) (i.e.: named first, second or third generation, respectively). Each cell line derives from a single cell that survived and divided after Cr(VI) exposure. Hence, the phenotypes that are observed in each cell line can be considered heritable and permanent. Cells with amplified centrosomes appeared as early as the first generation and remained present throughout the second and third generations. The highest percent of cells with centrosome amplification was observed in clone T5 with 22% of cells with centrosome amplification. This percent is consistent with the highest values found in multiple cancer cell lines (Nigg, 2002).

It is curious that the 3rd generation of clones had a lower percent of clones with centrosome amplification than the first two. This outcome is most likely due to increased cell death in the 3rd generation. However, the decrease may also indicate that over time the phenotype is lost as a result of the clonal selection and expansion. Chiba et al. (2000) used cell lines from single p53-deficient mouse epithelial cells to study the fate of

the centrosome amplification phenotype. As expected, these cell lines have centrosome amplification due to p53 deficiency as well as abnormal chromosome numbers. Interestingly, these cell lines retained the centrosome amplification phenotype approximately until passage 30, but at later passages the surviving cells had normal number of centrosomes. In addition, chromosome numbers were abnormal but highly heterogeneous in the earlier passages (i.e.: 30 passages) but at later passages surviving cells had abnormal but stable number of chromosomes. This raises the possibility that centrosome amplification might be selected out as chromate-treated clones are expanded. However, the consequences of centrosome amplification, such as numerical changes in chromosomes, would persist.

In order to further understand the presence of centrosome amplification and numerical CIN, we analyzed clonal pedigrees. Clones from different generations are related to each other, hence family pedigrees allow us to analyze how centrosome amplification and numerical CIN phenotypes change as clones are treated, selected and expanded. The pedigrees show that clones with a high percentage of cells with centrosome amplification, such as T5, have truncated pedigrees because there are not enough surviving daughter colonies. In addition, the only surviving colonies have normal karyotypes and do not have centrosome amplification. Lack of surviving colonies is also observed in clones that have intermediate centrosome amplification but extremely abnormal karyotypes such as T1-1 and T4-2. In contrast, clones with karyotypes closer to normal and intermediate levels of centrosome amplification give rise to clones that survive, such as T2-2 and T2-3. The surviving clones continue to have karyotypes closer to normal and intermediate levels of centrosome amplification.

We found numerical CIN increased significantly in the second and third generations. Moreover, this increase correlated with the increase in centrosome amplification in the previous generation. This is consistent with centrosome amplification

being a causative mechanism that leads to induction of numerical CIN (Lingle et al, 2002). An interesting observation is that the majority of cell lines that have numerical CIN in the form of a near-tetraploid or tetraploid complement (i.e.: 92, XXYY) did not show centrosome amplification. Given that tetraploidy most likely derives from mitotic failure or lack of cytokinesis, it is expected that these cells would also acquire extra centrosomes. Thus, the observation that these clones do not show centrosome amplification is intriguing. One explanation, albeit untested, is that these cells lose centrosomes by actively extruding them, a phenomenon previously described in oocytes (Sutovsky and Schatten, 1999). However, it is currently unknown if centrosome extrusion can happen in somatic cells or cells that have undergone transformation.

The pedigree analysis shows cell lines with low to moderate levels of centrosome amplification and numerical CIN survive even in response to a new Cr(VI) treatment. Supporting this observation, Weaver et al. (2007) used CENP-$E^{+/-}$ mice to show that numerical CIN can act both oncogenically as well as a tumor suppressor depending on the level of genomic instability that is induced.

Our data show cells with centrosome amplification survive and duplicate and that cell lines can survive with a certain percent of the population with centrosome amplification. This outcome is consistent with what has been observed in multiple cancer cell lines (Nigg, 2002). In summary, the analysis of centrosome amplification in clonal cell lines developed after Cr(VI) exposure confirms this phenotype is stable and persistent and that it correlates with the presence of numerical CIN, which is also persistent. In addition, these cell lines can also become useful tools for addressing pending questions regarding centrosome biology.

4.3. Part 2: Particulate Cr(VI) Induces Premature Centriole Disengagement Through Deregulation of Plk1, Separase, and Securin

After confirming that centrosome amplification after Cr(VI) exposure is a permanent phenotype, we sought to investigate the underlying mechanisms that contribute to its development. Centriole disengagement is a key step in the centrosome cycle because it is the licensing step for centriole duplication (Tsou and Stearns, 2006a; 2006b). If centrioles disengage at other points of the cell cycle, the result is centrosome amplification because each disengaged centriole can become a centrosome. Moreover, centriole disengagement triggers centriole duplication which further increases centrosome numbers.

Centriole disengagement normally occurs at the end of mitosis (telophase) or very early in G1 phase (Kuriyama and Borisy, 1981). We hypothesized that Cr(VI) exposure causes premature centriole disengagement. To address this, we used centriole markers that distinguish if centrioles from a centrosome remain engaged to each other or not (Tsou and Stearns, 2006b). Our data show that chronic exposure to Cr(VI) caused a time- and dose-dependent increase in centriole disengagement in S/G2 interphase cells. These results are in agreement with other studies that have shown premature centriole disengagement in human cells after exposure to DNA damaging agents such as radiation and doxorubucin (Saladino et al., 2009; Conroy et al., 2012; Douthwright and Sluder, 2014). This data suggest that premature centriole disengagement might be a general response to DNA damaging agents. Interestingly, mitotic cells did not show premature centriole disengagement after Cr(VI) exposure. In addition, centriole disengagement was not observed in telophase cells, which would be considered a normal phase for disengagement. In contrast, about 50% of G1 cells had disengaged centrioles suggesting that in human lung fibroblasts normal centriole disengagement occurs in G1 phase.

Because centriole disengagement is the licensing step for centriole duplication (Tsou and Stearns, 2006b) an increase in the number of centrioles would also be expected in Cr(VI)-treated cells. Centrin staining confirms that chronic exposure to Cr(VI) induces supernumerary centrioles in both interphase and mitotic cells. Because we did not observe centriole disengagement in mitotic cells, the mitotic cells with supernumerary centrioles likely derive from interphase cells with premature centriole disengagement and supernumerary centrioles that entered mitosis (Douthwright and Sluder, 2014).

After confirming Cr(VI) induces centriole disengagement we investigated how Cr(VI) affects the proteins involved in this phenotype. Centriole disengagement appears to be regulated by Plk1 and the separase/securin complex (Tsou and Stearns, 2006b; Wang et al., 2008; Nakamura et al., 2009; Tsou et al., 2009; Hatano and Sluder, 2012) acting on the S-M linker which remains poorly defined but includes cohesin, sSgo1 as well as components of the PCM (Sluder, 2014). We hypothesized that Cr(VI)-induced premature centriole disengagement might be the result of Plk1 activity which promotes separase activity through securin degradation (Waizenegger et al., 2002, Tsou et al., 2009).

We found that after a 24 h exposure levels of active and inactive Plk1 were similar to the control. In contrast, 72 and 120 h exposures greatly decreased the levels of inactive Plk1 but did not affect the levels of active Plk1. This results in an increased p-Plk1/Plk1 ratio and suggests that after chronic exposure to Cr(VI) the majority of Plk1 is in its active form. In normal conditions Plk1 is activated late in G2 by Aurora A-dependent phosporylation of threonine 210 (Macurek et al., 2008). However, in the presence of DNA damage, cells with an intact DNA damage response inactivate Plk1 through dephosphorylation (Smits et al., 2000). Our data suggest that despite the presence of Cr(VI)-induced DNA damage, cells do not dephosphorylate Plk1.

Considering that Cr(VI) is a potent genotoxicant, it is surprising that after 72 and 120 h exposures Cr(VI)-treated cells most of Plk1 is phosphorylated. This outcome suggests defective Plk1 inactivation. Moreover, Plk1 activity also regulates mitotic entry and checkpoint recovery (van Vugt et al., 2004; Macurek et al., 2008). Since Cr(VI)-treated cells arrest at G2 (Holmes et al., 2010), failure to inactivate Plk1 could allow cells with DNA damage (Smits et al, 2000) and centrosome defects to enter mitosis.

Only one previous study has Cr(VI) impacts on Plk1 (Chun et al., 2010). In this study, human lung fibroblasts were treated for 24 h with soluble Cr(VI) did not show changes in Plk1 kinase activity as measured by an in vitro kinase assay, but did observe a decrease in Plk1 protein levels and nuclear localization. The kinase activity data is consistent with the data showing the ratio of active vs. inactive Plk1 remains unchanged after 24 h exposure suggesting no changes in Plk1 activity after this exposure time.

In addition, two studies have analyzed Plk1 after exposure to other metals. Chen et al. (2011) performed western blot analysis of active Plk1 in HeLa cells arrested in mitosis after a 24 h treatment with arsenic trioxide and showed that active Plk1 was present and that it might be involved in maintaining the arrest. Huang et al. (2009) observed subtle localization changes in Plk1 localization in the midbody during cytokinesis in NIH3T3 cells exposed to titanium dioxide nanoparticles. The authors suggested that these changes may underlie failure of cytokinesis under the same treatment conditions. In contrast, Cr(VI) does not induce failure of cytokinesis or mitotic arrest (Holmes et al., 2010). However, these studies suggest that Plk1 might be a common target in metal toxicity, albeit through different mechanisms.

So how does Plk1 remain active after Cr(VI) treatment? One possibility, yet untested, might involve Cr(VI)-induced defects in DNA damage response and repair proteins. Several studies have shown that Plk1 inactivation upon DNA damage depends on ATM, ATR and BRCA1 (van Vugt et al, 2001; Tsvetkov and Stern, 2005; Zou et al.,

2013). Even though a 24h exposure to Cr(VI) induces ATM phosphorylation (i.e.:activation), longer exposures greatly decrease the levels of phosphorylated (i.e.: active) ATM (Qin et al., 2014). Hence, a diminished DNA damage response after Cr(VI) treatment might be partially responsible for lack of Plk1 inactivation.

We also considered the protease separase whose activation is regulated by Plk1 (Cohen et al., 1996; Waizenegger et al., 2002; Moshe et al., 2004) and leads to centriole disengagement (Tsou et al., 2009). Upon activation separase undergoes autocleavage and the resulting cleaved fragments migrate differentially on gels and can be detected by western blotting (Zou et al. 2002). We used interphase cell lysates to analyze full-length and cleaved separase after Cr(VI) exposure. Our data shows prolonged Cr(VI) exposure decreases full-length and inactive separase levels, while increasing its cleaved and active products, showing separase activation in interphase cells. Since separase activation is controlled by association with its inhibitor securin (Cohen et al., 1996) we also analyzed securin levels. After chronic exposure to Cr(VI), securin levels dropped significantly, which is consistent with separase activation.

Only a few studies have considered changes in securin and separase after exposure to metals. Similar to our study, Chao et al. (2006) observed a decrease in securin and slight increase in separase cleavage products after exposure to arsenite in vascular endothelial cells. In contrast, McNeelly et al. (2008) have reported increased securin protein levels after arsenite exposure in human malignant melanoma cells. The difference in response between these studies could be attributed to different cell lines or higher arsenite concentrations used by Chao et al. (2006). Consistent with our findings, Prosser et al. (2012) analyzed Plk1, APC/C, separase and securin in HeLa cells exposed to ionizing radiation. They found premature centriole disengagement during a G2 arrest which could be blocked by overexpressing inactive Plk1 or securin or by depleting APC or separase. The authors concluded that oscillations in APC/C activity

during a G2 arrest lead to securin degradation, separase activation and premature centriole disengagement.

In summary, chronic exposure to Cr(VI) induces premature centriole disengagement during interphase and affects the proteins that are involved in regulating this important step of the centrosome cycle. This data also provides novel targets for Cr(VI) toxicity and offers mechanistic insights into Cr(VI)-induced centrosome amplification. Moreover, the observed effects can also help explain changes in other Cr(VI) targets other than centrosomes.

4.4. Part 3: Particulate Cr(VI) Induces Premature Centrosome Separation Likely Independent of Nek2 and Eg5

We also considered whether Cr(VI) affects the other centrosome linker: the G1-G2 tether. In a normal cell cycle, the G1-G2 tether is formed between centrioles soon after they disengage in late mitotis/early G1, (Nigg and Stearns, 2011). Since each centriole will soon become an individual centrosome, the G1-G2 tether maintains the two centrosomes together and thereby ensures that they function as one microtubule organizing center throughout interphase. Late in G2 the tether is broken to allow centrosome separation during mitosis and bipolar spindle formation (Agircan et al., 2014).

In addition, a recent study by Conroy et al. (2012) showed that this linker is also involved in preventing centriole disengagement caused by ionizing radiation-induced DNA damage. Even more interesting is that the dissolution of this linker is dependent on Plk1 activity (Zhang et al., 2005; Mardin et al., 2011). Considering that Cr(VI) causes premature centriole disengagement, activates Plk1 and causes DNA damage, we hypothesized that exposure to Cr(VI) could cause premature centrosome separation in interphase cells.

To analyze this we measured the distance between centrosomes in interphase cells after Cr(VI) exposure. We observed after 24 h exposure that the percent of cells with separated centrosomes decreased compared to background levels. This decrease after 24 h is actually considered a normal response, as cells with damaged DNA inhibit centrosome separation as part of the overall cell cycle arrest (Zhang et al., 2005). Since Cr(VI) causes DNA damage at later time points (Holmes et al., 2008), the decrease in centrosome separation should persist. However, after 72 and 120 h, this percent increased significantly showing that chronic exposure to Cr(VI) induces premature centrosome separation in interphase.

The overall separation of centrosomes proceeds in two steps. The first step, linker dissolution, involves the phosphorylation of the linker components C-Nap1 and Rootletin by the Nek2A kinase causing their removal from centrosomes (Fry et al., 1998b; Helps et al., 2000; Bahe et al., 2005). The second step, termed centrosome separation or elongation, refers to the migration of centrosomes away from each other. This requires microtubule forces primarily driven by the motor protein Eg5 (Blangy et al., 1995).

To further understand the mechanism underlying Cr(VI)-induced premature centrosome separation in interphase we focused our attention on Nek2 as this kinase is present and active during S and G2 phases (Fry et al., 1995). Specifically, the isoform Nek2A is involved in centrosome separation (Hames and Fry, 2002). Western blot analysis showed that Cr(VI) exposure decreases Nek2A protein levels. Next, we analyzed its centrosomal localization. For this, isoforms A and B cannot be distinguished from each other. In agreement with the decrease in protein levels, we also observed a decrease in Nek2 centrosomal localization in interphase cells. Interestingly, this decrease did not affect G2 cells, as all G2 cells analyzed had Nek2 localization to centrosomes. We then tried to asses levels of phosphorylated Nek2, which is the active

form (Fry et al., 1999). Since no commercially available antibodies exist, we immunoprecipitated Nek2 and blotted for phospho-threonine and phospho-serine. Unfortunately, we were not able to detect good bands in the blots and hence, could not quantify active Nek2.

Even though we could not assess active Nek2, our data shows an overall decrease in protein levels and centrosomal localization. These trends are not consistent with the observed increase in centrosome separation. Multiple studies have analyzed Nek2 protein levels, centrosomal localization and kinase activity, and increased centrosome separation is only observed when these parameters are increased (Fry et al., 1995; Fry et al., 1998a, Hames and Fry., 2002; Faragher and Fry, 2003). Interestingly, DNA damage has been shown to inhibit Nek2 activity as well as decrease its protein levels (Fletcher et al., 2004; Mi et al., 2007). However, in these studies centrosome separation was also inhibited.

Only one study has analyzed premature centrosome separation. Mardin et al., (2013) showed that epithelial growth factor (EGF) signaling can drive premature centrosome separation in non-transformed as well as tumor-derived cell lines. Premature centrosome separation was mediated by Nek2 activity and reduced the requirement for Eg5. An interesting observation from this study is that in tumor-derived cell lines premature centrosome separation allows for a more accurate segregation of chromosomes and hence increases the survival of genetically unstable cells (Mardin et al. 2013). This increase in accurate chromosome segregation is due to centrosomes separating and being positioned at opposite poles before nuclear envelope breakdown, which decreases the incidence of abnormal kinetochore-microtubule attachments (Kaseda et al., 2012; Mchedlishvili et al., 2012; Silkworth et al., 2012).

Because the decreases in Nek2 protein levels and centrosomal localization cannot explain the increase in premature centrosome separation we considered Eg5. It

has been shown that in the absence of Nek2, Eg5 activity is enough to separate centrosomes without the release of the linker protein Rootletin (Mardin et al., 2010). Most likely the microtubule forces exerted by Eg5 can tear the linker apart. As with Nek2, we measured protein levels of Eg5 and Eg5 phosphorylated at threonine 927, which allows binding to microtubules and centrosomes (Blangy et al, 1995; Cahu et al., 2008). In interphase cells, Cr(VI) decreased levels of both Eg5 and phospho-Eg5 and Eg5 localization to the microtubules.

The decreases in Nek2 and Eg5 do not explain the increased centrosome separation after Cr(VI) exposure. Recently, new players have been proposed to act on centrosomes and cause centrosome separation. These include kinetochore-generated forces via the microtubules and motor proteins such as Kif15 and dynein (Tanenbaum and Medema, 2010; Mchedlishvili et al., 2012; van Heesben et al., 2013). The effects of Cr(VI) on these proteins is currently unknown.

If microtubule forces generated by other motor proteins were acting on centrosomes, one could expect Rootletin to still be localized to separated centrosomes, as it has been previously observed for Eg5-induced centrosome separation in cells with deficient Nek2 (Mardin et al., 2010). Rootletin presence in separated centrosomes is likely due to the microtubule forces acting on the linker and disrupting Rootletin, as opposed to its complete removal when it is phosphorylated by Nek2 (Bahe et al., 2005). To test this, and at the same time, rule out a deficiency of linker proteins at the centrosomes, we analyzed Rootletin and C-Nap1 localization to centrosomes in interphase cells.

The vast majority of cells had both proteins localized to centrosomes, and this was unaffected by Cr(VI) exposure. Hence, premature centrosome separation is not likely due to a lack of linker proteins. Next, we focused the analysis on separated centrosomes. Interestingly, both C-Nap1 and Rootletin were also present with no

changes after Cr(VI) exposure, indicating that the mechanism separating centrosomes does not involve Rootletin release from the centrosomes.

The presence of Rootletin in separated centrosomes suggests a mechanism involving microtubule forces. Even though not a focus of this dissertation, we do observe centrosomes that lack centrioles (i.e.: acentriolar centrosomes) in cells exposed to Cr(VI). These have been proposed to arise due to microtubule forces acting on the pericentriolar material and fragmenting it (Maiato and Logarinho, 2014). These microtubule forces could also act on linker proteins and cause their fragmentation as well. Even without motor proteins, centrosomes would separate, albeit slowly, by diffusion or through other microtubule movements.

Taken together our data show that Cr(VI) causes premature centrosome separation in interphase cells. This increase correlates with the increase in centriole disengagement, but whether these two phenotypes are related remains unknown. The decreases in Nek2 and Eg5 protein and localization, and the presence of Rootletin in separated centrosomes suggest a mechanism in which microtubule forces may be the driving force behind Cr(VI)-induced centrosome separation. The effects of the premature centrosome separation phenotype also remain unknown. It would be interesting to test if this allows for increased survival in Cr(VI)-treated cells, as previously observed in HeLa cells with premature centrosome separation (Mardin et al., 2013).

In summary, this work further shows that centrosomes and centrosomal proteins are targets of Cr(VI) toxicity and that the effects are multiple and diverse, and highlights the complexity of this human carcinogen.

4.5. Proposed Mechanism for Cr(VI)-Induced Centrosome Amplification

Considering our data we propose a mechanism by which Cr(VI) induces centrosome defects that lead to centrosome amplification (Figure 4.1). When a cell is

exposed to particulate Cr(VI) [1], the particle dissolves on the extracellular medium [2]. The chromate anion enters the cells using generic anion transporters [3] (DeFlora and Wetterhahn, 1989) and once inside the cells is rapidly reduced to Cr(III) producing Cr(V) and Cr(IV) species, as well as reactive oxygen intermediates [4] (De Flora and Wetterhahn, 1989; Shi et al., 2009). The reduction of Cr(VI) induces DNA damage, particularly DNA double strand breaks [5] (Xie et al., 2005; Xie et al., 2009) which lead to a G2 arrest [6] (Holmes et al., 2010). In a normal scenario, the cell cycle arrest should inhibit Plk1 via phospho-ATM (van Vugt et al., 2001) but since Cr(VI) decreases phospho-ATM levels [7] (Qin et al., 2014) Plk1 remains active [8]. Plk1 activity triggers securin degradation and frees separase [9], which acts on the proteins of the S-M linker causing premature centriole disengagement in interphase [10]. This event licenses centriole duplication and causes centrosome amplification [11] (Holmes et al., 2010). Centrosome amplification leads to numerical CIN [12] (Holmes et al., 2006b; Holmes et al., 2010). Centrosome amplification and numerical CIN are persistent phenotypes [13], which can drive tumorigenesis causing neoplastic transformation [14] (Xie et al., 2007) and ultimately, cancer. By an unknown mechanism Cr(VI) also induces premature centrosome separation [15]. This may favor the survival of genetically unstable cells, thus contributing to the permanence of the phenotypes involved in tumorigenesis [16].

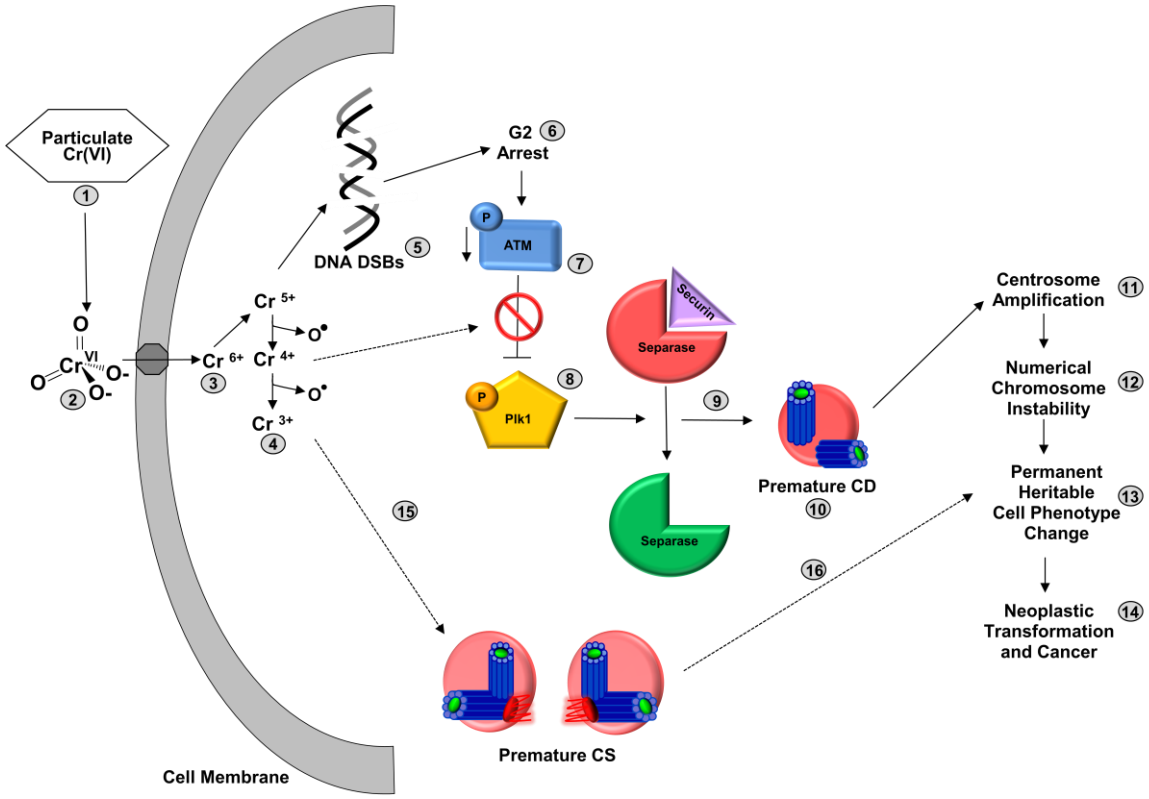

Figure 4.1. Proposed Mechanism for Cr(VI)-Induced Centrosome Amplification. This figure shows a proposed mechanism of how Cr(VI) induces centrosome amplification. Particulate Cr(VI) (1) dissolves in the extracellular medium (2). The chromate anion enters the cells using generic anion transporters (3) and once inside the cells is rapidly reduced to Cr(III) producing Cr(V) and Cr(IV) species, as well as reactive oxygen intermediates (4). The reduction of Cr(VI) induces DNA double strand breaks (DBSs) (5) causing a G2 arrest (6). The cell cycle arrest should inhibit Plk1 via phospho-ATM but since Cr(VI) decreases phospho-ATM levels (7) Plk1 remains active (8). Plk1 activity triggers securin degradation and frees separase (9) causing premature centriole disengagement (CD) (10). This causes centrosome amplification (11) and numerical chromosome instability (12) both of which are persistent phenotypes (13) which can drive tumorigenesis causing neoplastic transformation and ultimately, cancer (14). By an unknown mechanism Cr(VI) also induces premature centrosome separation (CS) (15). This may favor the survival of genetically unstable cells, thus contributing to the permanence of the phenotypes involved in tumorigenesis (16).

4.6. Future Work

The phenotypes observed in this study have mostly been described in the literature under conditions in which tumor cells are manipulated to become synchronous, to arrest at certain cell cycle phases, or to express or repress proteins. Our work is the first to show the effects of relevant doses of a chemical carcinogen and environmental pollutant on centrosome biology in normal human cells. It also provides further knowledge of Cr(VI) toxicity and new targets that had not been described for Cr(VI) or other metal carcinogens. However, this study also raises new questions to pursue and opens many future research directions.

First, there are experiments that could not be addressed in this dissertation due to time constraints or experimental issues. One such experiment is the confirmation that Plk1 is indeed driving the phenotypes we observe. As mentioned previously, reversal experiments are instrumental to proving cause-effect relationships. Fortunately, Plk1 is a widely studied target and highly specific inhibitors as well as plasmid systems allow for its manipulation in cells. It would be of extreme interest to either inhibit Plk1 or overexpress a kinase-dead protein and show that we can revert premature centriole disengagement, the changes observed in separase and securin protein levels, and, most importantly, centrosome amplification and numerical CIN after Cr(VI) exposure. Currently, there are several clinical trials with Plk1 inhibitors. If Plk1 proves to be a driver of numerical CIN after Cr(VI) exposure, it could become a potential target for therapy of Cr(VI) workers with lung cancer.

Moreover, since the mechanism underlying premature centrosome separation remains elusive, Plk1 manipulation could help find targets to study this phenotype, provided that it was also reversed. In addition, specific kinesin inhibitors could be tested to see if they contribute to centrosome separation and even unravel new players involved in this important aspect of centrosome biology. Another interesting question to

address is when centrosome separation is happening. Preliminary testing using cyclin D1 as a marker shows that it could be as early as G1, but more in depth analyses need to be performed.

For centriole disengagement, the timing also needs to be confirmed. Even though our studies show that it happens in S and/or G2 cells, it would be important to distinguish between these. This distinction would also allow assessing the involvement of the G2 arrest in the induction of this phenotype. Since many studies show that cell cycle arrest allows for centrosome defects, a possible way to overcome centrosome-associated defects could be by means of overriding a cell cycle arrest and push cells into mitosis where they are more sensitive to therapeutical approaches.

Time-lapse imaging of cells expressing GFP-centrin would provide insight into the timing and interconnectedness of centrosome separation and centriole disengagement, as well as answer other interesting questions. Can both phenotypes happen in the same cell? Or are they mutually exclusive? Does centrosome separation precede centriole disengagement? Or vice versa? When does centriole duplication begin after centriole disengagement? Do these phenotypes slow or accelerate the time spent in interphase or mitosis? Do Cr(VI)-treated cells cluster supernumerary centrioles and centrosomes? The clonal cell lines would be good candidates for the time-lapse studies because we know that in these the phenotypic changes are permanent.

Future studies should also use the clonal cell lines to test permanent changes in protein levels and localization of key centrosome proteins that are involved in numerical CIN, as well as other phenotypes. Also, considering the reports that suggest that premature centrosome separation may allow for an increase in the fidelity of mitosis, it would be interesting to analyze premature centrosome separation in the clones. Clones with low, medium and high levels of premature centrosome separation could be further observed using live imaging to assess time spent in mitosis and observe the incidence of

lagging chromosomes, anaphase bridges and mitotic figures that contribute to numerical CIN. Moreoever, it would be interesting to see the growth curves of the clones with different degrees of premature centrosome separation to see if the phenotype provides a proliferative advantage.

Another promising future area of research is the link between the DNA damage response and centrosome biology. Given that Cr(VI) is such a potent genotoxicant and causes defects in DNA repair, it would be interesting to study if a defective DNA damage response is involved in centrosome amplification after Cr(VI) exposure. Multiple DNA repair proteins have been shown to localize to the centrosome and cause centrosome abnormalities, many of which (i.e.: MRN complex, ATM, Rad51, Rad51C, BRCA1) are affected by Cr(VI). Because these proteins are downregulated by Cr(VI), it would be interesting to study if their overexpression can revert centrosome amplification. At the same time, multiple centrosomes could also contribute to defective DNA repair by affecting key signaling pathways involved in the DNA damage response. To our knowledge, this has not been explored but Cr(VI) might be a good model to use for these studies.

In summary, the study of centrosomes has the potential to shed light on many aspects of Cr(VI) toxicity and carcinogenesis. Because of their pivotal role in cell division, microtubule-related functions and due to their emerging connections to the entire cell signaling machinery, the study of centrosomes forces us to think in the totality of mechanisms that are present in a cell. As such, they provide with new ways to address the insult of environmental toxicants and chemical carcinogens, and will likely prove to be epicenters for therapeutic interventions in cancer cells.

REFERENCES

Agency for Toxic Substances and Disease Registry (ATSDR). 2012. Toxicological profile for chromium. U.S. Department of Health and Human Services, Public Health Service, ATSDR, Atlanta, GA.

Agircan FG, Schiebel E, Mardin BR. 2014. Separate to operate: control of centrosome positioning and separation. Philos Trans R Soc Lond B Biol Sci 369: 20130461.

Akella A, Deshpande SB. 2013. Pulmonary surfactants and their role in pathophysiology of lung disorders. Indian J Exp Biol 51:5-22.

Albert RE. 1991. Issues in the risk assessment of chromium. Environ Health Perspect 92:91-92.

Alderson MR, Rattan NS, Bidstrup L. 1981. Health of workmen in the chromate-producing industry in Britain. Br J Ind Med 38:117-124.

Ali AH, Kondo K, Namura T, Senba Y, Takizawa H, Nakagawa Y, Toba H, Kenzaki K, Sakiyama S, Tangoku A. 2011. Aberrant DNA methylation of some tumor suppressor genes in lung cancers from workers with chromate exposure. Mol Carcinog 50:89-99.

Bahe S, Stierhof YD, Wilkinson CJ, Leiss F, Nigg EA. 2005. Rootletin forms centriole-associated filaments and functions in centrosome cohesion. J Cell Biol 171:27-33.

Baldin V, Lukas J, Marcote MJ, Pagano M, Draetta G. 1993. Cyclin D1 is a nuclear protein required for cell cycle progression in G1. Genes Dev 7:812-821.

Balsara BR, Testa JR. 2002. Chromosomal imbalances in human lung cancer. Oncogene 21:6877-6883.

Blangy A, Lane HA, d'Hérin P, Harper M, Kress M, Niggt EA. 1995. Phosphorylation by $p34^{cdc2}$ regulates spindle association of human Eg5, a kinesin-related motor essential for bipolar spindle formation in vivo. Cell 83:1159-1169.

Boveri T. 1902. On multipolar mitosis as a means of analysis of the cell nucleus. Foundations of experimental embryology 1964:74-97.

Braver ER, Infante P, Chu K. 1985. An analysis of lung cancer risk from exposure to hexavalent chromium. Teratog Carcinog Mutagen 5:365-378.

Bridgewater LC, Manning FC, Woo ES, Patierno SR. 1994. DNA polymerase arrest by adducted trivalent chromium. Mol Carcinog 9:122-133.

Brooks B, O'Brien TJ, Ceryak S, Wise JP Sr, Wise SS, Wise JP Jr, Defabo E, Patierno SR. 2008. Excision repair is required for genotoxin-induced mutagenesis in mammalian cells. Carcinogenesis 29:1064-1069.

Bryant HE, Ying S, Helleday T. 2006. Homologous recombination is involved in repair of chromium-induced DNA damage in mammalian cells. Mutat Res-Fund Mol M 599:116-123.

Cahu J, Olichon A, Hentrich C, Schek H, Drinjakovic J, Zhang C, Doherty-Kirby A, Lajoie G, Surrey T. 2008. Phosphorylation by Cdk1 increases the binding of Eg5 to microtubules in vitro and in Xenopus egg extract spindles. PLoS One 3:e3936.

Casadevall M, Kortenkamp A. 1995. The formation of both purinic/apyrimidinic sites and single-strand breaks by chromate and glutathione arises from attack by the same single reactive species and is dependent on molecular oxygen. Carcinogenesis 16:805-809.

Chan JY. 2011. A clinical overview of centrosome amplification in human cancers. Int J Biol Sci 7:1122-1144.

Chao JI, Hsu SH, Tsou TC. 2006. Depletion of securin increases arsenite-induced chromosome instability and apoptosis via a p53-independent pathway. Tox Sci 90:73-86.

Chen YJ, Lin Y, Chow L, Lee T. 2011. Proteomic identification of Hsp70 as a new Plk1 substrate in arsenic trioxide-induced mitotically arrested cells. Proteomics 11:4331-4345.

Cheng L, Liu S, Dixon K. 1998. Analysis of repair and mutagenesis of chromium-induced DNA damage in yeast, mammalian cells, and transgenic mice. Environ Health Perspect 106 Suppl 4:1027-1032.

Cheng L, Sonntag DM, de Boer J, Dixon K. 2000. Chromium(VI)-induced mutagenesis in the lungs of big blue transgenic mice. J Environ Pathol Toxicol Oncol 19:239-249.

Chiba S, Okuda M, Mussman JG, Fukasawa K. 2000. Genomic convergence and suppression of centrosome hyperamplification in primary p53−/− cells in prolonged culture. Exp Cell Res 258:310-321.

Chun G, Bae D, Nickens K, O'Brien TJ, Patierno SR, Ceryak S. 2010. Polo-like kinase 1 enhances survival and mutagenesis after genotoxic stress in normal cells through cell cycle checkpoint bypass. Carcinogenesis 31:785-793.

Ciosk R, Zachariae W, Michaelis C, Shevchenko A, Mann M, Nasmyth K. 1998. An ESP1/PDS1 complex regulates loss of sister chromatid cohesion at the metaphase to anaphase transition in yeast. Cell 93:1067-1076.

Cohen-Fix O, Peters JM, Kirschner MW, Koshland D. 1996. Anaphase initiation in Saccharomyces cerevisiae is controlled by the APC-dependent degradation of the anaphase inhibitor Pds1p. Genes Dev 10:3081-3093.

Conroy PC, Saladino C, Dantas TJ, Lalor P, Dockery P, Morrison CG. 2012. C-NAP1 and rootletin restrain DNA damage-induced centriole splitting and facilitate ciliogenesis. Cell Cycle 11:3769-3778.

D'Assoro AB, Lingle WL, Salisbury JL. 2002. Centrosome amplification and the development of cancer. Oncogene 21:6146-6153.

Davidson T, Kluz T, Burns F, Rossman T, Zhang Q, Uddin A, Nadas A, Costa M. 2004. Exposure to chromium (VI) in the drinking water increases susceptibility to UV-induced skin tumors in hairless mice. Toxicol Appl Pharmacol 196:431-437.

Davies JM. 1984. Lung cancer mortality among workers making lead chromate and zinc chromate pigments at three English factories. Br J Ind Med 41:158-169.

De Flora S, Wetterhahn K. 1989. Mechanisms of chromium metabolism and genotoxicity. Life Chem Rep 7:169-244.

De Flora S, Bagnasco M, Serra D, Zanacchi P. 1990. Genotoxicity of chromium compounds. A review. Mutat Res-Rev Genet 238:99-172.

De Flora S, Camoirano A, Bagnasco M, Bennicelli C, Corbett GE, Kerger BD. 1997. Estimates of the chromium(VI) reducing capacity in human body compartments as a mechanism for attenuating its potential toxicity and carcinogenicity. Carcinogenesis 18:531-537.

Debec A, Courgeon AM, Maingourd M, Maisonhaute C. 1990. The response of the centrosome to heat shock and related stresses in a Drosophila cell line. J Cell Sci 96:403-412.

Domingo-Sananes MR, Kapuy O, Hunt T, Novak B. 2011. Switches and latches: a biochemical tug-of-war between the kinases and phosphatases that control mitosis. Philos Trans R Soc Lond B Biol Sci 366:3584-3594.

Douthwright S, Sluder G. 2014. Link between DNA damage and centriole disengagement/reduplication in untransformed human cells. J Cell Physiol 229:1427-1436.

Doxsey S. 2001. Re-evaluating centrosome function. Nat Rev Mol Cell Bio 2:688-698.

Elias Z, Poirot O, Pezerat H, Suquet H, Schneider O, Daniere MC, Terzetti F, Baruthio F, Fournier M, Cavelier C. 1989. Cytotoxic and neoplastic transforming effects of industrial hexavalent chromium pigments in Syrian hamster embryo cells. Carcinogenesis 10:2043-2052.

Elias Z, Poirot O, Baruthio F, Daniere MC. 1991. Role of solubilized chromium in the induction of morphological transformation of Syrian hamster embryo (SHE) cells by particulate chromium(VI) compounds. Carcinogenesis 12:1811-1816.

Environmental Protection Agency (EPA). 1984. Health assessment document for chromium. Environmental Criteria and Assessment Office, U.S. EPA, Research Triangle Park, NC.

Environmental Protection Agency (EPA). 1990. Non-carcinogenic effects of chromium: Update to health assessment document. Environmental Criteria and Assessment Office, U.S. EPA, Research Triangle Park, NC.

Environmental Working Group (EWG). 2010. Chromium-6 in U.S. tap water. EWG, Washington D.C.

European Food Safety Authority (EFSA). 2014. Scientific opinion on dietary reference values for chromium. EFSA Panel on Dietetic Products, Nutrition and Allergies, EFSA, Parma, Italy.

Ewis AA, Kondo K, Lee J, Tsuyuguchi M, Hashimoto M, Yokose T, Mukai K, Kodama T, Shinka T, Monden Y. 2001. Occupational cancer genetics: infrequent ras oncogenes point mutations in lung cancer samples from chromate workers. Am J Ind Med 40:92-97.

Ewis AA, Kondo K, Dang F, Nakahori Y, Shinohara Y, Ishikawa M, Baba Y. 2006. Surfactant protein B gene variations and susceptibility to lung cancer in chromate workers. Am J Ind Med 49:367-373.

Fang G, Zhang D, Yin H, Zheng L, Bi X, Yuan L. 2014. Centlein maintains centrosome cohesion by bridging and interaction between C-Nap1 and Cep68. J Cell Sci 127:1631-1639.

Faragher AJ, Fry AM. 2003. Nek2A kinase stimulates centrosome disjunction and is required for formation of bipolar mitotic spindles. Mol Biol Cell 14:2876-2889.

Feinberg AP. 2004. The epigenetics of cancer etiology. Semin Cancer Biol 14:427-432.

Fletcher L, Cerniglia GJ, Nigg EA, Yend TJ, Muschel RJ. 2004. Inhibition of centrosome separation after DNA damage: a role for Nek2. Radiat Res 162:128-135.

Freeman NC, Lioy PJ, Stern AH. 2000. Reduction in residential chromium following site remediation. J Air Waste Manage Assoc 50:948-953.

Freeman N, Wainman T, Lioy P, Stern A, Shupack S. 1995. The effect of remediation of chromium waste sites on chromium levels in urine of children living in the surrounding neighborhood. J Air Waste Manage Assoc 45:604-614.

Fry AM, Schultz SJ, Bartek J, Nigg EA. 1995. Substrate specificity and cell cycle regulation of the Nek2 protein kinase, a potential human homolog of the mitotic regulator NIMA of Aspergillus nidulans. J Biol Chem 270:12899-12905.

Fry AM, Meraldi P, Nigg EA. 1998a. A centrosomal function for the human Nek2 protein kinase, a member of the NIMA family of cell cycle regulators. EMBO J 17:470-481.

Fry AM, Mayor T, Meraldi P, Stierhof YD, Tanaka K, Nigg EA. 1998b. C-Nap1, a novel centrosomal coiled-coil protein and candidate substrate of the cell cycle-regulated protein kinase Nek2. J Cell Biol 141:1563-1574.

Fry AM, Arnaud L, Nigg EA. 1999. Activity of the human centrosomal kinase, Nek2, depends on an unusual leucine zipper dimerization motif. J Biol Chem 274:16304-16310.

Fukasawa K. 2005. Centrosome amplification, chromosome instability and cancer development. Cancer Lett 230:6-19.

Gibb HJ, Lees PS, Pinsky PF, Rooney BC. 2000. Lung cancer among workers in chromium chemical production. Am J Ind Med 38:115-126.

Graser S, Stierhof YD, Nigg EA. 2007. Cep68 and Cep215 (Cdk5rap2) are required for centrosome cohesion. J Cell Sci 120:4321-4331.

Guan J, Ekwurtzel E, Kvist U, Yuan L. 2008. Cohesin protein SMC1 is a centrosomal protein. Biochem Biophys Res Commun 372:761-764.

Güerci A, Seoane A, Dulout F. 2000. Aneugenic effects of some metal compounds assessed by chromosome counting in MRC-5 human cells. Mut Res-Gen Tox En 469:35-40.

Ha L, Ceryak S, Patierno SR. 2004. Generation of S phase-dependent DNA double-strand breaks by Cr(VI) exposure: involvement of ATM in Cr(VI) induction of γ-H2AX. Carcinogenesis 25:2265-2274.

Habedanck R, Stierhof YD, Wilkinson CJ, Nigg EA. 2005. The Polo kinase Plk4 functions in centriole duplication. Nat Cell Biol 7:1140-1146.

Hames RS, Fry AM. 2002. Alternative splice variants of the human centrosome kinase Nek2 exhibit distinct patterns of expression in mitosis. Biochem J 361:77-85.

Hanahan D, Weinberg RA. 2000. The hallmarks of cancer. Cell 100:57-70.

Hanahan D, Weinberg RA. 2011. Hallmarks of cancer: the next generation. Cell 144:646-674.

Hardy T, Lee M, Hames RS, Prosser SL, Cheary DM, Samant MD, Schultz F, Baxter JE, Rhee K, Fry AM. 2014. Multisite phosphorylation of C-Nap1 releases it from Cep135 to trigger centrosome disjunction. J Cell Sci 127:2493-2506.

Haruki N, Harano T, Masuda A, Kiyono T, Takahashi T, Tatematsu Y, Shimizu S, Mitsudomi T, Konishi H, Osada H. 2001. Persistent increase in chromosome instability in lung cancer: possible indirect involvement of p53 inactivation. Am J Pathol 159:1345-1352.

Hatano T, Sluder G. 2012. The interrelationship between APC/C and Plk1 activities in centriole disengagement. Biol Open 1:1153-1160.

Hayes RB, Lilienfeld AM, Snell LM. 1979. Mortality in chromium chemical production workers: a prospective study. Int J Epidemiol 8:365-374.

Hayes RB, Sheffet A, Spirtas R. 1989. Cancer mortality among a cohort of chromium pigment workers. Am J Ind Med 16:127-133.

He R, Huang N, Bao Y, Zhou H, Teng J, Chen J. 2013. LRRC45 is a centrosome linker component required for centrosome cohesion. Cell Rep 4:1100-1107.

Helps NR, Luo X, Barker HM, Cohen PT. 2000. NIMA-related kinase 2 (Nek2), a cell-cycle-regulated protein kinase localized to centrosomes, is complexed to protein phosphatase 1. Biochem J 349:509-518.

Hirose T, Kondo K, Takahashi Y, Ishikura H, Fujino H, Tsuyuguchi M, Hashimoto M, Yokose T, Mukai K, Kodama T, Monden Y. 2002. Frequent microsatellite instability in lung cancer from chromate-exposed workers. Mol Carcinogen 33:172-180.

Holmes AL, Wise SS, Sandwick SJ, Wise JP S. 2006a. The clastogenic effects of chronic exposure to particulate and soluble Cr(VI) in human lung cells. Mutat Res 610:8-13.

Holmes AL, Wise SS, Sandwick SJ, Lingle WL, Negron VC, Thompson WD, Wise JP S. 2006b. Chronic exposure to lead chromate causes centrosome abnormalities and aneuploidy in human lung cells. Cancer Res 66:4041-4048.

Holmes AL, Wise SS, Wise JP S. 2008. Carcinogenicity of hexavalent chromium. Indian J Med Res 128:353-372.

Holmes AL, Wise SS, Pelsue SC, Aboueissa A, Lingle W, Salisbury, J, Gallagher J, Wise JP Sr. 2010. Chronic exposure to zinc chromate induces centrosome amplification and spindle assembly checkpoint bypass un human lung fibroblasts. Chem Res Toxicol 23:386-395.

Holmes AL, Wise JP. 2010. Mechanisms of metal-induced centrosome amplification. Biochem Soc Trans 38:1687-1690.

Holmes AL. 2011. Elucidating a mechanism of particulate hexavalent chromium-induced carcinogenesis. Ph.D. Dissertation, University of Maine, Orono.

Huang S, Chueh PJ, Lin Y, Shih T, Chuang S. 2009. Disturbed mitotic progression and genome segregation are involved in cell transformation mediated by nano-TiO2 long-term exposure. Toxicol Appl Pharmacol 241:182-194.

Indjeian VB, Murray AW. 2007. Budding yeast mitotic chromosomes have an intrinsic bias to biorient on the spindle. Curr Biol 17:1837-1846.

International Agency for Research on Cancer (IARC). 1990. IARC Monographs on the evaluation of carcinogenic risks to humans Volume 49: Chromium, nickel and welding. World Health Organization, IARC.

Ishikawa Y, Nakagawa K, Satoh Y, Kitagawa T, Sugano H, Hirano T, Tsuchiya E. 1994a. "Hot spots" of chromium accumulation at bifurcations of chromate workers' bronchi. Cancer Res 54:2342-2346.

Ishikawa Y, Nakagawa K, Satoh Y, Kitagawa T, Sugano H, Hirano T, Tsuchiya E. 1994b. Characteristics of chromate workers' cancers, chromium lung deposition and precancerous bronchial lesions: an autopsy study. Br J Cancer 70:160-166.

Izzotti A, Bagnasco M, Camoirano A, Orlando M, De Flora S. 1998. DNA fragmentation, DNA-protein crosslinks, ^{32}P postlabeled nucleotidic modifications, and 8-hydroxy-2′-deoxyguanosine in the lung but not in the liver of rats receiving intratracheal instillations of chromium (VI). Chemoprevention by oral N-acetylcysteine. Mut Res-Fund Mol M 400:233-244.

Jantzen C, Jørgensen HL, Duus BR, Sporring SL, Lauritzen JB. 2013. Chromium and cobalt ion concentrations in blood and serum following various types of metal-on-metal hip arthroplasties. A literature overview. Acta Orthopaedica 84:229-236.

Johnson J, Schewel L, Graedel T. 2006. The contemporary anthropogenic chromium cycle. Environ Sci Technol 40:7060-7069.

Jung CK, Jung JH, Lee KY, Kang CS, Kim M, Ko YH, Oh CS. 2007. Centrosome abnormalities in non-small cell lung cancer: correlations with DNA aneuploidy and expression of cell cycle regulatory proteins. Pathol Res Pract 203:839-847.

Kalluri R, Zeisberg M. 2006. Fibroblasts in cancer. Nat Rev Cancer 6:392-401.

Karran P. 1996. Microsatellite instability and DNA mismatch repair in human cancer. Semin Cancer Biol 7:15-24.

Karri ND, Xie H, Wise J. 2013. Chronic Exposure to Particulate Hexavalent Chromium Alters Cdc20 Protein Localization, Interactions and Expression. J Carcinogen Mutagen 4:140.

Kaseda K, McAinsh AD, Cross RA. 2012. Dual pathway spindle assembly increases both the speed and the fidelity of mitosis. Biol Open 1:12-18.

Katabami M, Dosaka-Akita H, Mishina T, Honma K, Kimura K, Uchida Y, Morikawa K, Mikami H, Fukuda S, Inuyama Y. 2000. Frequent cyclin D1 expression in chromate-induced lung cancers. Hum Pathol 31:973-979.

Kim K, Lee S, Chang J, Rhee K. 2008. A novel function of CEP135 as a platform protein of C-NAP1 for its centriolar localization. Exp Cell Res 314:3692-3700.

Kimbrough DE, Cohen Y, Winer AM, Creelman L, Mabuni C. 1999. A critical assessment of chromium in the environment. Crit Rev Environ Sci Technol 29:1-46.

Klein CB, Su L, Bowser D, Leszczynska J. 2002. Chromate-induced epimutations in mammalian cells. Environ Health Perspect 110 Suppl 5:739-743.

Kondo K, Hino N, Sasa M, Kamamura Y, Sakiyama S, Tsuyuguchi M, Hashimoto M, Uyama T, Monden Y. 1997. Mutations of the p53 gene in human lung cancer from chromate-exposed workers. Biochem Biophys Res Commun 239:95-100.

Kondo K, Takahashi Y, Ishikawa S, Uchihara H, Hirose Y, Yoshizawa K, Tsuyuguchi M, Takizawa H, Miyoshi T, Sakiyama S. 2003. Microscopic analysis of chromium accumulation in the bronchi and lung of chromate workers. Cancer 98:2420-2429.

Kondo K, Takahashi Y, Hirose Y, Nagao T, Tsuyuguchi M, Hashimoto M, Ochiai A, Monden Y, Tangoku A. 2006. The reduced expression and aberrant methylation of $p16^{INK4a}$ in chromate workers with lung cancer. Lung Cancer 53:295-302.

Koutsami M, Tsantoulis P, Kouloukoussa M, Apostolopoulou K, Pateras I, Spartinou Z, Drougou A, Evangelou K, Kittas C, Bartkova J. 2006. Centrosome abnormalities are frequently observed in non-small-cell lung cancer and are associated with aneuploidy and cyclin E overexpression. J Pathol 209:512-521.

Kuo HW, Chang SF, Wu KY, Wu FY. 2003. Chromium (VI) induced oxidative damage to DNA: increase of urinary 8-hydroxydeoxyguanosine concentrations (8-OHdG) among electroplating workers. Occup Environ Med 60:590-594.

Kuriyama R, Borisy GG. 1981. Centriole cycle in Chinese hamster ovary cells as determined by whole-mount electron microscopy. J Cell Biol 91:814-821.

Lacey KR, Jackson PK, Stearns T. 1999. Cyclin-dependent kinase control of centrosome duplication. Proc Natl Acad Sci USA 96:2817-2822.

Langard S, Vigander T. 1983. Occurrence of lung cancer in workers producing chromium pigments. Br J Ind Med 40:71-74.

Lee K, Rhee K. 2012. Separase-dependent cleavage of pericentrin B is necessary and sufficient for centriole disengagement during mitosis. Cell Cycle 11:2476-2485.

Lengauer C, Kinzler KW, Vogelstein B. 1998. Genetic instabilities in human cancers. Nature 396:643-649.

Leonard A, Lauwerys R. 1980. Carcinogenicity and mutagenicity of chromium. Mut Res-Rev Genet 76:227-239.

Levina A, Harris HH, Lay PA. 2006. Binding of chromium (VI) to histones: implications for chromium (VI)-induced genotoxicity. JBIC Journal of Biological Inorganic Chemistry 11:225-234.

Levy LS, Martin PA, Bidstrup PL. 1986. Investigation of the potential carcinogenicity of a range of chromium containing materials on rat lung. Br J Ind Med 43:243-256.

Levy LS, Venitt S. 1986. Carcinogenicity and mutagenicity of chromium compounds: the association between bronchial metaplasia and neoplasia. Carcinogenesis 7:831-835.

Liao W, Lin P, Cheng T, Yu H, Chang LW. 2007. Arsenic promotes centrosome abnormalities and cell colony formation in p53 compromised human lung cells. Toxicol Appl Pharmacol 225:162-170.

Liao W, Yu H, Lin P, Chang LW. 2010. Arsenite promotes centrosome abnormalities under a p53 compromised status induced by 4-(methylnitrosamino)-1-(3-pyridyl)-1-butanone (NNK). Tox Appl Pharm 243:55-62.

Lingle WL, Barrett SL, Negron VC, D'Assoro AB, Boeneman K, Liu W, Whitehead CM, Reynolds C, Salisbury JL. 2002. Centrosome amplification drives chromosomal instability in breast tumor development. Proc Natl Acad Sci U S A 99:1978-1983.

Liu KJ, Jiang J, Swartz HM, Shi X. 1994. Low-frequency EPR detection of chromium (V) formation by chromium (VI) reduction in whole live mice. Arch Biochem Biophys 313:248-252.

Liu KJ, Shi X, Jang JJ, Goda F, Dalal N, Swartz HM. 1995. Chromate-induced chromium(V) formation in live mice and its control by cellular antioxidants: An L-band electron paramagnetic resonance study. Arch Biochem Biophys 323:33-39.

Liu S, Dixon K. 1996. Induction of mutagenic DNA damage by chromium (VI) and glutathione. Environ Mol Mutagen 28:71-79.

Loeb LA. 1994. Microsatellite instability: marker of a mutator phenotype in cancer. Cancer Res 54:5059-5063.

Luippold RS, Mundt KA, Austin RP, Liebig E, Panko J, Crump C, Crump K, Proctor D. 2003. Lung cancer mortality among chromate production workers. Occup Environ Med 60:451-457.

Machle W, Gregorius F. 1948. Cancer of the respiratory system in the United States chromate-producing industry. Public Health Reports (1896-1970):1114-1127.

Macůrek L, Lindqvist A, Lim D, Lampson MA, Klompmaker R, Freire R, Clouin C, Taylor SS, Yaffe MB, Medema RH. 2008. Polo-like kinase-1 is activated by aurora A to promote checkpoint recovery. Nature 455:119-123.

Maeng S, Chung H, Yu I, Kim H, Lim C, Kim K, Kim S, Ootsuyama Y, Kasai H. 2003. Changes of 8-OH-dG levels in DNA and its base excision repair activity in rat lungs after inhalation exposure to hexavalent chromium. Mut Res-Gen Tox En 539:109-116.

Maiato H, Logarinho E. 2014. Mitotic spindle multipolarity without centrosome amplification. Nat Cell Biol 16:386-394.

Mancuso TF. 1997. Chromium as an industrial carcinogen: Part I. Am J Ind Med 31:129-139.

Mardin BR, Lange C, Baxter JE, Hardy T, Scholz SR, Fry AM, Schiebel E. 2010. Components of the Hippo pathway cooperate with Nek2 kinase to regulate centrosome disjunction. Nat Cell Biol 12:1166-1176.

Mardin BR, Agircan FG, Lange C, Schiebel E. 2011. Plk1 controls the Nek2A-PP1γ antagonism in centrosome disjunction. Curr Biol 21:1145-1151.

Mardin BR, Schiebel E. 2012. Breaking the ties that bind: new advances in centrosome biology. J Cell Biol 197:11-18.

Mardin BR, Isokane M, Cosenza MR, Kramer A, Ellenberg J, Fry AM, Schiebel E. 2013. EGF-induced centrosome separation promotes mitotic progression and cell survival. Dev Cell 25:229-240.

Marshall WF. 2007. What is the function of centrioles?. J Cell Biochem 100:916-922.

Masuda A, Takahashi T. 2002. Chromosome instability in human lung cancers: possible underlying mechanisms and potential consequences in the pathogenesis. Oncogene 21:6884-6897.

Matsumoto Y, Hayashi K, Nishida E. 1999. Cyclin-dependent kinase 2 (Cdk2) is required for centrosome duplication in mammalian cells. Curr Biol 9:429-432.

Matsuo K, Ohsumi K, Iwabuchi M, Kawamata T, Ono Y, Takahashi M. 2012. Kendrin is a novel substrate for separase involved in the licensing of centriole duplication. Curr Biol 22:915-921.

Mayor T, Stierhof YD, Tanaka K, Fry AM, Nigg EA. 2000. The centrosomal protein C-Nap1 is required for cell cycle-regulated centrosome cohesion. J Cell Biol 151:837-846.

Mayor T, Hacker U, Stierhof YD, Nigg EA. 2002. The mechanism regulating the dissociation of the centrosomal protein C-Nap1 from mitotic spindle poles. J Cell Sci 115:3275-3284.

Mchedlishvili N, Wieser S, Holtackers R, Mouysset J, Belwal M, Amaro AC, Meraldi P. 2012. Kinetochores accelerate centrosome separation to ensure faithful chromosome segregation. J Cell Sci 125:906-918.

McNeely SC, Taylor BF, States JC. 2008. Mitotic arrest-associated apoptosis induced by sodium arsenite in A375 melanoma cells is BUBR1-dependent. Tox Appl Pharm 231:61-67.

Mi J, Guo C, Brautigan DL, Larner JM. 2007. Protein phosphatase-1alpha regulates centrosome splitting through Nek2. Cancer Res 67:1082-1089.

Mitsuuchi Y, Testa JR. 2002. Cytogenetics and molecular genetics of lung cancer. Am J Med Genet 115:183-188.

Moritz M, Braunfeld MB, Sedat JW, Alberts B, Agard DA. 1995. Microtubule nucleation by g-tubulin-containing rings in the centrosome. Nature 378:638-640.

Moshe Y, Boulaire J, Pagano M, Hershko A. 2004. Role of Polo-like kinase in the degradation of early mitotic inhibitor 1, a regulator of the anaphase promoting complex/cyclosome. Proc Natl Acad Sci USA 101:7937-7942.

Moulin JJ. 1997. A meta-analysis of epidemiologic studies of lung cancer in welders. Scand J Work Environ Health 23:104-113.

National Institute for Occupational Safety and Health (NIOSH). 1988. NIOSH testimony on the Occupational Safety and Health Administration's proposed rule on air contaminants. U.S. Department of Health and Human Services, Public Health Service, Centers for Disease Control, NIOSH, Cincinnati, OH:

National Toxicology Program (NTP). 1980. Report on carcinogens. NTP, U.S. Department of Health and Human Services, Research Triangle Park, NC.

National Toxicology Program (NTP). 2008. NTP Technical report on the toxicology and carcinogenesis studies of sodium dichromate dihydrate in F344/N rats and B6C3F1 mice. NTP, Research Triangle Park, NC.

National Toxicology Program (NTP). 2011. 12th Report on carcinogens. NTP, U.S. Department of Health and Human Services, Research Triangle Park, NC.

Nakamura A, Arai H, Fujita N. 2009. Centrosomal Aki1 and cohesin function in separase-regulated centriole disengagement. J Cell Biol 187:607-614.

Navara CS, Benyumov A, Vassilev A, Narla RK, Ghosh P, Uckun FM. 2001. Vanadocenes as potent anti-proliferative agents disrupting mitotic spindle formation in cancer cells. Anti Cancer Drug 12:369-376.

Negrini S, Gorgoulis VG, Halazonetis TD. 2010. Genomic instability-an evolving hallmark of cancer. Nature Rev Mol Cell Bio 11:220-228.

Nettesheim P, Hanna MG,Jr, Doherty DG, Newell RF, Hellman A. 1971. Effect of calcium chromate dust, influenza virus, and 100 R whole-body x radiation on lung tumor incidence in mice. J Natl Cancer Inst 47:1129-1144.

Newman D. 1890. A case of adeno-carcinoma of the left inferior turbinated body, and perforation of the nasal septum, in the person of a worker in chrome pigments. Glasgow Med J 33:469-470.

Nickens KP, Patierno SR, Ceryak S. 2010. Chromium genotoxicity: a double-edged sword. Chem Biol Interact 188:276-288.

Nigg EA. 2002. Centrosome aberrations: cause or consequence of cancer progression?. Nature Reviews Cancer 2:815-825.

Nigg EA, Stearns T. 2011. The centrosome cycle: Centriole biogenesis, duplication and inherent asymmetries. Nat Cell Biol 13:1154-1160.

O'Brien TJ, Xu J, Patierno SR. 2001. Effects of glutathione on chromium-induced DNA crosslinking and DNA polymerase arrest. Mol Cell Biochem 222:173-182.

O'Brien TJ, Ceryak S, Patierno SR. 2003. Complexities of chromium carcinogenesis: role of cellular response, repair and recovery mechanisms. Mut Res-Fund Mol M 533:3-36.

O'Brien TJ, Brooks BR, Patierno SR. 2005. Nucleotide excision repair functions in the removal of chromium-induced DNA damage in mammalian cells. Mol Cell Biochem 279:85-95.

Occupational Safety and Health Administration (OSHA). 2006. 29 CFR Parts 1910, 1915, 1917, 1918, and 1926. Occupational exposure to hexavalent chromium: Final rule. Department of Labor, OSHA.

Ochi T, Nakajima F, Shimizu A, Harada M. 1999a. Induction of multinucleated cells in V79 Chinese hamster cells exposed to dimethylarsinic acid, a methylated derivative of inorganic arsenics: mechanism associated with the formation of aberrant mitotic spindles. Toxicol In vitro 13:11-25.

Ochi T, Nakajima F, Nasui M. 1999b. Distribution of γ-tubulin in multipolar spindles and multinucleated cells induced by dimethylarsinic acid, a methylated derivative of inorganic arsenics, in Chinese hamster V79 cells. Toxicology 136:79-88.

Ochi T. 2000. Induction of centrosome injury, multipolar spindles and multipolar division in cultured V79 cells exposed to dimethylarsinic acid: role for microtubules in centrosome dynamics. Mut Res-Fund Mol M 454:21-33.

Ochi T. 2002a. Role of mitotic motors, dynein and kinesin, in the induction of abnormal centrosome integrity and multipolar spindles in cultured V79 cells exposed to dimethylarsinic acid. Mut Res-Fund Mol M 499:73-84.

Ochi T. 2002b. Methylmercury, but not inorganic mercury, causes abnormality of centrosome integrity (multiple foci of γ-tubulin), multipolar spindles and multinucleated cells without microtubule disruption in cultured Chinese hamster V79 cells. Toxicology 175:111-121.

Ochi T, Suzuki T, Isono H, Schlagenhaufen C, Goessler W, Tsutsui T. 2003. Induction of structural and numerical changes of chromosome, centrosome abnormality, multipolar spindles and multipolar division in cultured Chinese hamster V79 cells by exposure to a trivalent dimethylarsenic compound. Mut Res-Fund Mol M 530:59-71.

Ochi T, Suzuki T, Barrett JC, Tsutsui T. 2004. A trivalent dimethylarsenic compound, dimethylarsine iodide, induces cellular transformation, aneuploidy, centrosome abnormality and multipolar spindle formation in Syrian hamster embryo cells. Toxicology 203:155-163.

Ochi T, Kita K, Suzuki T, Rumpler A, Goessler W, Francesconi KA. 2008. Cytotoxic, genotoxic and cell-cycle disruptive effects of thio-dimethylarsinate in cultured human cells and the role of glutathione. Toxicol Appl Pharm 228:59-67.

Paoletti A, Moudjou M, Paintrand M, Salisbury JL, Bornens M. 1996. Most of centrin in animal cells is not centrosome-associated and centrosomal centrin is confined to the distal lumen of centrioles. J Cell Sci 109:3089-3102.

Patierno S, Banh D, Landolph J. 1988. Transformation of C3H/10T1/2 mouse embryo cells by insoluble lead chromate but not soluble calcium chromate: relationship to mutagenesis and internalization of lead chromate particles. Cancer Res 47:3815-3823.

Peterson-Roth E, Reynolds M, Quievryn G, Zhitkovich A. 2005. Mismatch repair proteins are activators of toxic responses to chromium-DNA damage. Mol Cell Biol 25:3596-3607.

Pihan GA, Purohit A, Wallace J, Knecht H, Woda B, Quesenberry P, Doxsey SJ. 1998. Centrosome defects and genetic instability in malignant tumors. Cancer Res 58:3974-3985.

Pihan GA, Purohit A, Wallace J, Malhotra R, Liotta L, Doxsey SJ. 2001. Centrosome defects can account for cellular and genetic changes that characterize prostate cancer progression. Cancer Res 61:2212-2219.

Pihan GA, Wallace J, Zhou Y, Doxsey SJ. 2003. Centrosome abnormalities and chromosome instability occur together in pre-invasive carcinomas. Cancer Res 63:1398-1404.

Proctor DM, Suh M, Campleman SL, Thompson CM. 2014. Assessment of the mode of action for hexavalent chromium-induced lung cancer following inhalation exposures. Toxicology 325:160-179.

Prosser SL, Samant MD, Baxter JE, Morrison CG, Fry AM. 2012. Oscillation of APC/C activity during cell cycle arrest promotes centrosome amplification. J Cell Sci 125:5353-5368.

Qin Q. 2013. Characterizing the impact of prolonged exposure to particulate hexavalent chromium on DNA double strand break repair. Ph.D. Dissertation, University of Maine, Orono.

Qin Q, Xie H, Wise SS, Browning CL, Thompson KN, Holmes AL, Wise JP S. 2014. Homologous recombination repair signaling in chemical carcinogenesis: prolonged particulate hexavalent chromium exposure suppresses the Rad51 response in human lung cells. Toxicol Sci 142:117-125.

Quievryn G, Peterson E, Messer J, Zhitkovich A. 2003. Genotoxicity and mutagenicity of chromium(VI)/ascorbate-generated DNA adducts in human and bacterial cells. Biochemistry 42:1062-1070.

Reynolds M, Peterson E, Quievryn G, Zhitkovich A. 2004. Human nucleotide excision repair efficiently removes chromium-DNA phosphate adducts and protects cells against chromate toxicity. J Biol Chem 279:30419-30424.

Reynolds M, Stoddard L, Bespalov I, Zhitkovich A. 2007. Ascorbate acts as a highly potent inducer of chromate mutagenesis and clastogenesis: linkage to DNA breaks in G2 phase by mismatch repair. Nucleic Acids Res 35:465-476.

Reynolds M, Zhitkovich A. 2007. Cellular vitamin C increases chromate toxicity via a death program requiring mismatch repair but not p53. Carcinogenesis 285:1613-1620.

Reynolds MF, Peterson-Roth EC, Bespalov IA, Johnston T, Gurel VM, Menard HL, Zhitkovich A. 2009. Rapid DNA double-strand breaks resulting from processing of Cr-DNA cross-links by both MutS dimers. Cancer Res 69:1071-1079.

Robbins E, Jentzsch G, Micali A. 1968. The centriole cycle in synchronized HeLa cells. J Cell Biol 36:329-339.

Rodrigues C, Urbano A, Matoso E, Carreira I, Almeida A, Santos P, Botelho F, Carvalho L, Alves M, Monteiro C. 2009. Human bronchial epithelial cells malignantly transformed by hexavalent chromium exhibit an aneuploid phenotype but no microsatellite instability. Mut Res-Fund Mol M 670:42-52.

Saladino C, Bourke E, Conroy PC, Morrison CG. 2009. Centriole separation in DNA damage-induced centrosome amplification. Environ Mol Mutagen 50:725-732.

Schnekenburger M, Talaska G, Puga A. 2007. Chromium cross-links histone deacetylase 1-DNA methyltransferase 1 complexes to chromatin, inhibiting histone-remodeling marks critical for transcriptional activation. Mol Cell Biol 27:7089-7101.

Schöckel L, Mockel M, Mayer B, Boos D, Stemmann O. 2011. Cleavage of cohesin rings coordinates the separation of centrioles and chromatids. Nat Cell Biol 13:966-972.

Schwarz K, Mertz W. 1959. Chromium (III) and the glucose tolerance factor. Arch Biochem Biophys 85:292-295.

Seifart C, Seifart U, Plagens A, Wolf M, Von Wichert P. 2002. Surfactant protein B gene variations enhance susceptibility to squamous cell carcinoma of the lung in German patients. Br J Cancer 87:212-217.

Seoane A, Güerci A, Dulout F. 2002. Malsegregation as a possible mechanism of aneuploidy induction by metal salts in MRC-5 human cells. Environ Mol Mutagen 40:200-206.

Sheffet A, Thind I, Miller AM, Louria DB. 1982. Cancer mortality in a pigment plant utilizing lead and zinc chromates. Arch Environ Health 37:44-52.

Shi X, Chiu A, Chen CT, Halliwell B. 1999. Reduction of chromium (VI) and its relationship to carcinogenesis. J Toxicol Env Heal B 2:87-104.

Silkworth WT, Nardi IK, Paul R, Mogilner A, Cimini D. 2012. Timing of centrosome separation is important for accurate chromosome segregation. Mol Biol Cell 23:401-411.

Slade R, Stead AG, Graham JA, Hatch GE. 1985. Comparison of lung antioxidant levels in humans and laboratory animals. Am Rev Respir Dis 131:742-746.

Sluder G. 2005. Two-way traffic: centrosomes and the cell cycle. Nat Rev Mol Cell Biol 6:743-748.

Sluder G, Nordberg JJ. 2004. The good, the bad and the ugly: the practical consequences of centrosome amplification. Curr Opin Cell Biol 16:49-54.

Sluder G. 2013. Centriole engagement: It's not just cohesin anymore. Curr Biol 23:R659-R660.

Smith C, Livingston S, Doolittle D. 1997. An international literature survey of "IARC Group I carcinogens" reported in mainstream cigarette smoke. Food Chem Toxicol 35:1107-1130.

Smits VA, Klompmaker R, Arnaud L, Rijksen G, Nigg EA, Medema RH. 2000. Polo-like kinase-1 is a target of the DNA damage checkpoint. Nat Cell Biol 2:672-676.

Snyder CA, Sellakumar A, Waterman S. 1997. An assessment of the tumorigenic properties of a Hudson County soil sample heavily contaminated with hexavalent chromium. Arch Environ Health 52:220-226.

Sorahan T, Harrington JM. 2000. Lung cancer in Yorkshire chrome platers, 1972-97. Occup Environ Med 57:385-389.

Stackpole MM, Wise SS, Goodale BC, Duzevik EG, Munroe RC, Thompson WD, Thacker J, Thompson LH, Hinz JM, Wise Sr JP. 2007. Homologous recombination repair protects against particulate chromate-induced chromosome instability in Chinese hamster cells. Mut Res-Fund Mol M 625:145-154.

Standeven AM, Wetterhahn KE. 1992. Ascorbate is the principal reductant of chromium(VI) in rat lung ultrafiltrates and cytosols, and mediates chromium-DNA binding in vitro. Carcinogenesis 13:1319-1324.

Stearns DM. 2000. Is chromium a trace essential metal?. Biofactors 11:149-162.

Steinhoff D, Gad SC, Hatfiled GK, Mohr U. 1986. Carcinogenicity study with sodium dichromate in rats. Exp Pathol 30:129-141.

Stern RM. 1982. Chromium compounds: production and occupational exposure. In: Biological and environmental aspects of chromium. Langård S (ed.). Amsterdam: Elsevier Biomedical Press. p5.

Stern AH, Freeman NC, Pleban P, Boesch RR, Wainman T, Howell T, Shupack SI, Johnson BB, Lioy PJ. 1992. Residential exposure to chromium waste—urine biological

monitoring in conjunction with environmental exposure monitoring. Environ Res 58:147-162.

Stout MD, Herbert RA, Kissling GE, Collins BJ, Travlos GS, Witt KL, Melnick RL, Abdo KM, Malarkey DE, Hooth MJ. 2009. Hexavalent chromium is carcinogenic to F344/N rats and B6C3F1 mice after chronic oral exposure. Environ Health Perspect 117:716-722.

Sun H, Zhou X, Chen H, Li Q, Costa M. 2009. Modulation of histone methylation and MLH1 gene silencing by hexavalent chromium. Toxicol Appl Pharmacol 237:258-266.

Sutovsky P, Schatten G. 1999. Paternal contributions to the mammalian zygote: fertilization after sperm-egg fusion. Int Rev Cytol 195:1-65.

Suzuki Y, Fukuda K. 1990. Reduction of hexavalent chromium by ascorbic acid and glutathione with special reference to the rat lung. Arch Toxicol 64:169-176.

Takahashi Y, Kondo K, Hirose T, Nakagawa H, Tsuyuguchi M, Hashimoto M, Sano T, Ochiai A, Monden Y. 2005. Microsatellite instability and protein expression of the DNA mismatch repair gene, hMLH1, of lung cancer in chromate-exposed workers. Mol Carcinog 42:150-158.

Tanenbaum ME, Medema RH. 2010. Mechanisms of centrosome separation and bipolar spindle assembly. Dev Cell 19:797-806.

Taylor FH. 1966. The relationship of mortality and duration of employment as reflected by a cohort of chromate workers. Am J Public Health N 56:218-229.

Testa JR, Siegfried JM. 1992. Chromosome abnormalities in human non-small cell lung cancer. Cancer Res 52:2702s-2706s.

Tsou MF, Stearns T. 2006a. Controlling centrosome number: licenses and blocks. Curr Opin Cell Biol 18:74-78.

Tsou MF, Stearns T. 2006b. Mechanism limiting centrosome duplication to once per cell cycle. Nature 442:947-951.

Tsou MF, Wang WJ, George KA, Uryu K, Stearns T, Jallepalli PV. 2009. Polo kinase and separase regulate the mitotic licensing of centriole duplication in human cells. Dev Cell 17:344-354.

Tsvetkov L, Stern DF. 2005. Phosphorylation of Plk1 at S137 and T210 is inhibited in response to DNA damage. Cell Cycle 4:166-171.

Uddin AN, Burns FJ, Rossman TG, Chen H, Kluz T, Costa M. 2007. Dietary chromium and nickel enhance UV-carcinogenesis in skin of hairless mice. Toxicol Appl Pharmacol 221:329-338.

U.S. Geological Survey (USGS). 2014. Mineral commodity summaries: Chromium. U.S. Geological Survey, Reston, Virginia.

van Heesbeen RG, Raaijmakers JA, Tanenbaum ME, Medema RH. 2013. Nuclear envelope-associated dynein cooperates with Eg5 to drive prophase centrosome separation. Commun Integr Biol 6:e23841.

van Vugt MA, Smits VA, Klompmaker R, Medema RH. 2001. Inhibition of Polo-like kinase-1 by DNA damage occurs in an ATM- or ATR-dependent fashion. J Biol Chem 276:41656-41660.

van Vugt MA, van de Weerdt BC, Vader G, Janssen H, Calafat J, Klompmaker R, Wolthuis RM, Medema RH. 2004. Polo-like kinase-1 is required for bipolar spindle formation but is dispensable for anaphase promoting complex/Cdc20 activation and initiation of cytokinesis. J Biol Chem 279:36841-36854.

Vincent JB. 2014. Is chromium pharmacologically relevant?. Journal of Trace Elements in Medicine and Biology.

Vogelstein B, Kinzler KW. 1993. The multistep nature of cancer. Trends in Genetics 9:138-141.

Voitkun V, Zhitkovich A, Costa M. 1998. Cr(III)-mediated crosslinks of glutathione or amino acids to the DNA phosphate backbone are mutagenic in human cells. Nucleic Acids Res 26:2024-2030.

Wakeman TP, Kim WJ, Callens S, Chiu A, Brown KD, Xu B. 2004. The ATM-SMC1 pathway is essential for activation of the chromium[VI]-induced S-phase checkpoint. Mutat Res 554:241-251.

Waizenegger IC, Giménez-Abián JF, Wernic D, Peters J. 2002. Regulation of human separase by securin binding and autocleavage. Curr Biol 12:1368-1378.

Wang X, Yang Y, Duan Q, Jiang N, Huang Y, Darzynkiewicz Z, Dai W. 2008. sSgo1, a major splice variant of Sgo1, functions in centriole cohesion where it is regulated by Plk1. Dev Cell 14:331-341.

Wang T, Song Y, Wang H, Zhang J, Yu S, Gu Y, Chen T, Wang Y, Shen H, Jia G. 2012. Oxidative DNA damage and global DNA hypomethylation are related to folate deficiency in chromate manufacturing workers. J Hazard Mater 213:440-446.

Weaver BA, Silk AD, Montagna C, Verdier-Pinard P, Cleveland DW. 2007. Aneuploidy acts both oncogenically and as a tumor suppressor. Cancer Cell 11:25-36.

Wise JP Sr, Stearns DM, Wetterhahn KE, Patierno SR. 1994. Cell-enhanced dissolution of carcinogenic lead chromate particles: the role of individual dissolution products in clastogenesis. Carcinogenesis 15:2249-2254.

Wise JP Sr, Wise SS, Little JE. 2002. The cytotoxicity and genotoxicity of particulate and soluble hexavalent chromium in human lung cells. Mutat Res 517:221-229.

Wise SS, Holmes AL, Ketterer ME, Hartsock WJ, Fomchenko E, Katsifis S, Thompson WD, Wise JP S. 2004a. Chromium is the proximate clastogenic species for lead chromate-induced clastogenicity in human bronchial cells. Mutat Res 560:79-89.

Wise SS, Elmore LW, Holt SE, Little JE, Antonucci PG, Bryant BH, Wise JP S. 2004b. Telomerase-mediated lifespan extension of human bronchial cells does not affect hexavalent chromium-induced cytotoxicity or genotoxicity. Mol Cell Biochem 255:103-111.

Wise SS, Holmes AL, Wise JP S. 2006a. Particulate and soluble hexavalent chromium are cytotoxic and genotoxic to human lung epithelial cells. Mutat Res 610:2-7.

Wise SS, Holmes AL, Xie H, Thompson WD, Wise JP S. 2006b. Chronic exposure to particulate chromate induces spindle assembly checkpoint bypass in human lung cells. Chem Res Toxicol 19:1492-1498.

Wise SS, Holmes AL, Wise JP S. 2008. Hexavalent chromium-induced DNA damage and repair mechanisms. Rev Environ Health 23:39-57.

Wise SS, Holmes AL, Qin Q, Xie H, Katsifis S, Thompson WD, Wise JP Sr. 2010. Comparative genotoxicity and cytotoxicity of four hexavalent chromium compounds in human bronchial cells. Chem Res Toxicol 23:365-372.

Wise SS. 2013. Characterizing the role of chromosome instability in particulate hexavalent chromium-induced carcinogenesis. Ph.D. Dissertation, University of Maine, Orono.

Wu CH, Tseng YS, Kao YT, Sheu HM, Liu HS. 2013. Low concentration of arsenic-induced aberrant mitosis in keratinocytes through E2F1 transcriptionally regulated Aurora-A. Toxicol Sci 132:43-52.

Wunderlich V. 2002. Chromosomes and cancer: Theodor Boveri's predictions 100 years later. J Mol Med 80:545-548.

Xie H, Holmes AL, Wise SS, Gordon N, Wise JP S. 2004. Lead chromate-induced chromosome damage requires extracellular dissolution to liberate chromium ions but does not require particle internalization or intracellular dissolution. Chem Res Toxicol 17:1362-1367.

Xie H, Wise SS, Holmes AL, Xu B, Wakeman TP, Pelsue SC, Singh NP, Wise JP S. 2005. Carcinogenic lead chromate induces DNA double-strand breaks in human lung cells. Mutat Res 586:160-172.

Xie H, Holmes AL, Wise SS, Huang S, Peng C, Wise JP S. 2007. Neoplastic transformation of human bronchial cells by lead chromate particles. Am J Respir Cell Mol Biol 37:544-552.

Xie H, Wise SS, Wise JP S. 2008. Deficient repair of particulate hexavalent chromium-induced DNA double strand breaks leads to neoplastic transformation. Mutat Res 649:230-238.

Xie H, Holmes AL, Young JL, Qin Q, Joyce K, Pelsue SC, Peng C, Wise SS, Jeevarajan AS, Wallace WT, Hammond D, Wise JP Sr. 2009. Zinc chromate induces chromosome instability and DNA double strand breaks in human lung cells. Toxicol Appl Pharm 234:293-299.

Yang J, Adamian M, Li T. 2006. Rootletin interacts with C-Nap1 and may function as a physical linker between the pair of centrioles/basal bodies in cells. Mol Biol Cell 17:1033-1040.

Yao H, Guo L, Jiang B, Luo J, Shi X. 2008. Oxidative stress and chromium (VI) carcinogenesis. J Environ Pathol Tox 27.

Yih LH, Tseng YY, Wu YC, Lee TC. 2006. Induction of centrosome amplification during arsenite-induced mitotic arrest in CGL-2 cells. Cancer Res 66:2098-2106.

Yih LH, Wu YC, Hsu NC, Kuo HH. 2012. Arsenic trioxide induces abnormal mitotic spindles through a PIP4KIIgamma/Rho pathway. Toxicol Sci 128:115-125.

Zhang W, Fletcher L, Muschel RJ. 2005. The role of Polo-like kinase 1 in the inhibition of centrosome separation after ionizing radiation. J Biol Chem 280:42994-42999.

Zhitkovich A, Voitkun V, Costa M. 1996. Formation of the amino acid-DNA complexes by hexavalent and trivalent chromium in vitro: importance of trivalent chromium and the phosphate group. Biochemistry 35:7275-7282.

Zhitkovich A, Song Y, Quievryn G, Voitkun V. 2001. Non-oxidative mechanisms are responsible for the induction of mutagenesis by reduction of Cr (VI) with cysteine: role of ternary DNA adducts in Cr (III)-dependent mutagenesis. Biochemistry 40:549-560.

Zhitkovich A. 2004. Importance of chromium-DNA adducts in mutagenicity and toxicity of chromium(VI). Chem Res Toxicol 18:3-11.

Zou H, Stemman O, Anderson JS, Mann M, Kirschner MW. 2002. Anaphase specific auto-cleavage of separase. FEBS Lett 528:246-250.

Zou J, Rezvani K, Wang H, Lee KS, Zhang D. 2013. BRCA1 down-regulates the kinase activity of polo-like kinase 1 in response to replication stress. Cell Cycle 12:2255-2265.

BIOGRAPHY OF THE AUTHOR

Julieta Martino was born in Córdoba, Argentina on September 21, 1981. She graduated from the Universidad Nacional de Córdoba in 2005 with a degree in Biology. After graduating she worked for two years for the non-profit Instituto de Conservación de Ballenas performing field research on whales. During this work she became interested in the links between disease and environmental pollutants. In 2006, she met Dr. Wise and visited his laboratory, after which she decided to join the cooperative Ph.D. program between the University of Maine and University of Southern Maine. For this purpose, she was awarded a Fulbright Fellowship from the U.S. Department of State. She moved to Maine in 2007. She is a candidate for the Doctor of Philosophy degree in Biochemistry and Molecular Biology from The University of Maine in May 2015.